4 Validation tests

The verification of a seismic hazard computer code is crucial for ensuring the user that the calculations performed with it are reliable. The numerical verification process of R-CRISIS has been carried out considering a set of tests developed in a project sponsored by the Pacific Earthquake Engineering Research Center (PEER) documented by Thomas et al. (2010) for the first phase and by Thomas et al. (2014) in the second phase. The results presented herein correspond to the work developed by Villani et al. (2010) and by Ordaz and Aguilar (2015) and explains with detail the procedures, assumptions and options used for each particular case.

Finally, additional validation tests of geometrical, rupture, seismicity and attenuation parameters are included in this section in order to show that R-CRISIS performs well under the framework of the selected methodologies and is suitable for the development of probabilistic seismic hazard analyses.

4.1 PEER validation tests (set 1)

For these validation and verification exercises, two sets of test problems were used for testing some fundamental aspects of the R-CRISIS code such as the treatment of fault sources, recurrence models and rates, strong ground motion attenuation relationships and their associated uncertainties. For the simplest cases analytical solutions were also provided by the PEER project coordinators.

4.1.1 Geometry of the earthquake sources

Three different types of earthquake sources were adopted for the tests:

- Two (2) fault sources and,
- One (1) area source with constant depth.

The two fault sources are shown in Figure 4-1 where the thick black line in the plan view corresponds to the trace of the two faults on the surface. Fault 1 (black line) corresponds to a strike-slip vertical source with depth between 0 and 12km, whereas fault 2 (red line) corresponds to a reverse fault with dip of 60° and with depth between 1 and 11km.

The area source is illustrated in Figure 4-2 and corresponds to a circular area with radius of 100km at a constant depth of 5km and with uniform seismicity. The black points identified with numbers in Figures 4-1 and 4-2 show the location of the sites (or observation sites) where the computation of the seismic hazard was made.

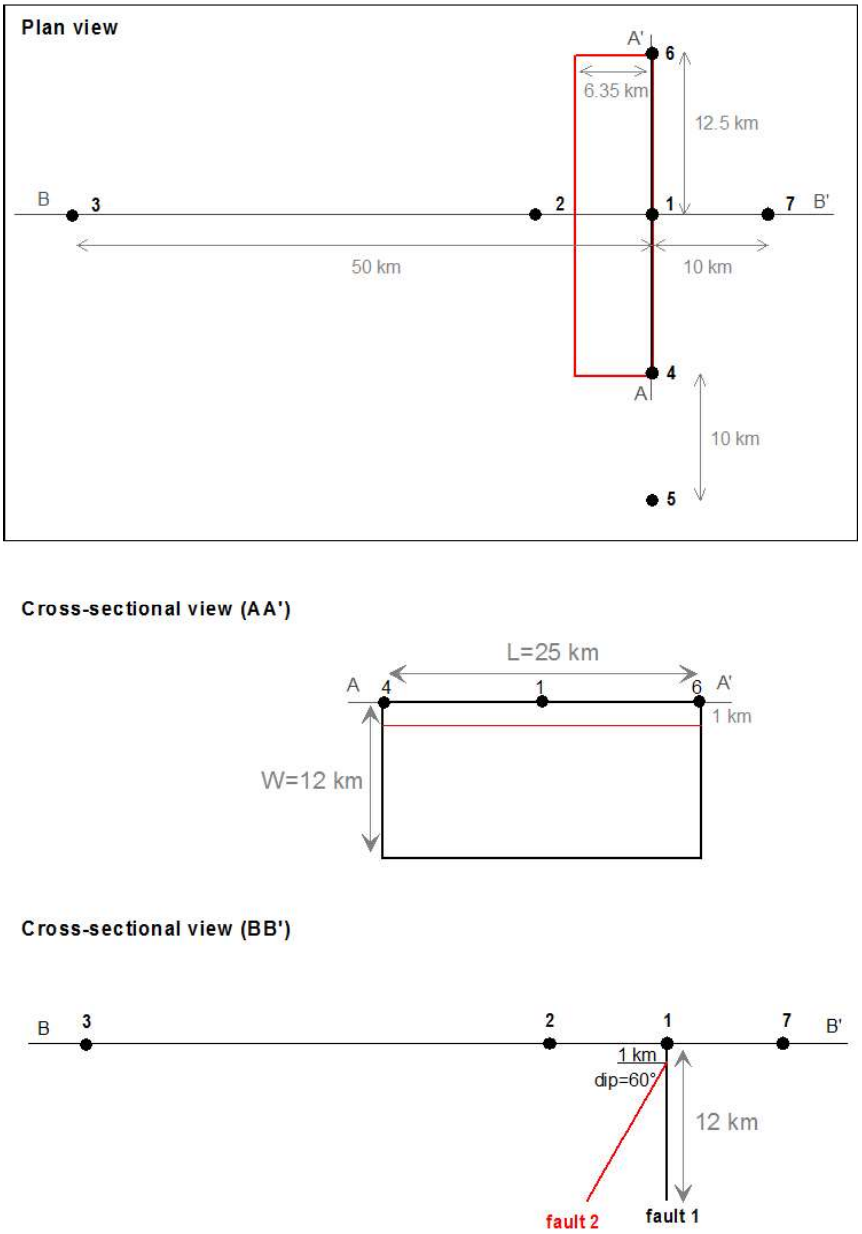

Figure 4-1 Geometry of the fault sources (1 & 2) and location of the observation sites

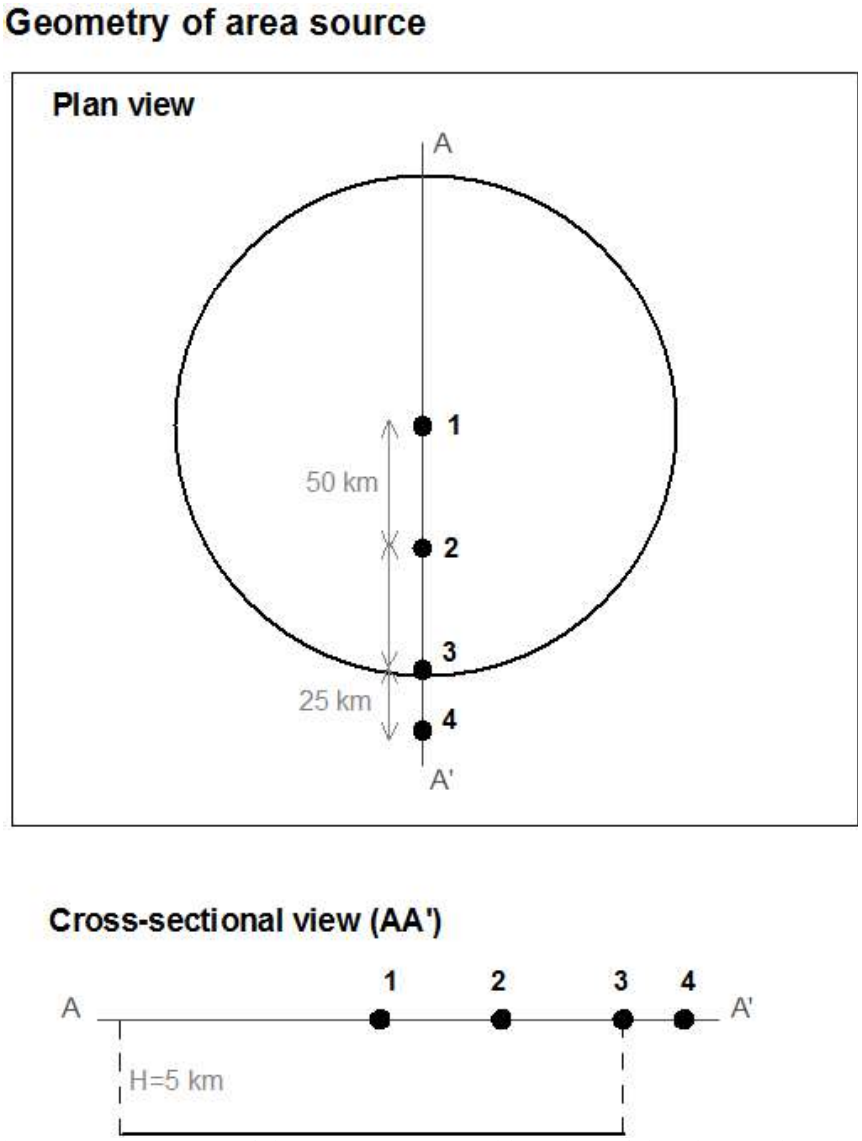

Figure 4-2 Geometry of the area sources and location of the observation sites

4.1.2 Rupture areas

Considering that since R-CRISIS the rectangular fault type was introduced and bearing in mind that for R-CRISIS the definition of the geometry also implies the definition of the shape of the rupture area. Comparisons of the results obtained between different rupture shapes (elliptical and rectangular) are included in this section with the aim of presenting, in a transparent way, the implications the selection of this parameter has in the final hazard results. It is anyhow important to highlight that, from a theoretical point of view, the rupture areas can be rectangular or elliptical (Villani et al., 2010).

Figure 4-3 shows the schematic representation of the elliptical rupture areas, using the strict boundary behavior which, from the theoretical point of view are considered as valid. Anyhow, the inconvenient with them, for locations such as computation sites 4 and 6 (for the cases

when the fault type sources are used) is that when elliptical ruptures exist, regions near the corners of the source do not have sub-sources included and then, the seismic hazard intensities are lower than in the case where rectangular shapes are used.

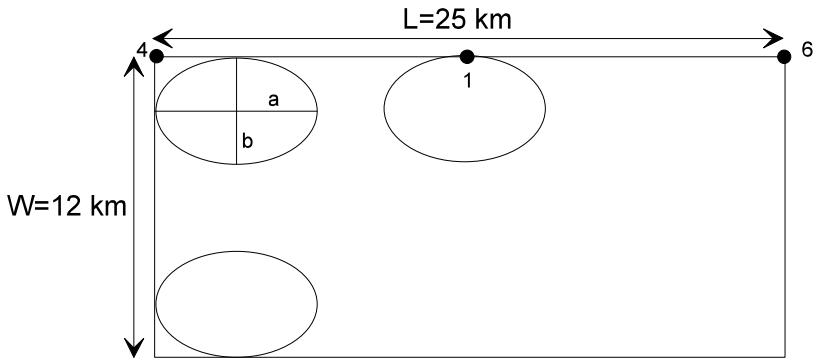

Figure 4-3 Schematic representation of elliptical rupture areas in R-CRISIS

4.1.3 Description of ground motion attenuation

In the PEER tests, the ground motion attenuation is described by means of the strong ground motion attenuation relationship proposed by Sadigh et al. (1997). In R-CRISIS, the Sadigh et al. (1997) model is using the built-in GMPM that accounts for magnitudes between 4.0 and 7.5 (with ΔM=0.1) and for distances (R_{rup}) between 0.01 and 150km.

Note: in most cases the associated ground motion variability (σ) is assumed to be null. Hence, in the attenuation table a sigma value equal to 0.0001 was used (this because a null value is not accepted by the R-CRISIS code).

4.1.4 Other instructions from PEER

PEER provided some additional instructions to the developers of the tests, such as:

- The rupture area, A, should depend on magnitude in the form of $Log(A)=M_W-4$ with σ_A=0.25. In all tests, except in case #3, this variability is not included.
- For all faults the slip rate is 2mm/yr and the Gutenberg-Richter b-value is 0.9.
- The results should provide the mean probability of exceedance for peak horizontal acceleration between 0.001 and 1g.

4.1.5 Set 1 case1

Input parameters

The source adopted corresponds to fault 1 (see Figure 4-1). In Thomas et al. (2010; 2014) the seismicity input is specified through a b-value of 0.9, a slip rate of 2mm/yr and a magnitude density function in the form of a delta-function centered at 6.5.

Table 4-1 summarizes the input data whereas Table 4-2 shows the data associated to the geometry of the fault source. Table 4-3 includes the coordinates of the computation sites together with an explanation about its relevance for validation and verification purposes.

Table 4-1 Summary of input data for Set 1, case 1

Name	Description	Source	Mag-Density Function	Ground Motion Model[1,2]	Rupture Dimension Relationships[3,4,5,6]
Set 1 Case 1	Single rupture of entire fault plane. Tests distance, rate, and ground motion calculations.	Fault 1(vertical SS) b-value=0.9 Slip rate=2mm/yr. The geometry and other characteristics of the source are shown in Figure 4-1	Delta function at M6.5	Sadigh et al. (1997), rock. σ = 0	$Log(A) = M - 4; \sigma_A = 0$ $Log(W) = 0.5 * M - 2.15; \sigma_W = 0$ $Log(L) = 0.5 * M - 1.85; \sigma_L = 0$

[1] Integration over magnitude zero.

[2] Use magnitude integration step size as small as necessary to model the magnitude density function.

[3] For all cases, uniform slip with tapered slip at edges.

[4] No ruptures are to extend beyond the edge of the fault plane.

[5] Aspect ratio to be maintained until maximum width is reached, then increase length (maintain area at the expense of aspect ratio).

[6] Down-dip and along strike integration step size should be as small as necessary for uniform rupture location.

Note: For all cases where the validation tests are performed using rupture dimension characteristics shown in Table 4-1, the following considerations are made. $Log(A)=M-4$ corresponds to the value proposed by Singh et al. (1980) and that is implemented as a built-in model in R-CRISIS. Instructions about $Log(W)$ and $Log(L)$ are handled by estimating the aspect ratio of L/W equal to 2.0 which correspond to elliptical ruptures.

Table 4-2 Coordinates of the fault source 1

Latitude	Longitude	Comment
38.0000	-122.0000	South end of fault
38.2248	-122.0000	North end of fault

Table 4-3 Coordinates and comments of the computation sites for fault sources 1 and 2

Site	Latitude	Longitude	Comment
1	38.113	-122.000	On fault, at midpoint along strike
2	38.113	-122.114	10 km west of fault, at midpoint along strike
3	38.111	-122.570	50 km west of fault, at midpoint along strike
4	38.000	-122.000	On fault, at southern end
5	37.910	-122.000	10 km south of fault along strike
6	38.225	-122.000	On fault, at northern end
7	38.113	-121.886	10 km east of fault, at midpoint along strike

In the R-CRISIS screen shown in Figures 4-4 and 4-5 (geometry of the seismic sources for rectangular and area sources), it is possible to assign the parameters that define the rupture dimensions. Particularly, in the case of sources with a surface, the rupture area is defined by means of equation 4-1 (which is the same as Eq. 2-27 but repeated herein for convenience of the reader). *K1* and *K2* parameters are user defined.

$$A = K_1 \cdot e^{K_2 M} \qquad \text{(Eq. 4-1)}$$

where A is the source area (in km²), M stands for magnitude and K_1 and K_2 are constants given by the user or chosen from a set of constants.

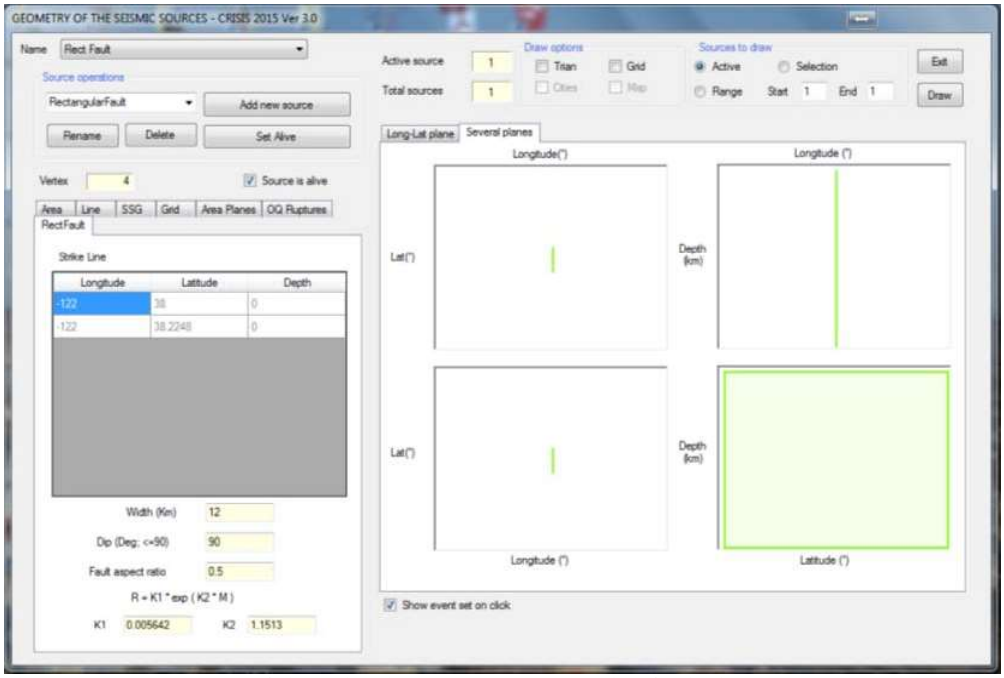

Figure 4-4 Geometry of the seismic source (rectangular fault) in R-CRISIS. Case 1, set 1

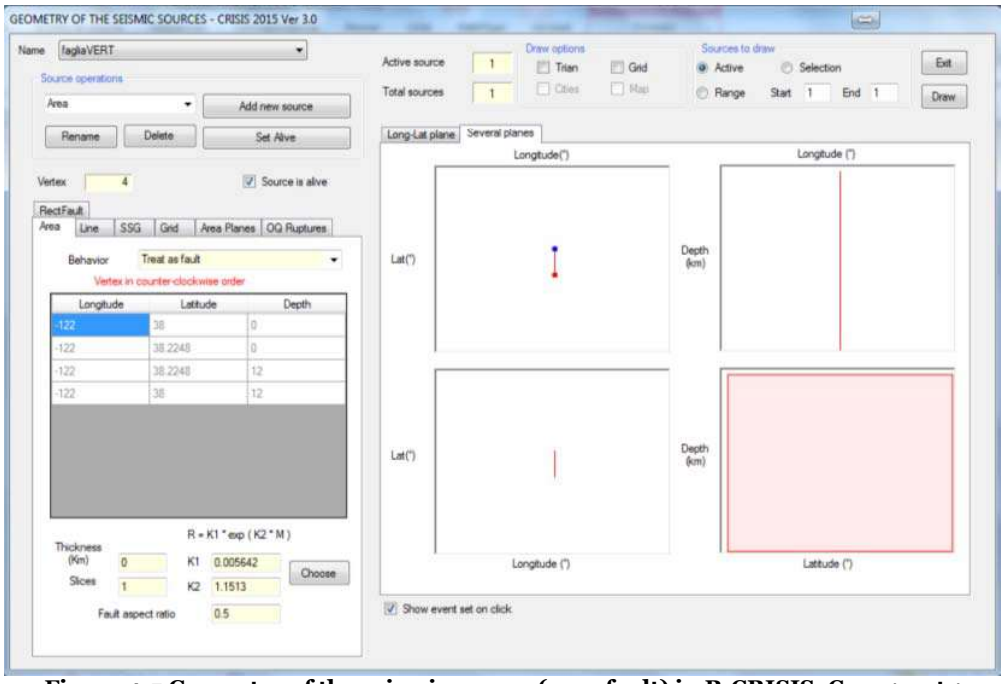

Figure 4-5 Geometry of the seismic source (area fault) in R-CRISIS. Case 1, set 1

In R-CRISIS, this input was described through a modified Gutenberg-Richter relation with minimum magnitude, M_{min}=6.49, and a maximum magnitude, M_{max}=6.51. The two parameters for the full description of the G-R relation are the slope b (equal to 0.9 as per the PEER instructions[21]) and the annual rate λ (i.e. the number of earthquakes with magnitude $M \geq M_{min}$. The latter can be computed from the slip rate using the scalar seismic moment, M_o as:

$$M_o = \mu A s \qquad \text{(Eq. 4-2)}$$

where:

- M=3x10^{11} (dyne/cm^2)
- A= source area (cm^2)
- s= average slip on the fault (cm)

Moreover, according to the definition of moment magnitude (M_W) by Hanks and Kanamori (1979):

$$M_W = \frac{2}{3}\log M_o\left[dyne \cdot cm\right] - 16.05 \qquad \text{(Eq. 4-3)}$$

From which it can be seen that:

[21] Since in this case only one magnitude is considered, the b-value is irrelevant

$$M_o\left[dyne \cdot cm\right] = 10^{1.5M+16.05} \quad \text{(Eq. 4-4)}$$

The seismic moment rate (i.e. the seismic moment released by the source in one year, can be obtained by replacing the average slip on the fault (s) with the slip rate. since only one magnitude value (m) is possible, the seismic moment rate is λ (the number of earthquakes of magnitude equal to m in one year) times the seismic moment related to such magnitude m:

$$\dot{M}_o = \mu A \dot{s} = \lambda(10^{1.5m+16.05}) \quad \text{(Eq. 4-5)}$$

where s correspond to the slip rate on the source (cm/yr).

From equation 4-5, for m=6.5, $\lambda_{6.5}$=0.002853. Figure 4-6 shows the seismicity screen of R-CRISIS and how these values were set for this case.

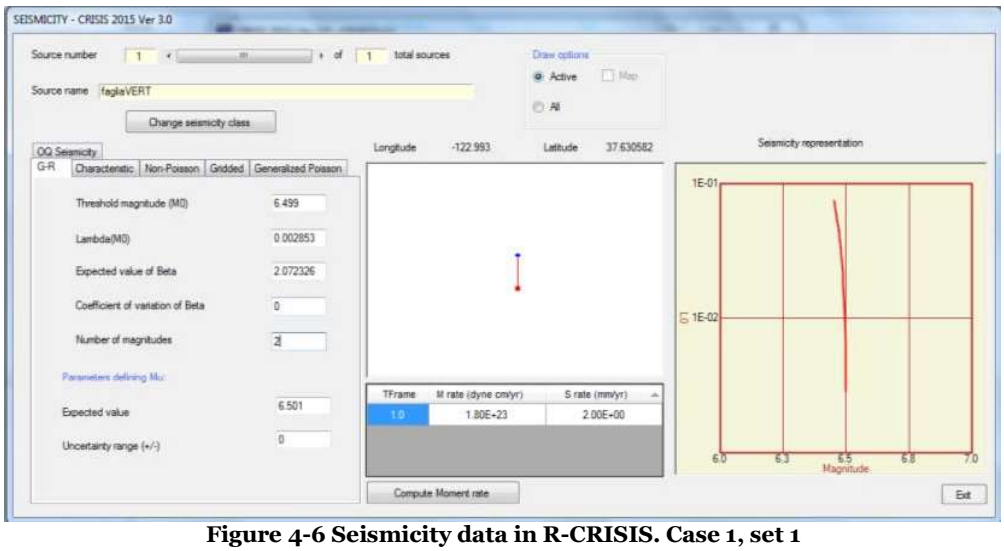

Figure 4-6 Seismicity data in R-CRISIS. Case 1, set 1

Finally, Figure 4-7 shows the attenuation data screen of R-CRISIS from where the Sadigh et al. (1997) GMPM has been assigned to the fault source.

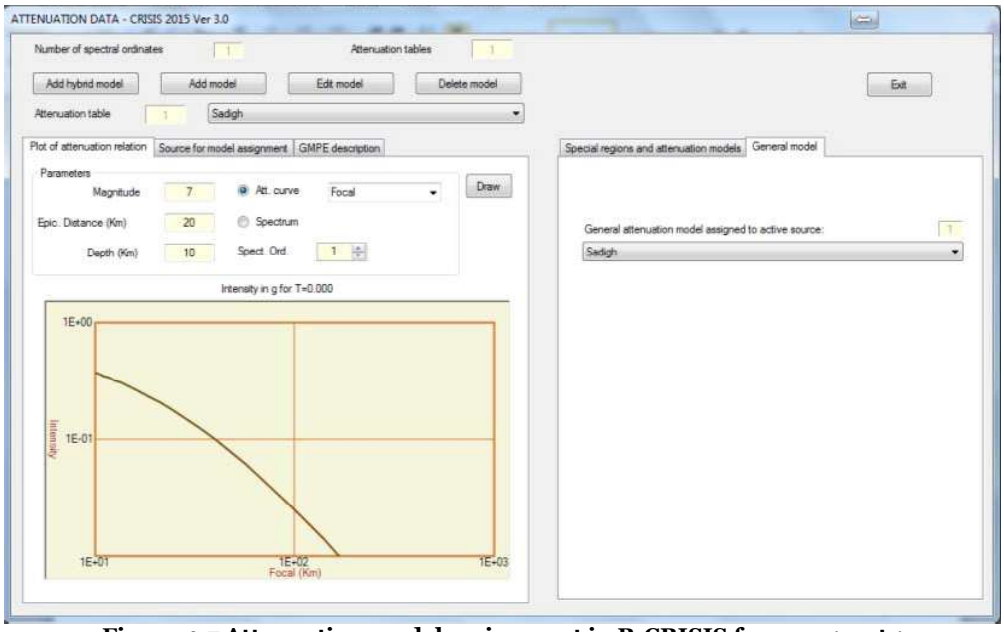

Figure 4-7 Attenuation model assignment in R-CRISIS for case 1, set 1

Results

Results obtained in R-CRISIS are summarized in Table 4-4. Additionally, in Table 4-5 it is possible to observe the results reported by PEER-2015 as benchmarks. Table 4-6 shows the results obtained analytically for the same case by the coordinators of the PEER-2015 project.

Figure 4-8 shows the plots of the seismic hazard results obtained by R-CRISIS and those considered as valid by the PEER-2015 project. In all the plots, it is seen a complete agreement between the results obtained by CRISIS and those provided by PEER-2015 and therefore, it is possible to conclude that CRISIS fulfills all the requirements evaluated by the PEER-2015 project in Set 1-Case 1.

Finally, for comparison purposes, Figure 4-9 shows the hazard plots comparing the results obtained with R-CRISIS (elliptical and rectangular options) and the ones provided by the PEER-2015 project. As expected, the differences occur in computation sites 4 and 6 for the reasons explained in Section 4.1.2.

Table 4-4 Annual exceedance probabilities obtained in R-CRISIS for Case 1, set 1

Peak Ground Acceleration (g)	Annual Exceedance Probability						
	Site 1	Site 2	Site 3	Site 4	Site 5	Site 6	Site 7
0.001	2.85E-03	2.85E-03	2.85E-03	2.85E-03	2.85E-03	2.85E-03	2.85E-03
0.01	2.85E-03	2.85E-03	2.85E-03	2.85E-03	2.85E-03	2.85E-03	2.85E-03
0.05	2.85E-03	2.85E-03	0.00E+00	2.85E-03	2.85E-03	2.85E-03	2.85E-03
0.10	2.85E-03	2.85E-03	0.00E+00	2.85E-03	2.85E-03	2.85E-03	2.85E-03
0.15	2.85E-03	2.85E-03	0.00E+00	2.85E-03	2.85E-03	2.85E-03	2.85E-03
0.20	2.85E-03	2.85E-03	0.00E+00	2.85E-03	2.85E-03	2.85E-03	2.85E-03
0.25	2.85E-03	2.85E-03	0.00E+00	2.85E-03	2.85E-03	2.85E-03	2.85E-03
0.30	2.85E-03	2.85E-03	0.00E+00	2.85E-03	2.85E-03	2.85E-03	2.85E-03
0.35	2.85E-03	0.00E+00	0.00E+00	2.85E-03	0.00E+00	2.85E-03	0.00E+00
0.40	2.85E-03	0.00E+00	0.00E+00	2.85E-03	0.00E+00	2.85E-03	0.00E+00
0.45	2.85E-03	0.00E+00	0.00E+00	2.85E-03	0.00E+00	2.85E-03	0.00E+00
0.50	2.85E-03	0.00E+00	0.00E+00	2.85E-03	0.00E+00	2.85E-03	0.00E+00
0.55	2.85E-03	0.00E+00	0.00E+00	2.85E-03	0.00E+00	2.85E-03	0.00E+00
0.60	2.85E-03	0.00E+00	0.00E+00	2.85E-03	0.00E+00	2.85E-03	0.00E+00
0.70	2.85E-03	0.00E+00	0.00E+00	2.85E-03	0.00E+00	2.85E-03	0.00E+00
0.80	0.00E+00	0.00E+00	0.00E+00	0.00E+00	0.00E+00	0.00E+00	0.00E+00
0.90	0.00E+00	0.00E+00	0.00E+00	0.00E+00	0.00E+00	0.00E+00	0.00E+00
1.00	0.00E+00	0.00E+00	0.00E+00	0.00E+00	0.00E+00	0.00E+00	0.00E+00

Table 4-5 Annual exceedance probabilities reported as benchmarks by PEER project coordinators for Case 1, set 1

Peak Ground Acceleration (g)	Annual Exceedance Probability						
	Site 1	Site 2	Site 3	Site 4	Site 5	Site 6	Site 7
0.001	2.85E-03	2.85E-03	2.85E-03	2.85E-03	2.85E-03	2.85E-03	2.85E-03
0.01	2.85E-03	2.85E-03	2.85E-03	2.85E-03	2.85E-03	2.85E-03	2.85E-03
0.05	2.85E-03	2.85E-03	0.00E+00	2.85E-03	2.85E-03	2.85E-03	2.85E-03
0.10	2.85E-03	2.85E-03	0.00E+00	2.85E-03	2.85E-03	2.85E-03	2.85E-03
0.15	2.85E-03	2.85E-03	0.00E+00	2.85E-03	2.85E-03	2.85E-03	2.85E-03
0.20	2.85E-03	2.85E-03	0.00E+00	2.85E-03	2.85E-03	2.85E-03	2.85E-03
0.25	2.85E-03	2.85E-03	0.00E+00	2.85E-03	2.85E-03	2.85E-03	2.85E-03
0.30	2.85E-03	2.85E-03	0.00E+00	2.85E-03	2.85E-03	2.85E-03	2.85E-03
0.35	2.85E-03	0.00E+00	0.00E+00	2.85E-03	0.00E+00	2.85E-03	0.00E+00
0.40	2.85E-03	0.00E+00	0.00E+00	2.85E-03	0.00E+00	2.85E-03	0.00E+00
0.45	2.85E-03	0.00E+00	0.00E+00	2.85E-03	0.00E+00	2.85E-03	0.00E+00
0.50	2.85E-03	0.00E+00	0.00E+00	2.85E-03	0.00E+00	2.85E-03	0.00E+00
0.55	2.85E-03	0.00E+00	0.00E+00	2.85E-03	0.00E+00	2.85E-03	0.00E+00
0.60	2.85E-03	0.00E+00	0.00E+00	2.85E-03	0.00E+00	2.85E-03	0.00E+00
0.70	2.85E-03	0.00E+00	0.00E+00	2.85E-03	0.00E+00	2.85E-03	0.00E+00
0.80	0.00E+00	0.00E+00	0.00E+00	0.00E+00	0.00E+00	0.00E+00	0.00E+00
0.90	0.00E+00	0.00E+00	0.00E+00	0.00E+00	0.00E+00	0.00E+00	0.00E+00
1.00	0.00E+00	0.00E+00	0.00E+00	0.00E+00	0.00E+00	0.00E+00	0.00E+00

Table 4-6 Analytical annual exceedance probabilities obtained by PEER project coordinators for Case 1, set 1

Peak Ground Acceleration (g)	Annual Exceedance Probability						
	Site 1	Site 2	Site 3	Site 4	Site 5	Site 6	Site 7
0.001	2.85E-03	2.85E-03	2.85E-03	2.85E-03	2.85E-03	2.85E-03	2.85E-03
0.01	2.85E-03	2.85E-03	2.85E-03	2.85E-03	2.85E-03	2.85E-03	2.85E-03
0.05	2.85E-03	2.85E-03	0.00E+00	2.85E-03	2.85E-03	2.85E-03	2.85E-03
0.10	2.85E-03	2.85E-03	0.00E+00	2.85E-03	2.85E-03	2.85E-03	2.85E-03
0.15	2.85E-03	2.85E-03	0.00E+00	2.85E-03	2.85E-03	2.85E-03	2.85E-03
0.20	2.85E-03	2.85E-03	0.00E+00	2.85E-03	2.85E-03	2.85E-03	2.85E-03
0.25	2.85E-03	2.85E-03	0.00E+00	2.85E-03	2.85E-03	2.85E-03	2.85E-03
0.30	2.85E-03	2.85E-03	0.00E+00	2.85E-03	2.85E-03	2.85E-03	2.85E-03
0.35	2.85E-03	0.00E+00	0.00E+00	2.85E-03	0.00E+00	2.85E-03	0.00E+00
0.40	2.85E-03	0.00E+00	0.00E+00	2.85E-03	0.00E+00	2.85E-03	0.00E+00
0.45	2.85E-03	0.00E+00	0.00E+00	2.85E-03	0.00E+00	2.85E-03	0.00E+00
0.50	2.85E-03	0.00E+00	0.00E+00	2.85E-03	0.00E+00	2.85E-03	0.00E+00
0.55	2.85E-03	0.00E+00	0.00E+00	2.85E-03	0.00E+00	2.85E-03	0.00E+00
0.60	2.85E-03	0.00E+00	0.00E+00	2.85E-03	0.00E+00	2.85E-03	0.00E+00
0.70	2.85E-03	0.00E+00	0.00E+00	2.85E-03	0.00E+00	2.85E-03	0.00E+00
0.80	0.00E+00	0.00E+00	0.00E+00	0.00E+00	0.00E+00	0.00E+00	0.00E+00
0.90	0.00E+00	0.00E+00	0.00E+00	0.00E+00	0.00E+00	0.00E+00	0.00E+00
1.00	0.00E+00	0.00E+00	0.00E+00	0.00E+00	0.00E+00	0.00E+00	0.00E+00

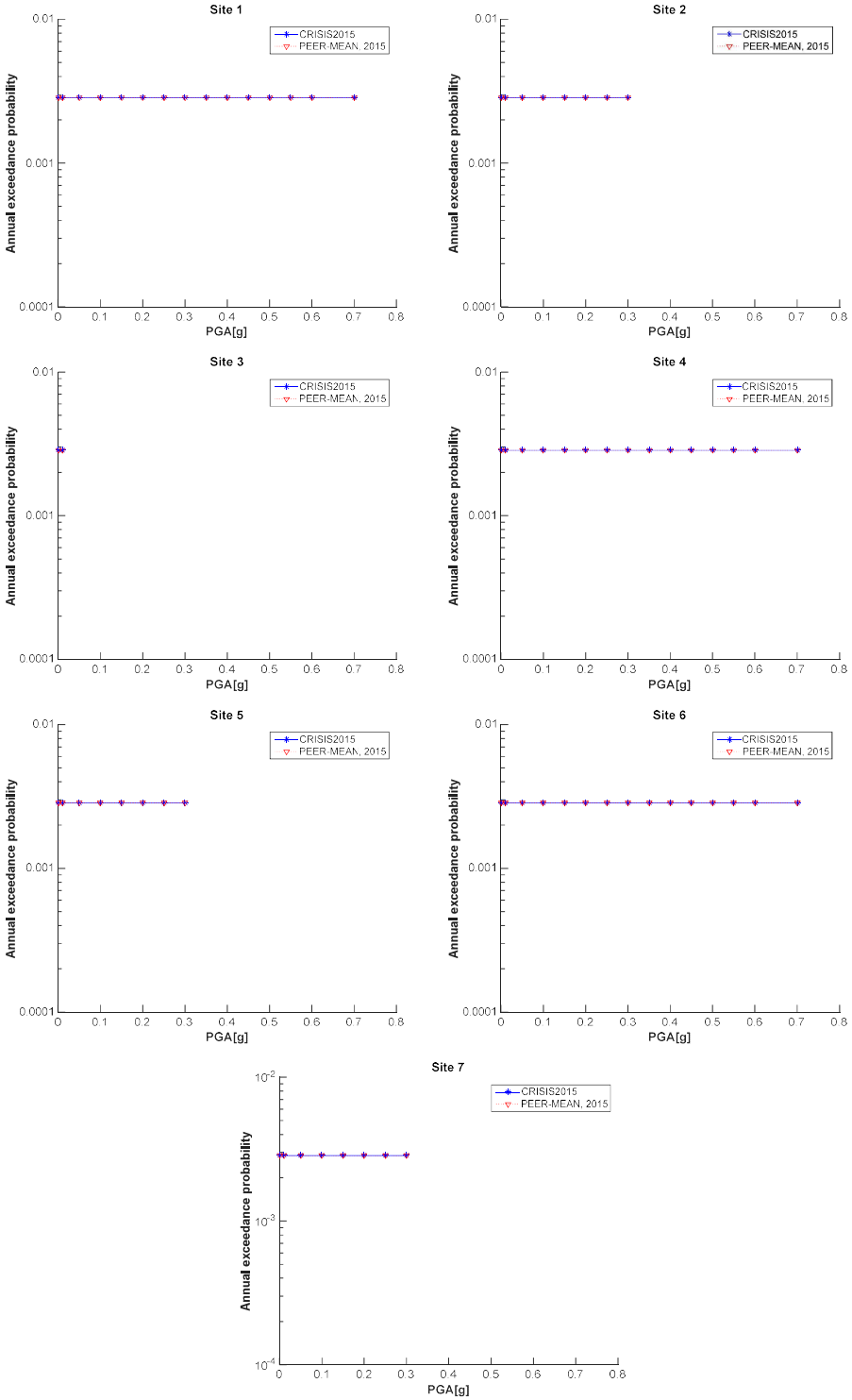

Figure 4-8 Comparison of the CRISIS and PEER-2015 results for Sites 1 to 7 (Set 1 Case 1)

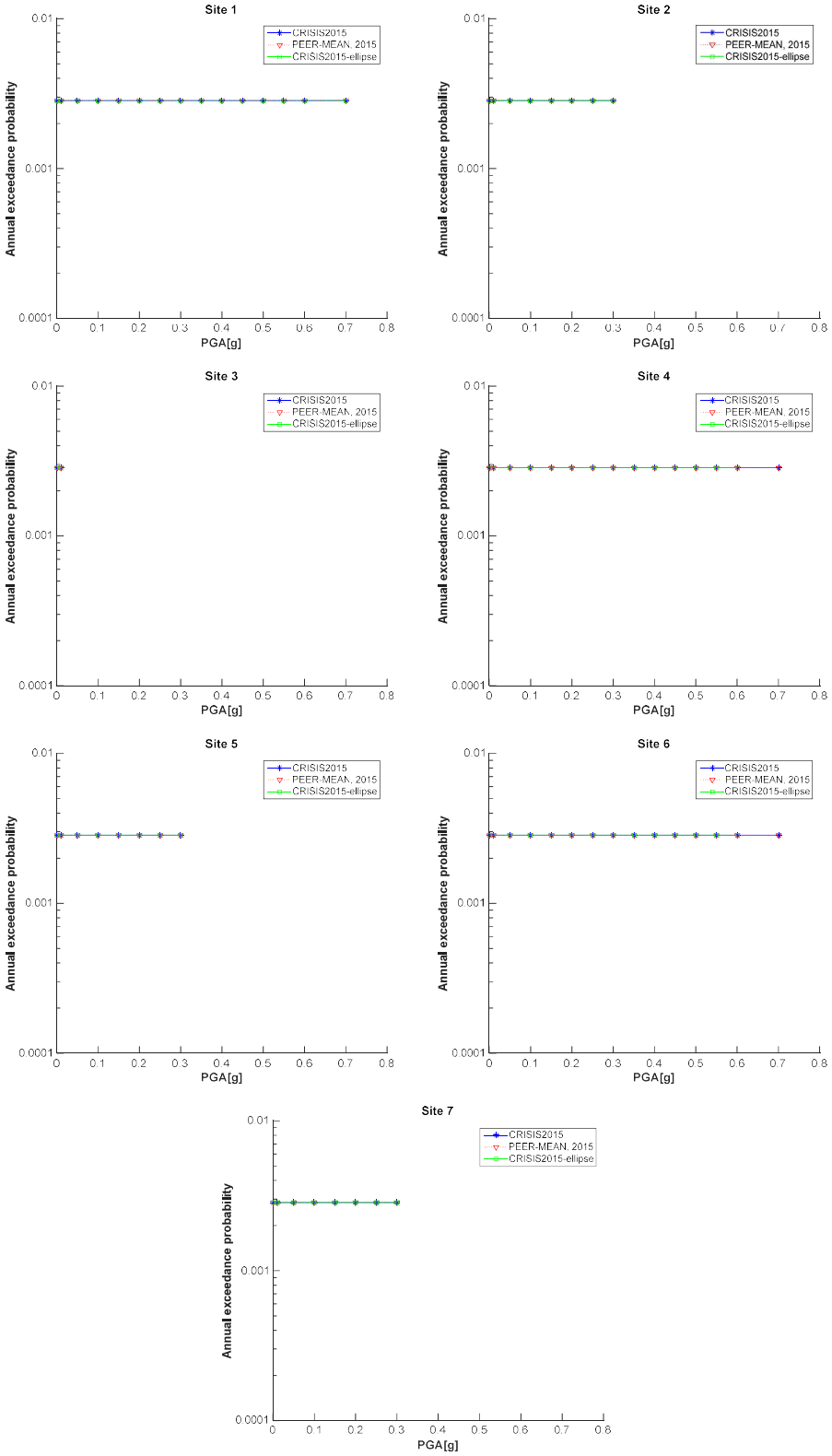

Figure 4-9 Comparison of elliptical and rectangular rupture shapes for PEER-2015 Set 1 Case 1

4.1.6 Set 1 case 2

Input parameters

The source adopted for this case corresponds to Fault 1. In Thomas et al. (2010; 2014) the seismicity input is specified by a *b*-value=0.9 a slip rate of 2mm/yr and a magnitude density function in the form of a delta-function centered at 6.0 as shown in Table 4-7.

Table 4-7 Summary of input data for Set 1, case 2

Name	Description	Source	Mag-Density Function	Ground Motion Model[1,2]	Rupture Dimension Relationships[3,4,5,6]
Set 1 Case 2	Single rupture of entire fault plane. Tests distance, rate, and ground motion calculations.	Fault 1(vertical SS) b-value=0.9 Slip rate=2mm/yr. The geometry and other characteristics of the source are shown in Figure 4-1	Delta function at M6.0	Sadigh et al. (1997), rock. σ = 0	$Log(A) = M - 4; \sigma_A = 0$ $Log(W) = 0.5 * M - 2.15; \sigma_W = 0$ $Log(L) = 0.5 * M - 1.85; \sigma_L = 0$

[1] Integration over magnitude zero.
[2] Use magnitude integration step size as small as necessary to model the magnitude density function.
[3] For all cases, uniform slip with tapered slip at edges.
[4] No ruptures are to extend beyond the edge of the fault plane.
[5] Aspect ratio to be maintained until maximum width is reached, then increase length (maintain area at the expense of aspect ratio).
[6] Down-dip and along strike integration step size should be as small as necessary for uniform rupture location.

As in case 1, set 1, a modified G-R relation was used in R-CRISIS with minimum magnitude, M_{min}=5.99, maximum magnitude, M_{max}=6.01 and λ=0.016043, obtained from equation 4-5 now with m=6. Figure 4-10 shows the seismicity data included in the R-CRISIS screen which is the only difference if compared to the geometry and attenuation screens shown before for case 1, set 1 of the PEER project tests.

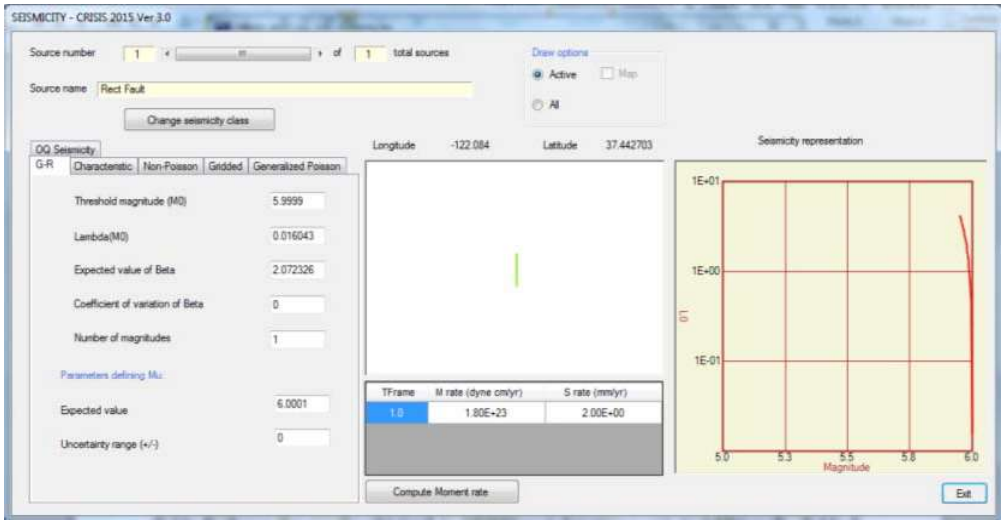

Figure 4-10 Seismicity values in R-CRISIS. Case 1, set 2

Results

Table 4-8 shows the results obtained in R-CRISIS for case 1, set 2. Additionally, Table 4-9 shows the mean values provided by PEER-2015 and finally Table 4-10 includes the analytical solution provided by the coordinators of the PEER-2015 project.

Figure 4-11 shows the comparison of the seismic hazard plots obtained by R-CRISIS and provided by PEER-2015. In all cases there is a full agreement between the results and therefore, it is possible to conclude that R-CRISIS fulfills all the requirements evaluated by the PEER project validation test in case 1, set 2.

Finally, Figure 4-12 shows the hazard plots comparing the results obtained with R-CRISIS (elliptical and rectangular options) and the ones provided by the PEER-2015 project. In this case differences exist at computation sites 1, 4, 5 and 6. The reason for these differences is the same explained before but it is worth noting that, as expected, it is much bigger at those computation sites in the corners than in other locations.

Table 4-8 Annual exceedance probabilities obtained in R-CRISIS for Case 1, set 2

Peak Ground Acceleration (g)	Annual Exceedance Probability						
	Site 1	Site 2	Site 3	Site 4	Site 5	Site 6	Site 7
0.001	1.59E-02	1.59E-02	1.59E-02	1.59E-02	1.59E-02	1.59E-02	1.59E-02
0.01	1.59E-02	1.59E-02	1.59E-02	1.59E-02	1.59E-02	1.59E-02	1.59E-02
0.05	1.59E-02	1.59E-02	0.00E+00	1.59E-02	1.59E-02	1.59E-02	1.59E-02
0.10	1.59E-02	1.59E-02	0.00E+00	1.59E-02	1.59E-02	1.59E-02	1.59E-02
0.15	1.59E-02	1.59E-02	0.00E+00	1.59E-02	7.78E-03	1.59E-02	1.59E-02
0.20	1.59E-02	1.59E-02	0.00E+00	1.58E-02	1.60E-03	1.58E-02	1.59E-02
0.25	1.59E-02	0.00E+00	0.00E+00	1.20E-02	0.00E+00	1.20E-02	0.00E+00
0.30	1.59E-02	0.00E+00	0.00E+00	8.68E-03	0.00E+00	8.63E-03	0.00E+00
0.35	1.59E-02	0.00E+00	0.00E+00	5.74E-03	0.00E+00	5.70E-03	0.00E+00
0.40	1.17E-02	0.00E+00	0.00E+00	3.10E-03	0.00E+00	3.07E-03	0.00E+00
0.45	8.24E-03	0.00E+00	0.00E+00	1.52E-03	0.00E+00	1.50E-03	0.00E+00
0.50	5.25E-03	0.00E+00	0.00E+00	6.09E-04	0.00E+00	6.00E-04	0.00E+00
0.55	2.63E-03	0.00E+00	0.00E+00	*	0.00E+00	*	0.00E+00
0.60	*	0.00E+00	0.00E+00	*	0.00E+00	*	0.00E+00
0.70	0.00E+00	0.00E+00	0.00E+00	0.00E+00	0.00E+00	0.00E+00	0.00E+00
0.80	0.00E+00	0.00E+00	0.00E+00	0.00E+00	0.00E+00	0.00E+00	0.00E+00
0.90	0.00E+00	0.00E+00	0.00E+00	0.00E+00	0.00E+00	0.00E+00	0.00E+00
1.00	0.00E+00	0.00E+00	0.00E+00	0.00E+00	0.00E+00	0.00E+00	0.00E+00

* for these cases a value different than zero was computed, however, it was considered by the PEER coordinators as inappropriate for comparative purposes since there are significant differences between the values obtained by the 5 reference codes used to estimate the mean value.

Table 4-9 Annual exceedance probabilities reported as benchmarks by PEER project coordinators for Case 1, set 2

Peak Ground Acceleration (g)	Annual Exceedance Probability						
	Site 1	Site 2	Site 3	Site 4	Site 5	Site 6	Site 7
0.001	1.59E-02	1.59E-02	1.59E-02	1.59E-02	1.59E-02	1.59E-02	1.59E-02
0.01	1.59E-02	1.59E-02	1.59E-02	1.59E-02	1.59E-02	1.59E-02	1.59E-02
0.05	1.59E-02	1.59E-02	0.00E+00	1.59E-02	1.59E-02	1.59E-02	1.59E-02
0.10	1.59E-02	1.59E-02	0.00E+00	1.59E-02	1.59E-02	1.59E-02	1.59E-02
0.15	1.59E-02	1.59E-02	0.00E+00	1.59E-02	7.78E-03	1.59E-02	1.59E-02
0.20	1.59E-02	1.59E-02	0.00E+00	1.58E-02	1.60E-03	1.58E-02	1.59E-02
0.25	1.59E-02	0.00E+00	0.00E+00	1.20E-02	0.00E+00	1.20E-02	0.00E+00
0.30	1.59E-02	0.00E+00	0.00E+00	8.68E-03	0.00E+00	8.63E-03	0.00E+00
0.35	1.59E-02	0.00E+00	0.00E+00	5.74E-03	0.00E+00	5.70E-03	0.00E+00
0.40	1.17E-02	0.00E+00	0.00E+00	3.10E-03	0.00E+00	3.07E-03	0.00E+00
0.45	8.24E-03	0.00E+00	0.00E+00	1.52E-03	0.00E+00	1.50E-03	0.00E+00
0.50	5.25E-03	0.00E+00	0.00E+00	6.09E-04	0.00E+00	6.00E-04	0.00E+00
0.55	2.63E-03	0.00E+00	0.00E+00	*	0.00E+00	*	0.00E+00
0.60	*	0.00E+00	0.00E+00	*	0.00E+00	*	0.00E+00
0.70	0.00E+00	0.00E+00	0.00E+00	0.00E+00	0.00E+00	0.00E+00	0.00E+00
0.80	0.00E+00	0.00E+00	0.00E+00	0.00E+00	0.00E+00	0.00E+00	0.00E+00
0.90	0.00E+00	0.00E+00	0.00E+00	0.00E+00	0.00E+00	0.00E+00	0.00E+00
1.00	0.00E+00	0.00E+00	0.00E+00	0.00E+00	0.00E+00	0.00E+00	0.00E+00

* for these cases a value different than zero was computed, however, it was considered by the PEER coordinators as inappropriate for comparative purposes since there are significant differences between the values obtained by the 5 reference codes used to estimate the mean value.

Table 4-10 Analytical annual exceedance probabilities obtained by PEER project coordinators for Case 1, set 2

Peak Ground Acceleration (g)	Annual Exceedance Probability						
	Site 1	Site 2	Site 3	Site 4	Site 5	Site 6	Site 7
0.001	1.59E-02	1.59E-02	1.59E-02	1.59E-02	1.59E-02	1.59E-02	1.59E-02
0.01	1.59E-02	1.59E-02	1.59E-02	1.59E-02	1.59E-02	1.59E-02	1.59E-02
0.05	1.59E-02	1.59E-02	0.00E+00	1.59E-02	1.59E-02	1.59E-02	1.59E-02
0.10	1.59E-02	1.59E-02	0.00E+00	1.59E-02	1.59E-02	1.59E-02	1.59E-02
0.15	1.59E-02	1.59E-02	0.00E+00	1.59E-02	7.75E-03	1.59E-02	1.59E-02
0.20	1.59E-02	1.59E-02	0.00E+00	1.58E-02	1.60E-03	1.58E-02	1.59E-02
0.25	1.59E-02	0.00E+00	0.00E+00	1.20E-02	0.00E+00	1.20E-02	0.00E+00
0.30	1.59E-02	0.00E+00	0.00E+00	8.64E-03	0.00E+00	8.64E-03	0.00E+00
0.35	1.59E-02	0.00E+00	0.00E+00	5.73E-03	0.00E+00	5.73E-03	0.00E+00
0.40	1.17E-02	0.00E+00	0.00E+00	3.09E-03	0.00E+00	3.09E-03	0.00E+00
0.45	8.23E-03	0.00E+00	0.00E+00	1.51E-03	0.00E+00	1.51E-03	0.00E+00
0.50	5.23E-03	0.00E+00	0.00E+00	6.09E-04	0.00E+00	6.08E-04	0.00E+00
0.55	2.64E-03	0.00E+00	0.00E+00	*	0.00E+00	*	0.00E+00
0.60	*	0.00E+00	0.00E+00	*	0.00E+00	*	0.00E+00
0.70	0.00E+00	0.00E+00	0.00E+00	0.00E+00	0.00E+00	0.00E+00	0.00E+00
0.80	0.00E+00	0.00E+00	0.00E+00	0.00E+00	0.00E+00	0.00E+00	0.00E+00
0.90	0.00E+00	0.00E+00	0.00E+00	0.00E+00	0.00E+00	0.00E+00	0.00E+00
1.00	0.00E+00	0.00E+00	0.00E+00	0.00E+00	0.00E+00	0.00E+00	0.00E+00

* for these cases a value different than zero was computed, however, it was considered by the PEER coordinators as inappropriate for comparative purposes since there are significant differences between the values obtained by the 5 reference codes used to estimate the mean value.

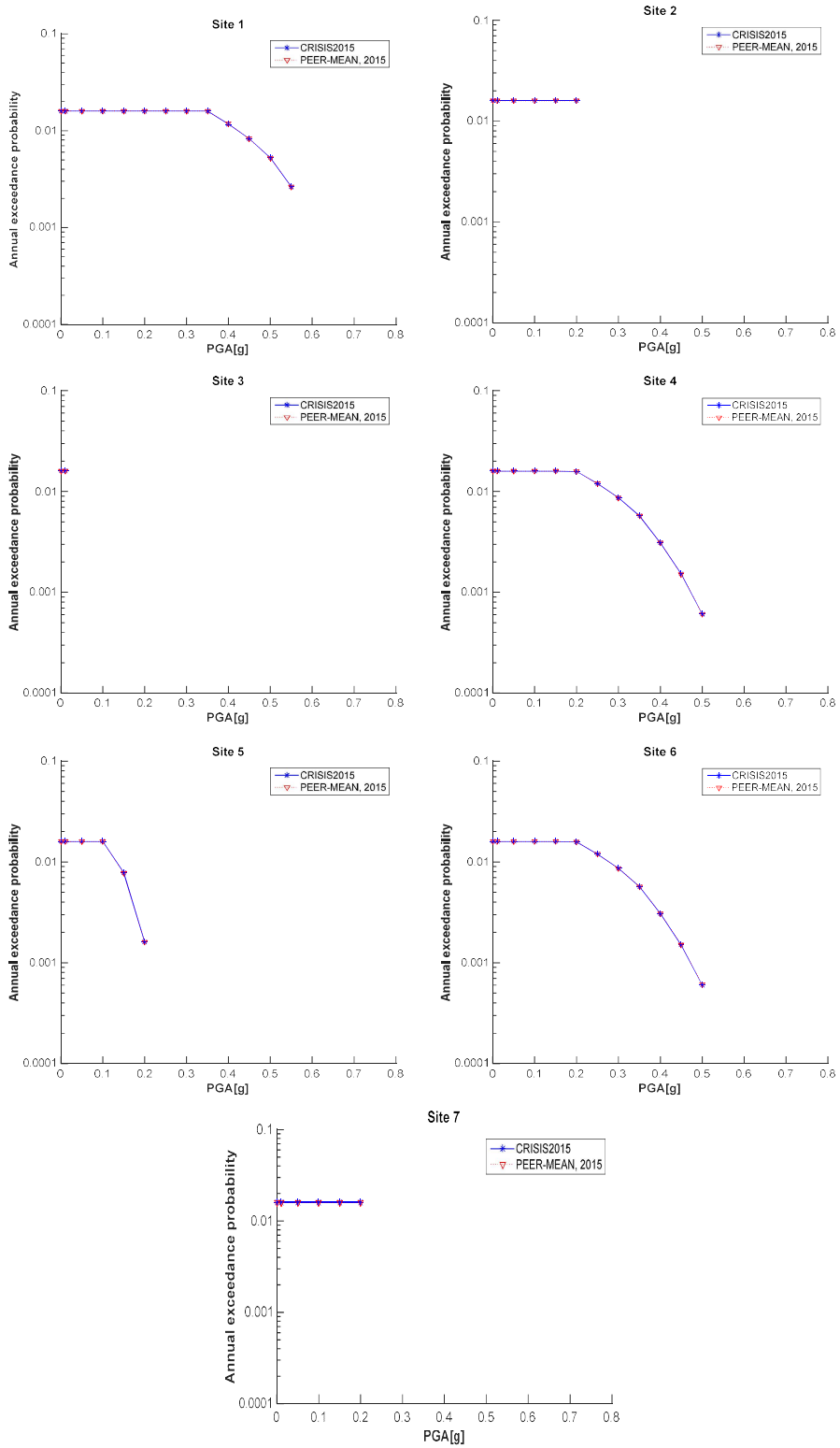

Figure 4-11 Comparison of the CRISIS and PEER-2015 results for Sites 1 to 7 (Set 1 Case 2)

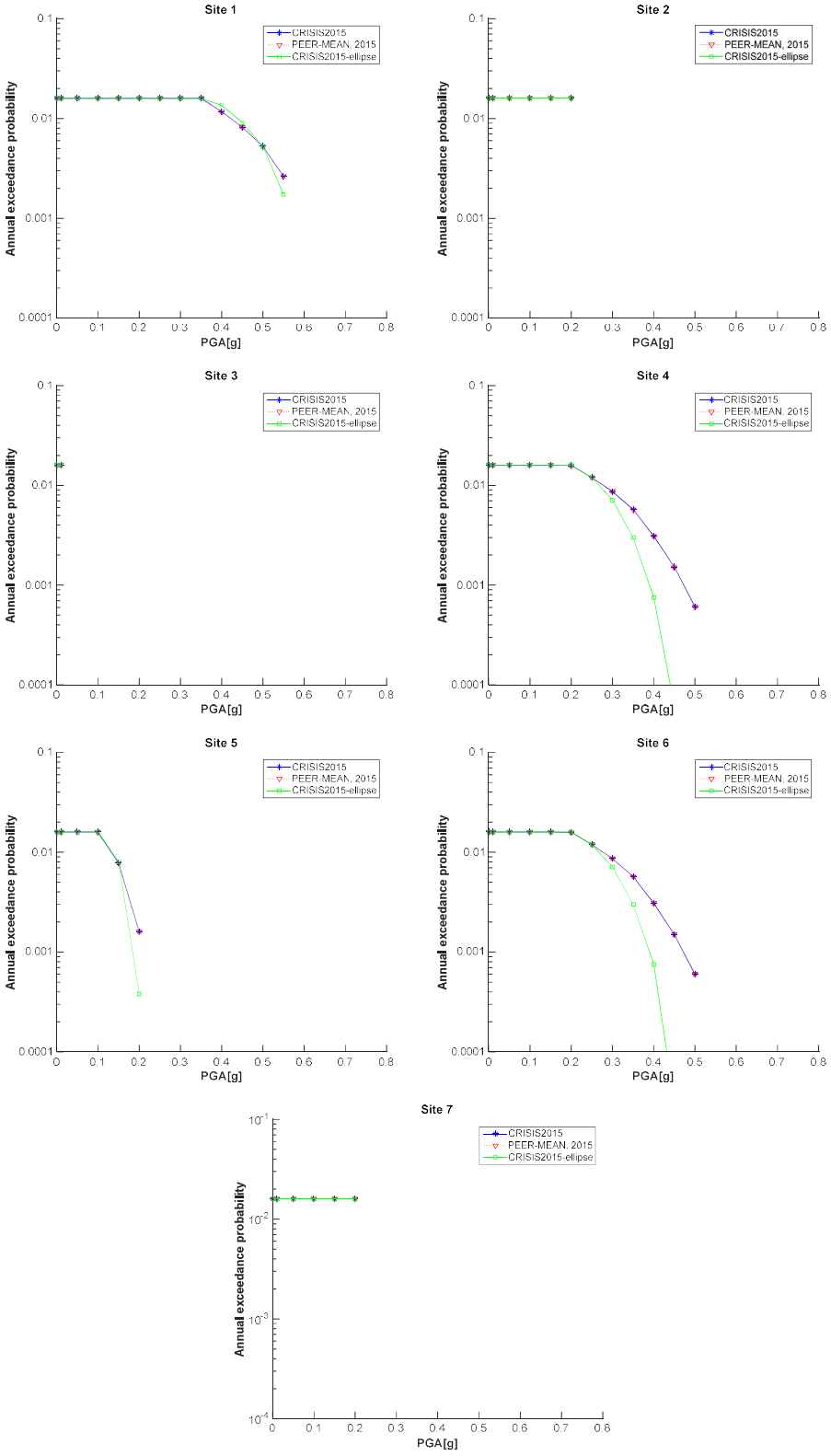

Figure 4-12 Comparison of elliptical and rectangular rupture shapes for PEER-2015 Set 1 Case 2

4.1.7 Set 1 case 3

The tests differ from case 2 due to the introduction of the variability of the rupture planes. A "sigma" is assigned to the rupture areas. This option is not yet available in R-CRISIS and thus, this test could not be carried out.

4.1.8 Set 1 case 4

Input parameters

The source used for this model corresponds to Fault 2 with a width W=12.7km [=H/sin(60°)]. The seismicity is similar to the set 1, case 2 except for the λ value that is in this case equal to 0.01698 (the area of the source is slightly different due to the depth and thus also the seismic moment rate). Table 4-11 summarizes the input data.

Table 4-11 Summary of input data for Set 1, case 4

Name	Description	Source	Mag-Density Function	Ground Motion Model[1,2]	Rupture Dimension Relationships[3,4,5,6]
Set 1 Case 4	Single rupture smaller than fault plane on dipping fault	Fault 2(reverse 60°) b-value=0.9 Slip rate=2mm/yr. The geometry and other characteristics of the source are shown in Figure 4-1	Delta function at M6.0	Sadigh et al. (1997), rock. σ = 0	$Log(A) = M - 4; \sigma_A = 0$ $Log(W) = 0.5 * M - 2.15; \sigma_W = 0$ $Log(L) = 0.5 * M - 1.85; \sigma_L = 0$

[1] Integration over magnitude zero.

[2] Use magnitude integration step size as small as necessary to model the magnitude density function.

[3] For all cases, uniform slip with tapered slip at edges.

[4] No ruptures are to extend beyond the edge of the fault plane.

[5] Aspect ratio to be maintained until maximum width is reached, then increase length (maintain area at the expense of aspect ratio).

[6] Down-dip and along strike integration step size should be as small as necessary for uniform rupture location.

Figure 4-13 shows the geometry data screen of R-CRISIS with the parameters that were used herein, whereas, Figure 4-14 shows the seismicity data screen of R-CRISIS with the assigned parameters for this particular case.

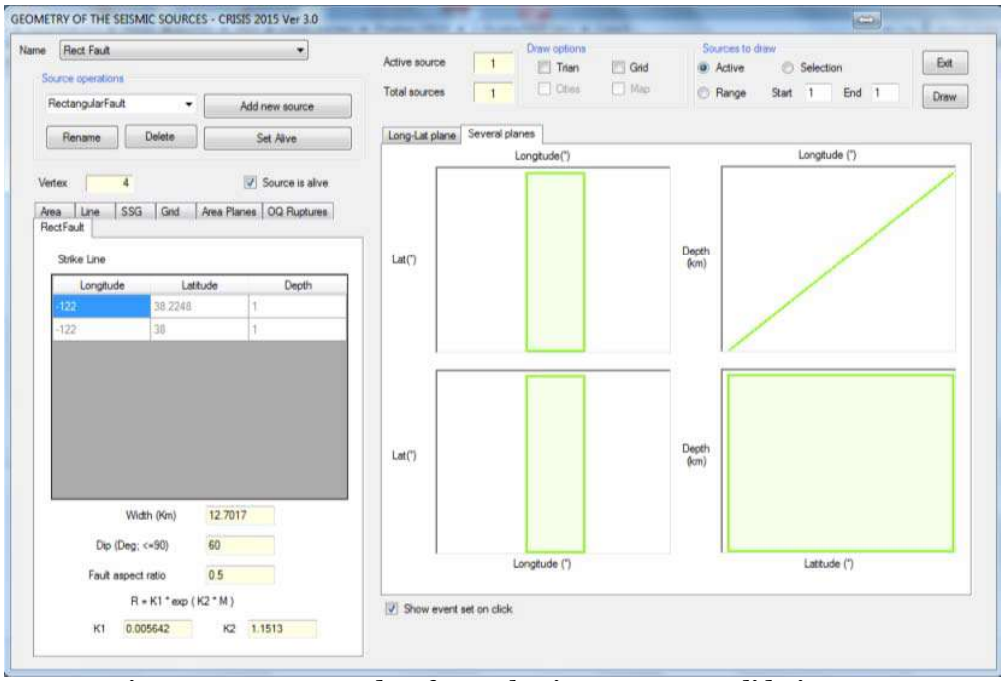

Figure 4-13 Geometry data for Fault 2 in PEER-2015 validation tests

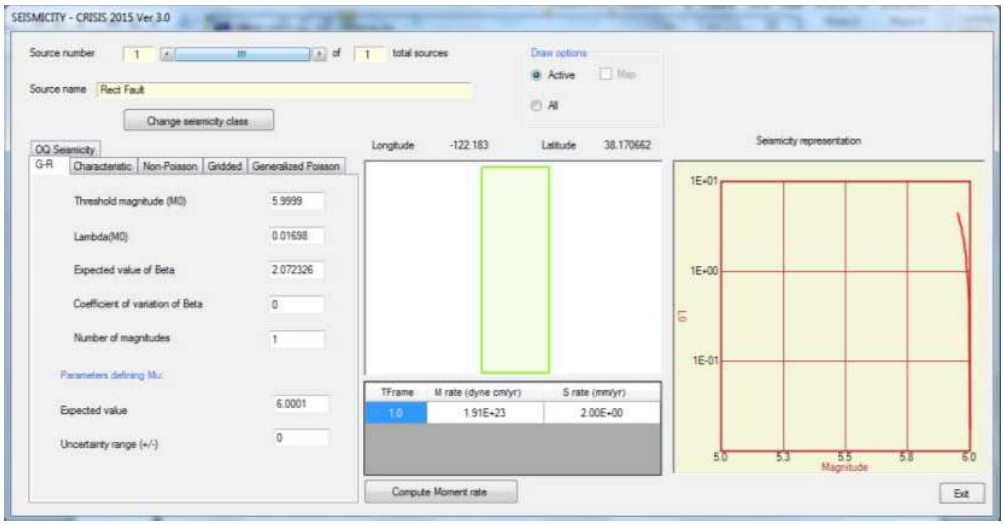

Figure 4-14 Seismicity parameters assigned in R-CRISIS for set 1, case 4

Results

Results computed in R-CRISIS for set 1, case 4 are shown in Table 4-12. Table 4-13 shows the results provided by the PEER-2015 project whereas Table 4-14 shows the analytical solution also provided by the coordinators of the PEER-2015 project. Figure 4-15 shows the hazard plots for the 7 computation sites. In all cases there is a full agreement between the results and therefore, it is possible to conclude that CRISIS fulfills all the requirements evaluated by the PEER-2015 project in Set 1-Case 4.

Figure 4-16 shows the hazard plots comparing the results obtained with R-CRISIS (elliptical and rectangular options) and the ones provided by the PEER-2015 project. Differences at computation sites 1, 4, 5 and 6 exist for exactly the same reasons explained in section 4.1.2.

Table 4-12 Annual exceedance probabilities obtained in R-CRISIS for Case 1, set 4

Peak Ground Acceleration (g)	Annual Exceedance Probability						
	Site 1	Site 2	Site 3	Site 4	Site 5	Site 6	Site 7
0.001	1.68E-02	1.68E-02	1.68E-02	1.68E-02	1.68E-02	1.68E-02	1.68E-02
0.01	1.68E-02	1.68E-02	1.68E-02	1.68E-02	1.68E-02	1.68E-02	1.68E-02
0.05	1.68E-02	1.68E-02	0.00E+00	1.68E-02	1.68E-02	1.68E-02	1.68E-02
0.10	1.68E-02	1.68E-02	0.00E+00	1.68E-02	1.68E-02	1.68E-02	1.68E-02
0.15	1.68E-02	1.68E-02	0.00E+00	1.68E-02	1.24E-02	1.68E-02	1.68E-02
0.20	1.68E-02	1.68E-02	0.00E+00	1.68E-02	5.26E-03	1.68E-02	1.66E-02
0.25	1.68E-02	1.68E-02	0.00E+00	1.57E-02	*	1.57E-02	4.37E-03
0.30	1.68E-02	0.00E+00	0.00E+00	1.18E-02	0.00E+00	1.18E-02	0.00E+00
0.35	1.68E-02	0.00E+00	0.00E+00	8.44E-03	0.00E+00	8.41E-03	0.00E+00
0.40	1.36E-02	0.00E+00	0.00E+00	5.10E-03	0.00E+00	5.07E-03	0.00E+00
0.45	1.01E-02	0.00E+00	0.00E+00	2.88E-03	0.00E+00	2.86E-03	0.00E+00
0.50	7.01E-03	0.00E+00	0.00E+00	1.48E-03	0.00E+00	1.46E-03	0.00E+00
0.55	4.37E-03	0.00E+00	0.00E+00	*	0.00E+00	6.17E-04	0.00E+00
0.60	*	0.00E+00	0.00E+00	*	0.00E+00	*	0.00E+00
0.70	0.00E+00	0.00E+00	0.00E+00	0.00E+00	0.00E+00	0.00E+00	0.00E+00
0.80	0.00E+00	0.00E+00	0.00E+00	0.00E+00	0.00E+00	0.00E+00	0.00E+00
0.90	0.00E+00	0.00E+00	0.00E+00	0.00E+00	0.00E+00	0.00E+00	0.00E+00
1.00	0.00E+00	0.00E+00	0.00E+00	0.00E+00	0.00E+00	0.00E+00	0.00E+00

* for these cases a value different than zero was computed, however, it was considered by the PEER coordinators as inappropriate for comparative purposes since there are significant differences between the values obtained by the 5 reference codes used to estimate the mean value.

Table 4-13 Annual exceedance probabilities reported as benchmarks by PEER project coordinators for Case 1, set 4

Peak Ground Acceleration (g)	Annual Exceedance Probability						
	Site 1	Site 2	Site 3	Site 4	Site 5	Site 6	Site 7
0.001	1.68E-02	1.68E-02	1.68E-02	1.68E-02	1.68E-02	1.68E-02	1.68E-02
0.01	1.68E-02	1.68E-02	1.68E-02	1.68E-02	1.68E-02	1.68E-02	1.68E-02
0.05	1.68E-02	1.68E-02	0.00E+00	1.68E-02	1.68E-02	1.68E-02	1.68E-02
0.10	1.68E-02	1.68E-02	0.00E+00	1.68E-02	1.68E-02	1.68E-02	1.68E-02
0.15	1.68E-02	1.68E-02	0.00E+00	1.68E-02	1.24E-02	1.68E-02	1.68E-02
0.20	1.68E-02	1.68E-02	0.00E+00	1.68E-02	5.24E-03	1.68E-02	1.63E-02
0.25	1.68E-02	1.68E-02	0.00E+00	1.57E-02	*	1.57E-02	4.18E-03
0.30	1.68E-02	0.00E+00	0.00E+00	1.18E-02	0.00E+00	1.18E-02	0.00E+00
0.35	1.68E-02	0.00E+00	0.00E+00	8.42E-03	0.00E+00	8.39E-03	0.00E+00
0.40	1.36E-02	0.00E+00	0.00E+00	5.09E-03	0.00E+00	5.07E-03	0.00E+00
0.45	1.01E-02	0.00E+00	0.00E+00	2.87E-03	0.00E+00	2.86E-03	0.00E+00
0.50	7.02E-03	0.00E+00	0.00E+00	1.47E-03	0.00E+00	1.47E-03	0.00E+00
0.55	4.37E-03	0.00E+00	0.00E+00	*	0.00E+00	6.25E-04	0.00E+00
0.60	*	0.00E+00	0.00E+00	*	0.00E+00	*	0.00E+00
0.70	0.00E+00	0.00E+00	0.00E+00	0.00E+00	0.00E+00	0.00E+00	0.00E+00
0.80	0.00E+00	0.00E+00	0.00E+00	0.00E+00	0.00E+00	0.00E+00	0.00E+00
0.90	0.00E+00	0.00E+00	0.00E+00	0.00E+00	0.00E+00	0.00E+00	0.00E+00
1.00	0.00E+00	0.00E+00	0.00E+00	0.00E+00	0.00E+00	0.00E+00	0.00E+00

* for these cases a value different than zero was computed, however, it was considered by the PEER coordinators as inappropriate for comparative purposes since there are significant differences between the values obtained by the 5 reference codes used to estimate the mean value.

Table 4-14 Analytical annual exceedance probabilities obtained by PEER project coordinators for Case 1, set 4

Peak Ground Acceleration (g)	Annual Exceedance Probability						
	Site 1	Site 2	Site 3	Site 4	Site 5	Site 6	Site 7
0.001	1.68E-02	1.68E-02	1.68E-02	1.68E-02	1.68E-02	1.68E-02	1.68E-02
0.01	1.68E-02	1.68E-02	1.68E-02	1.68E-02	1.68E-02	1.68E-02	1.68E-02
0.05	1.68E-02	1.68E-02	0.00E+00	1.68E-02	1.68E-02	1.68E-02	1.68E-02
0.10	1.68E-02	1.68E-02	0.00E+00	1.68E-02	1.68E-02	1.68E-02	1.68E-02
0.15	1.68E-02	1.68E-02	0.00E+00	1.68E-02	1.24E-02	1.68E-02	1.68E-02
0.20	1.68E-02	1.68E-02	0.00E+00	1.68E-02	5.25E-03	1.68E-02	1.64E-02
0.25	1.68E-02	1.68E-02	0.00E+00	1.57E-02	*	1.57E-02	4.17E-03
0.30	1.68E-02	0.00E+00	0.00E+00	1.18E-02	0.00E+00	1.18E-02	0.00E+00
0.35	1.68E-02	0.00E+00	0.00E+00	8.42E-03	0.00E+00	8.42E-03	0.00E+00
0.40	1.36E-02	0.00E+00	0.00E+00	5.09E-03	0.00E+00	5.09E-03	0.00E+00
0.45	1.01E-02	0.00E+00	0.00E+00	2.87E-03	0.00E+00	2.87E-03	0.00E+00
0.50	7.03E-03	0.00E+00	0.00E+00	1.47E-03	0.00E+00	1.47E-03	0.00E+00
0.55	4.37E-03	0.00E+00	0.00E+00	*	0.00E+00	6.26E-04	0.00E+00
0.60	*	0.00E+00	0.00E+00	*	0.00E+00	*	0.00E+00
0.70	0.00E+00	0.00E+00	0.00E+00	0.00E+00	0.00E+00	0.00E+00	0.00E+00
0.80	0.00E+00	0.00E+00	0.00E+00	0.00E+00	0.00E+00	0.00E+00	0.00E+00
0.90	0.00E+00	0.00E+00	0.00E+00	0.00E+00	0.00E+00	0.00E+00	0.00E+00
1.00	0.00E+00	0.00E+00	0.00E+00	0.00E+00	0.00E+00	0.00E+00	0.00E+00

* for these cases a value different than zero was computed, however, it was considered by the PEER coordinators as inappropriate for comparative purposes since there are significant differences between the values obtained by the 5 reference codes used to estimate the mean value.

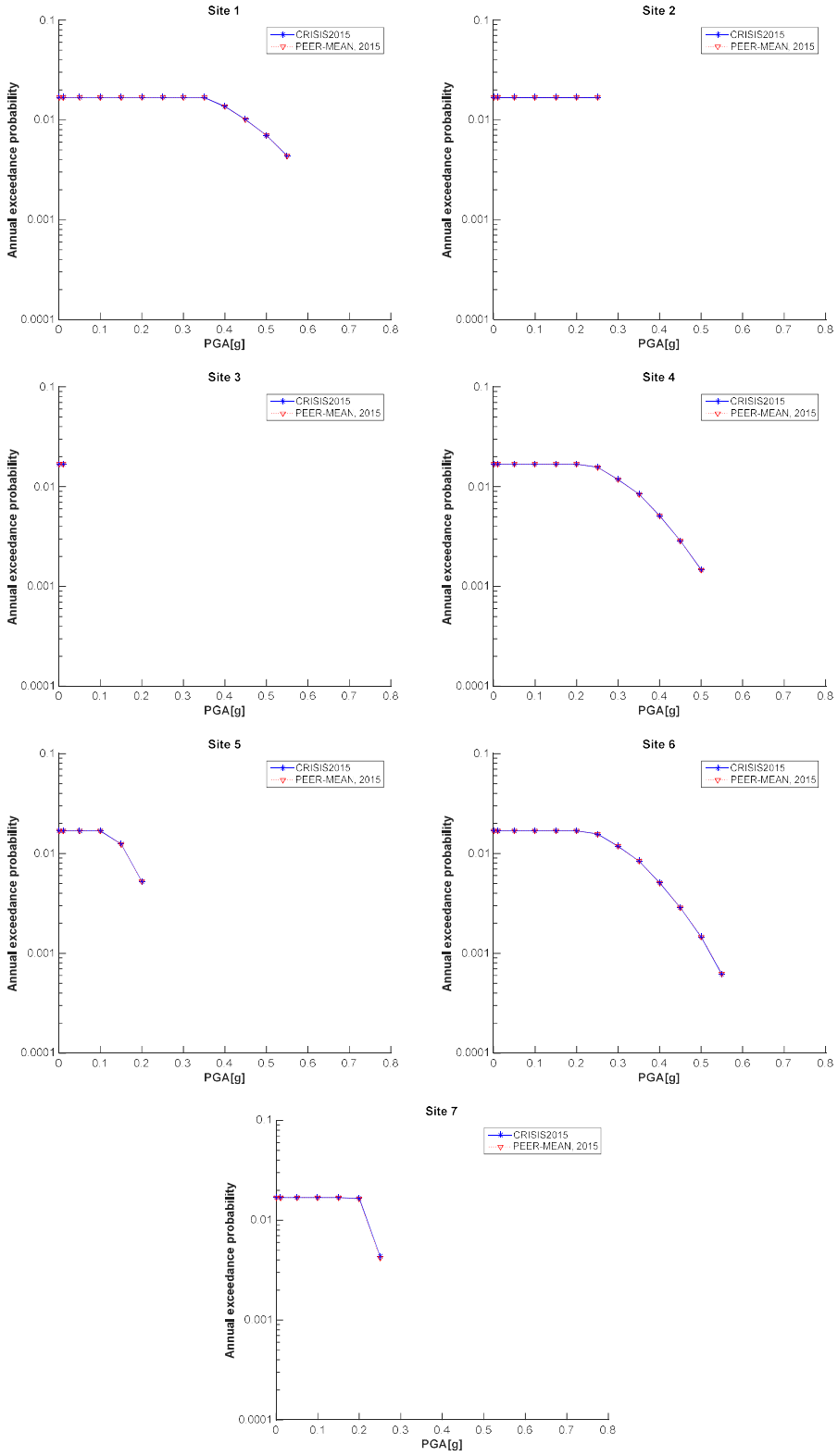

Figure 4-15 Comparison of the CRISIS and PEER-2015 results for Sites 1 to 7 (Set 1 Case 4)

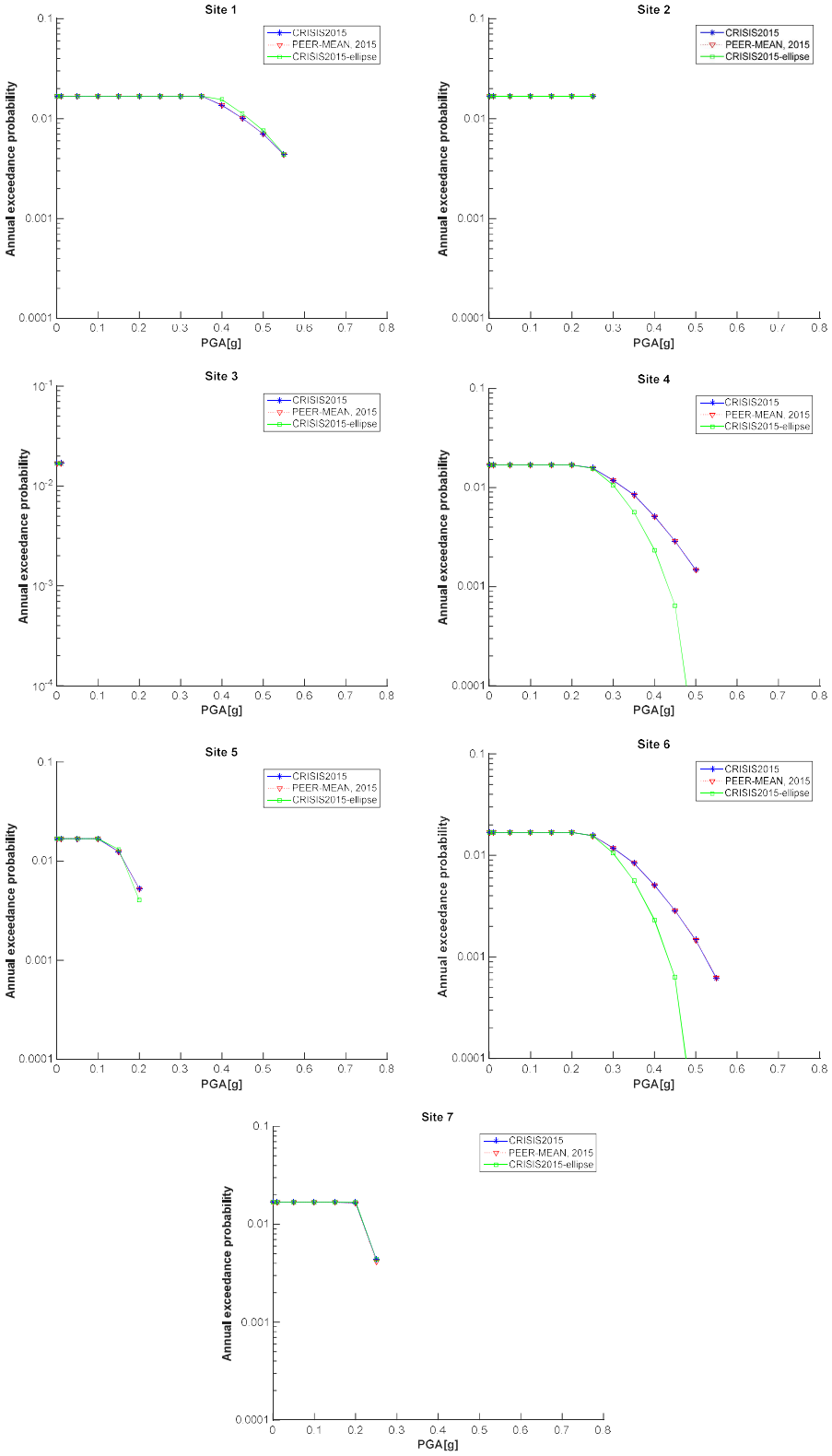

Figure 4-16 Comparison of elliptical and rectangular rupture shapes for PEER-2015 Set 1 Case 4

4.1.9 Set 1 case 5

Input parameters

The source adopted is fault 1. The seismic activity (magnitude distribution) is described by a truncated exponential model with a *b*-value=0.9, a slip rate of 2mm/yr, minimum magnitude *Mmin*=5 and maximum magnitude *Mmax*=6.5 as summarized in Table 4-15.

Table 4-15 Summary of input data for Set 1, case 5

Name	Description	Source	Mag-Density Function	Ground Motion Model[1,2]	Rupture Dimension Relationships[3,4,5,6]
Set 1 Case 5	Truncated exponential model	Fault 1(vertical SS) b-value=0.9 Slip rate=2mm/yr.	Truncated exponential model, Mmax=6.5, Mmin=5.0	Sadigh et al. (1997), rock. σ = 0	$Log(A) = M - 4; \sigma_A = 0$ $Log(W) = 0.5 * M - 2.15; \sigma_W = 0$ $Log(L) = 0.5 * M - 1.85; \sigma_L = 0$

[1] Integration over magnitude zero.
[2] Use magnitude integration step size as small as necessary to model the magnitude density function.
[3] For all cases, uniform slip with tapered slip at edges.
[4] No ruptures are to extend beyond the edge of the fault plane.
[5] Aspect ratio to be maintained until maximum width is reached, then increase length (maintain area at the expense of aspect ratio).
[6] Down-dip and along strike integration step size should be as small as necessary for uniform rupture location.

For this case, a modified G-R relation was adopted in R-CRISIS.Therefore, the seismicity rate, λ, is in this case the number of earthquakes with $M \geq 5$. The logic behind is the same as in set 1, case 1 but now, in this context, all the magnitudes between 5.0 and 6.5 are possible.

Following Youngs and Coppersmith (1985), the moment rate can be written as:

$$\dot{M}_o = \mu A \dot{s} = \int_{-\infty}^{M_{\max}} M_0(m) f(m) dm \qquad \text{(Eq. 4-6)}$$

where:

- $M_o(m)$ is given by equation 4-4.
- $f(m)$ is the probability density function of magnitude, that in the case of a truncated exponential is:

$$f(m) = \frac{\lambda\beta \exp(-\beta(m - M_{\min}))}{1 - \exp(-\beta(M_{\max} - M_{\min}))} \qquad \text{(Eq. 4-7)}$$

where $\beta = \ln(10) * b$

Hence, equation 4-6 becomes:

$$\dot{M}_o = \mu A \dot{s} = \frac{\lambda\beta \exp(-\beta(m - M_{\min})) \times M_o(M_{\max})}{\left[1 - \exp(-\beta(M_{\max} - M_{\min}))\right](1.5 - b)} \qquad \text{(Eq. 4-8)}$$

Solving equation 4-8 with respect to the unknown λ, gives λ_5=0.0407. Figure 4-17 shows the seismicity data screen of R-CRISIS for this case.

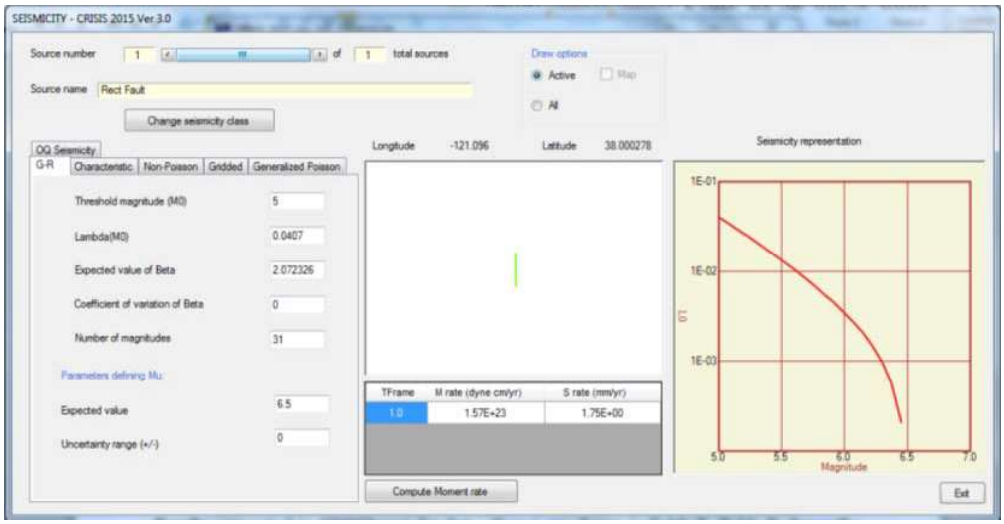

Figure 4-17 Seismicity parameters assigned in R-CRISIS for set 1, case 5

Results

Results computed in R-CRISIS for case 1, set 5 are shown in Table 4-16. Table 4-17 shows the results provided by the PEER-2015 project whereas Table 4-18 shows the analytical solution also provided by the coordinators of the PEER-2015 project. Figure 4.18 shows the hazard plots for the 7 computation sites. In all cases there is a full agreement between the results and therefore, it is possible to conclude that CRISIS fulfills all the requirements evaluated by the PEER-2015 project in Set 1-Case 5.

Figure X shows the hazard plots comparing the results obtained with R-CRISIS (elliptical and rectangular options) and the ones provided by the PEER-2015 project. Differences at computation sites 1, 4, 5 and 6 exist for exactly the same reasons explained before.

Table 4-16 Annual exceedance probabilities obtained in R-CRISIS for Case 1, set 5

Peak Ground Acceleration (g)	Annual Exceedance Probability						
	Site 1	Site 2	Site 3	Site 4	Site 5	Site 6	Site 7
0.001	3.99E-02	3.99E-02	3.99E-02	3.99E-02	3.99E-02	3.99E-02	3.99E-02
0.01	3.99E-02	3.99E-02	3.99E-02	3.99E-02	3.99E-02	3.99E-02	3.99E-02
0.05	3.99E-02	3.99E-02	0.00E+00	3.98E-02	3.14E-02	3.98E-02	3.99E-02
0.10	3.98E-02	3.35E-02	0.00E+00	2.99E-02	1.21E-02	2.99E-02	3.35E-02
0.15	3.49E-02	1.23E-02	0.00E+00	2.00E-02	4.41E-03	2.00E-02	1.23E-02
0.20	2.62E-02	4.90E-03	0.00E+00	1.30E-02	1.89E-03	1.30E-02	4.90E-03
0.25	1.91E-02	1.80E-03	0.00E+00	8.59E-03	7.53E-04	8.56E-03	1.80E-03
0.30	1.38E-02	*	0.00E+00	5.74E-03	*	5.71E-03	*
0.35	9.78E-03	0.00E+00	0.00E+00	3.89E-03	0.00E+00	3.87 E-03	0.00E+00
0.40	6.80E-03	0.00E+00	0.00E+00	2.69E-03	0.00E+00	2.68E-03	0.00E+00
0.45	4.74E-03	0.00E+00	0.00E+00	1.92E-03	0.00E+00	1.91E-03	0.00E+00
0.50	3.29E-03	0.00E+00	0.00E+00	1.37 E-03	0.00E+00	1.37 E-03	0.00E+00
0.55	2.24E-03	0.00E+00	0.00E+00	9.72E-04	0.00E+00	9.65E-04	0.00E+00
0.60	1.47 E-03	0.00E+00	0.00E+00	6.84E-04	0.00E+00	6.75E-04	0.00E+00
0.70	*	0.00E+00	0.00E+00	*	0.00E+00	*	0.00E+00
0.80	0.00E+00	0.00E+00	0.00E+00	0.00E+00	0.00E+00	0.00E+00	0.00E+00
0.90	0.00E+00	0.00E+00	0.00E+00	0.00E+00	0.00E+00	0.00E+00	0.00E+00
1.00	0.00E+00	0.00E+00	0.00E+00	0.00E+00	0.00E+00	0.00E+00	0.00E+00

* for these cases a value different than zero was computed, however, it was considered by the PEER coordinators as inappropriate for comparative purposes since there are significant differences between the values obtained by the 5 reference codes used to estimate the mean value.

Table 4-17 Annual exceedance probabilities reported as benchmarks by PEER project coordinators for Case 1, set 5

Peak Ground Acceleration (g)	Annual Exceedance Probability						
	Site 1	Site 2	Site 3	Site 4	Site 5	Site 6	Site 7
0.001	3.99E-02	3.99E-02	3.99E-02	3.99E-02	3.99E-02	3.99E-02	3.99E-02
0.01	3.99E-02	3.99E-02	3.99E-02	3.99E-02	3.99E-02	3.99E-02	3.99E-02
0.05	3.99E-02	3.99E-02	0.00E+00	3.98E-02	3.14E-02	3.98E-02	3.99E-02
0.10	3.98E-02	3.34E-02	0.00E+00	2.98E-02	1.21E-02	2.99E-02	3.34E-02
0.15	3.48E-02	1.23E-02	0.00E+00	2.00E-02	4.41E-03	2.00E-02	1.23E-02
0.20	2.62E-02	4.87 E-03	0.00E+00	1.30E-02	1.89E-03	1.30E-02	4.87 E-03
0.25	1.91E-02	1.78E-03	0.00E+00	8.58E-03	7.53E-04	8.58E-03	1.78E-03
0.30	1.37 E-02	*	0.00E+00	5.73E-03	*	5.73E-03	*
0.35	9.77 E-03	0.00E+00	0.00E+00	3.88E-03	0.00E+00	3.88E-03	0.00E+00
0.40	6.80E-03	0.00E+00	0.00E+00	2.69E-03	0.00E+00	2.69E-03	0.00E+00
0.45	4.74E-03	0.00E+00	0.00E+00	1.91E-03	0.00E+00	1.91E-03	0.00E+00
0.50	3.29E-03	0.00E+00	0.00E+00	1.36E-03	0.00E+00	1.37 E-03	0.00E+00
0.55	2.24E-03	0.00E+00	0.00E+00	9.70E-04	0.00E+00	9.70E-04	0.00E+00
0.60	1.47 E-03	0.00E+00	0.00E+00	6.71E-04	0.00E+00	6.73E-04	0.00E+00
0.70	*	0.00E+00	0.00E+00	*	0.00E+00	*	0.00E+00
0.80	0.00E+00	0.00E+00	0.00E+00	0.00E+00	0.00E+00	0.00E+00	0.00E+00
0.90	0.00E+00	0.00E+00	0.00E+00	0.00E+00	0.00E+00	0.00E+00	0.00E+00
1.00	0.00E+00	0.00E+00	0.00E+00	0.00E+00	0.00E+00	0.00E+00	0.00E+00

* for these cases a value different than zero was computed, however, it was considered by the PEER coordinators as inappropriate for comparative purposes since there are significant differences between the values obtained by the 5 reference codes used to estimate the mean value.

Table 4-18 Analytical annual exceedance probabilities obtained by PEER project coordinators for Case 1, set 5

Peak Ground Acceleration (g)	Annual Exceedance Probability						
	Site 1	Site 2	Site 3	Site 4	Site 5	Site 6	Site 7
0.001	3.99E-02	3.99E-02	3.99E-02	3.99E-02	3.99E-02	3.99E-02	3.99E-02
0.01	3.99E-02	3.99E-02	3.99E-02	3.99E-02	3.99E-02	3.99E-02	3.99E-02
0.05	3.99E-02	3.99E-02	0.00E+00	3.98E-02	3.14E-02	3.98E-02	3.99E-02
0.10	3.98E-02	3.33E-02	0.00E+00	2.99E-02	1.21E-02	2.99E-02	3.33E-02
0.15	3.49E-02	1.23E-02	0.00E+00	2.00E-02	4.41E-03	2.00E-02	1.23E-02
0.20	2.62E-02	4.85E-03	0.00E+00	1.30E-02	1.89E-03	1.30E-02	4.85E-03
0.25	1.91E-02	1.76E-03	0.00E+00	8.57E-03	7.52E-04	8.57E-03	1.76E-03
0.30	1.37E-02	*	0.00E+00	5.72E-03	*	5.72E-03	*
0.35	9.76E-03	0.00E+00	0.00E+00	3.88E-03	0.00E+00	3.87E-03	0.00E+00
0.40	6.79E-03	0.00E+00	0.00E+00	2.69E-03	0.00E+00	2.69E-03	0.00E+00
0.45	4.73E-03	0.00E+00	0.00E+00	1.91E-03	0.00E+00	1.91E-03	0.00E+00
0.50	3.28E-03	0.00E+00	0.00E+00	1.37E-03	0.00E+00	1.37E-03	0.00E+00
0.55	2.23E-03	0.00E+00	0.00E+00	9.72E-04	0.00E+00	9.72E-04	0.00E+00
0.60	1.47E-03	0.00E+00	0.00E+00	6.73E-04	0.00E+00	6.73E-04	0.00E+00
0.70	*	0.00E+00	0.00E+00	*	0.00E+00	*	0.00E+00
0.80	0.00E+00	0.00E+00	0.00E+00	0.00E+00	0.00E+00	0.00E+00	0.00E+00
0.90	0.00E+00	0.00E+00	0.00E+00	0.00E+00	0.00E+00	0.00E+00	0.00E+00
1.00	0.00E+00	0.00E+00	0.00E+00	0.00E+00	0.00E+00	0.00E+00	0.00E+00

* for these cases a value different than zero was computed, however, it was considered by the PEER coordinators as inappropriate for comparative purposes since there are significant differences between the values obtained by the 5 reference codes used to estimate the mean value.

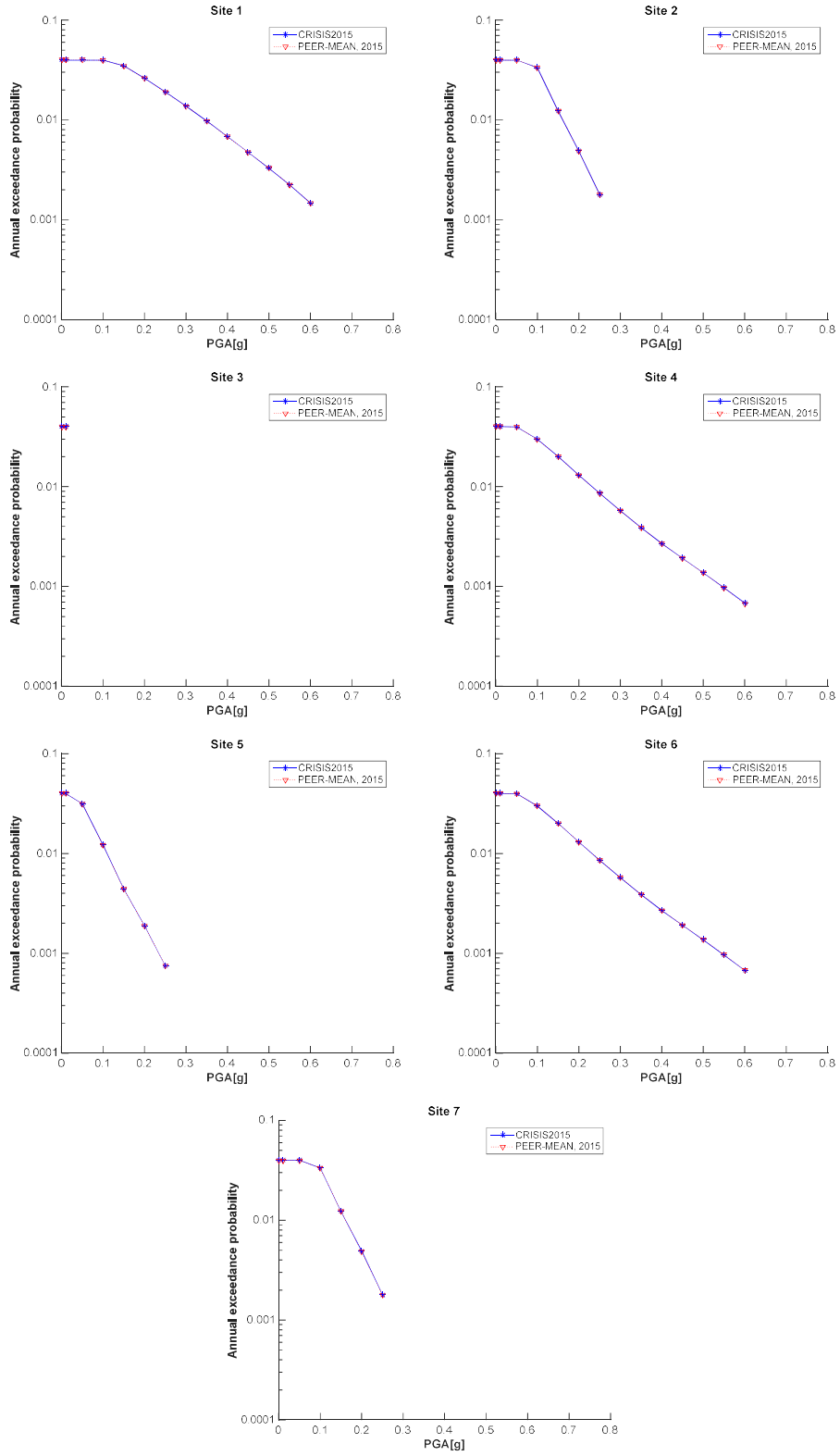

Figure 4-18 Comparison of the CRISIS and PEER-2015 results for Sites 1 to 7 (Set 1 Case 5)

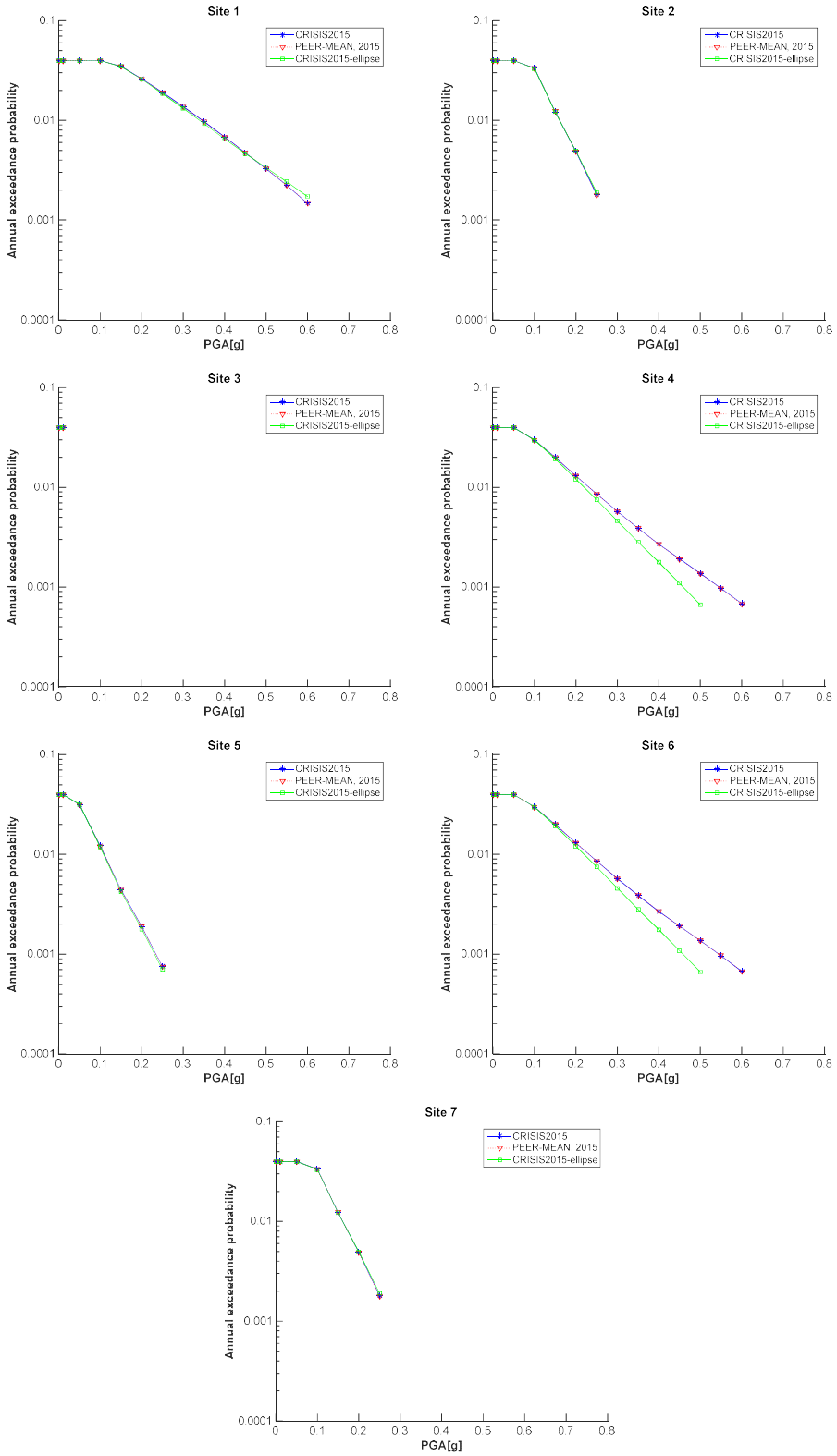

Figure 4-19 Comparison of elliptical and rectangular rupture shapes for PEER-2015 Set 1 Case 5

4.1.10 Set 1 case 6

Input parameters

The source adopted is Fault 1. The seismicity is described by a characteristic model with a truncated normal distribution with a *b*-value=0.9, a slip rate of 2mm/yr, Mmin=5, Mmax=6.5, a characteristic magnitude Mch=6.2 and a sigma σM=0.25. Table 4-19 summarizes the input parameters.

Table 4-19 Summary of input data for Set 1, case 6

Name	Description	Source	Mag-Density Function	Ground Motion Model[1,2]	Rupture Dimension Relationships[3,4,5,6]
Set 1 Case 6	Truncated normal model	Fault 1(vertical SS) b-value=0.9 Slip rate=2mm/yr.	Truncated normal model, Mmax=6.5, Mmin=5.0, Mchar=6.2, σ=0.25	Sadigh et al. (1997), rock. σ = 0	$Log(A) = M - 4; \sigma_A = 0$ $Log(W) = 0.5 * M - 2.15; \sigma_W = 0$ $Log(L) = 0.5 * M - 1.85; \sigma_L = 0$

[1] Integration over magnitude zero.
[2] Use magnitude integration step size as small as necessary to model the magnitude density function.
[3] For all cases, uniform slip with tapered slip at edges.
[4] No ruptures are to extend beyond the edge of the fault plane.
[5] Aspect ratio to be maintained until maximum width is reached, then increase length (maintain area at the expense of aspect ratio).
[6] Down-dip and along strike integration step size should be as small as necessary for uniform rupture location.

Using the same approach as the one explained in set 1, case 7 with the provided data, the mean recurrence time between earthquakes was obtained and the characteristic earthquake seismicity model was used in R-CRISIS. According to the provided data, the mean recurrence time between characteristic earthquakes is 129 years. Figure 4-20 shows the seismicity data screen (now for the characteristic earthquake model) of R-CRISIS.

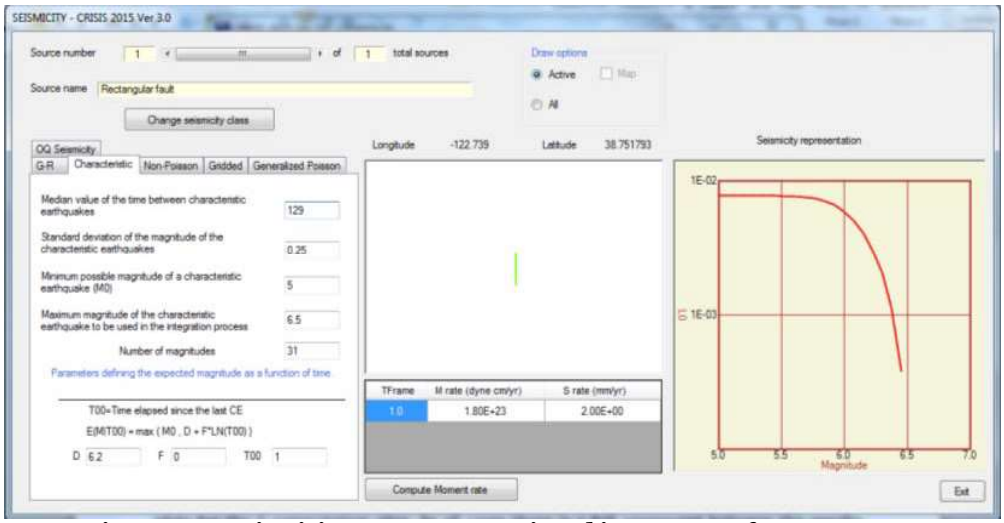

Figure 4-20 Seismicity parameters assigned in R-CRISIS for set 1, case 6

Results

Results computed in R-CRISIS for set 1, case 6 are shown in Table 4-20. Table 4-21 shows the results provided by the PEER-2015 project whereas Table 4-22 shows the analytical solution also provided by the coordinators of the PEER-2015 project. Figure 4-21 shows the hazard plots for the 7 computation sites. In all cases there is a full agreement between the results and therefore, it is possible to conclude that CRISIS fulfills all the requirements evaluated by the PEER-2015 project in Set 1-Case 6.

Figure 4-22 shows the hazard plots comparing the results obtained with R-CRISIS (elliptical and rectangular options) and the ones provided by the PEER-2015 project. Differences at computation sites 1, 4, 5 and 6 exist for exactly the same reasons explained in section 4.1.2.

Table 4-20 Annual exceedance probabilities obtained in R-CRISIS for Case 1, set 6

Peak Ground Acceleration (g)	Annual Exceedance Probability						
	Site 1	Site 2	Site 3	Site 4	Site 5	Site 6	Site 7
0.001	7.72E-03	7.72E-03	7.72E-03	7.72E-03	7.72E-03	7.72E-03	7.72E-03
0.01	7.72E-03	7.72E-03	7.72E-03	7.72E-03	7.72E-03	7.72E-03	7.72E-03
0.05	7.72E-03	7.72E-03	0.00E+00	7.72E-03	7.72E-03	7.72E-03	7.72E-03
0.10	7.72E-03	7.72E-03	0.00E+00	7.72E-03	7.35E-03	7.72E-03	7.72E-03
0.15	7.72E-03	7.67E-03	0.00E+00	7.62E-03	5.79E-03	7.62E-03	7.67E-03
0.20	7.72E-03	6.77E-03	0.00E+00	7.29E-03	3.54E-03	7.28E-03	6.77E-03
0.25	7.67E-03	3.65E-03	0.00E+00	6.72E-03	1.52E-03	6.71E-03	3.65E-03
0.30	7.52E-03	*	0.00E+00	5.98E-03	*	5.96E-03	*
0.35	7.20E-03	0.00E+00	0.00E+00	5.14E-03	0.00E+00	5.13E-03	0.00E+00
0.40	6.67E-03	0.00E+00	0.00E+00	4.27E-03	0.00E+00	4.25E-03	0.00E+00
0.45	5.92E-03	0.00E+00	0.00E+00	3.44E-03	0.00E+00	3.42E-03	0.00E+00
0.50	5.04E-03	0.00E+00	0.00E+00	2.64E-03	0.00E+00	2.63E-03	0.00E+00
0.55	3.99E-03	0.00E+00	0.00E+00	1.94E-03	0.00E+00	1.92E-03	0.00E+00
0.60	2.91E-03	0.00E+00	0.00E+00	1.37E-03	0.00E+00	1.35E-03	0.00E+00
0.70	*	0.00E+00	0.00E+00	*	0.00E+00	*	0.00E+00
0.80	0.00E+00	0.00E+00	0.00E+00	0.00E+00	0.00E+00	0.00E+00	0.00E+00
0.90	0.00E+00	0.00E+00	0.00E+00	0.00E+00	0.00E+00	0.00E+00	0.00E+00
1.00	0.00E+00	0.00E+00	0.00E+00	0.00E+00	0.00E+00	0.00E+00	0.00E+00

* for these cases a value different than zero was computed, however, it was considered by the PEER coordinators as inappropriate for comparative purposes since there are significant differences between the values obtained by the 5 reference codes used to estimate the mean value.

Table 4-21 Annual exceedance probabilities reported as benchmarks by PEER project coordinators for Case 1, set 6

Peak Ground Acceleration (g)	Annual Exceedance Probability						
	Site 1	Site 2	Site 3	Site 4	Site 5	Site 6	Site 7
0.001	7.73E-03	7.73E-03	7.73E-03	7.73E-03	7.73E-03	7.73E-03	7.73E-03
0.01	7.73E-03	7.73E-03	7.73E-03	7.73E-03	7.73E-03	7.73E-03	7.73E-03
0.05	7.73E-03	7.73E-03	0.00E+00	7.73E-03	7.73E-03	7.73E-03	7.73E-03
0.10	7.73E-03	7.73E-03	0.00E+00	7.72E-03	7.35E-03	7.72E-03	7.73E-03
0.15	7.73E-03	7.68E-03	0.00E+00	7.62E-03	5.79E-03	7.62E-03	7.68E-03
0.20	7.72E-03	6.77E-03	0.00E+00	7.28E-03	3.55E-03	7.28E-03	6.77E-03
0.25	7.68E-03	3.63E-03	0.00E+00	6.71E-03	1.52E-03	6.71E-03	3.65E-03
0.30	7.53E-03	*	0.00E+00	5.96E-03	*	5.96E-03	*
0.35	7.20E-03	0.00E+00	0.00E+00	5.12E-03	0.00E+00	5.12E-03	0.00E+00
0.40	6.66E-03	0.00E+00	0.00E+00	4.25E-03	0.00E+00	4.25E-03	0.00E+00
0.45	5.93E-03	0.00E+00	0.00E+00	3.41E-03	0.00E+00	3.41E-03	0.00E+00
0.50	5.03E-03	0.00E+00	0.00E+00	2.63E-03	0.00E+00	2.63E-03	0.00E+00
0.55	4.00E-03	0.00E+00	0.00E+00	1.93E-03	0.00E+00	1.93E-03	0.00E+00
0.60	2.92E-03	0.00E+00	0.00E+00	1.34E-03	0.00E+00	1.34E-03	0.00E+00
0.70	*	0.00E+00	0.00E+00	*	0.00E+00	*	0.00E+00
0.80	0.00E+00	0.00E+00	0.00E+00	0.00E+00	0.00E+00	0.00E+00	0.00E+00
0.90	0.00E+00	0.00E+00	0.00E+00	0.00E+00	0.00E+00	0.00E+00	0.00E+00
1.00	0.00E+00	0.00E+00	0.00E+00	0.00E+00	0.00E+00	0.00E+00	0.00E+00

* for these cases a value different than zero was computed, however, it was considered by the PEER coordinators as inappropriate for comparative purposes since there are significant differences between the values obtained by the 5 reference codes used to estimate the mean value.

Table 4-22 Analytical annual exceedance probabilities obtained by PEER project coordinators for Case 1, set 6

Peak Ground Acceleration (g)	Annual Exceedance Probability						
	Site 1	Site 2	Site 3	Site 4	Site 5	Site 6	Site 7
0.001	**	**	**	7.75E-03	7.75E-03	7.75E-03	**
0.01	**	**	**	7.75E-03	7.75E-03	7.75E-03	**
0.05	**	**	**	7.75E-03	7.75E-03	7.75E-03	**
0.10	**	**	**	7.74E-03	7.37E-03	7.74E-03	**
0.15	**	**	**	7.64E-03	5.81E-03	7.64E-03	**
0.20	**	**	**	7.31E-03	3.57E-03	7.31E-03	**
0.25	**	**	**	6.73E-03	1.52E-03	6.73E-03	**
0.30	**	**	**	5.99E-03	*	5.99E-03	**
0.35	**	**	**	**	**	**	**
0.40	**	**	**	4.27E-03	**	4.27E-03	**
0.45	**	**	**	**	**	**	**
0.50	**	**	**	2.64E-03	**	2.64E-03	**
0.55	**	**	**	**	**	**	**
0.60	**	**	**	1.35E-03	**	1.35E-03	**
0.70	**	**	**	*	**	*	**
0.80	**	**	**	**	**	**	**
0.90	**	**	**	**	**	**	**
1.00	**	**	**	**	**	**	**

* for these cases a value different than zero was computed, however, it was considered by the PEER coordinators as inappropriate for comparative purposes since there are significant differences between the values obtained by the 5 reference codes used to estimate the mean value.
** There are no data available for these cases

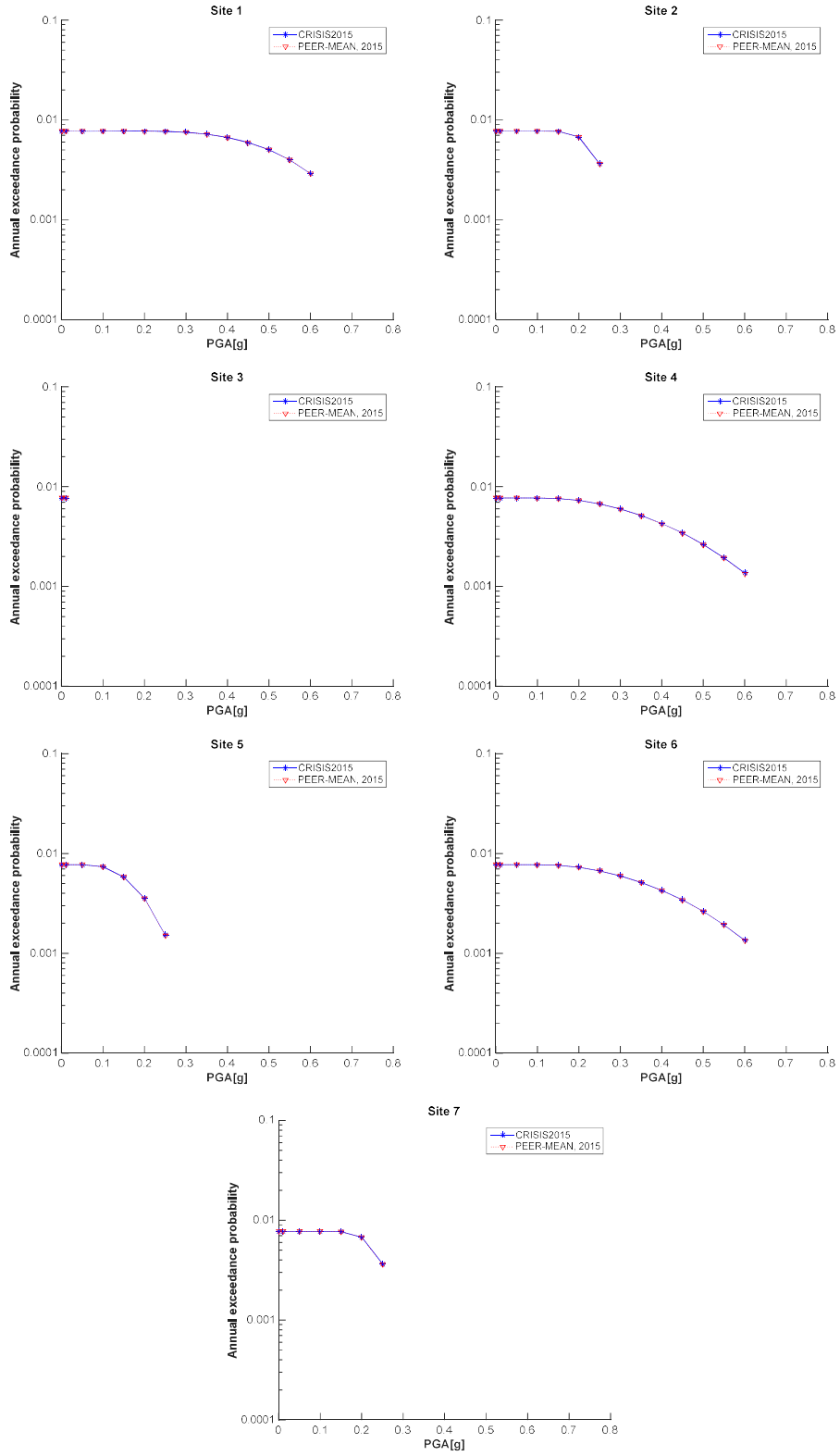

Figure 4-21 Comparison of the CRISIS and PEER-2015 results for Sites 1 to 7 (Set 1 Case 6)

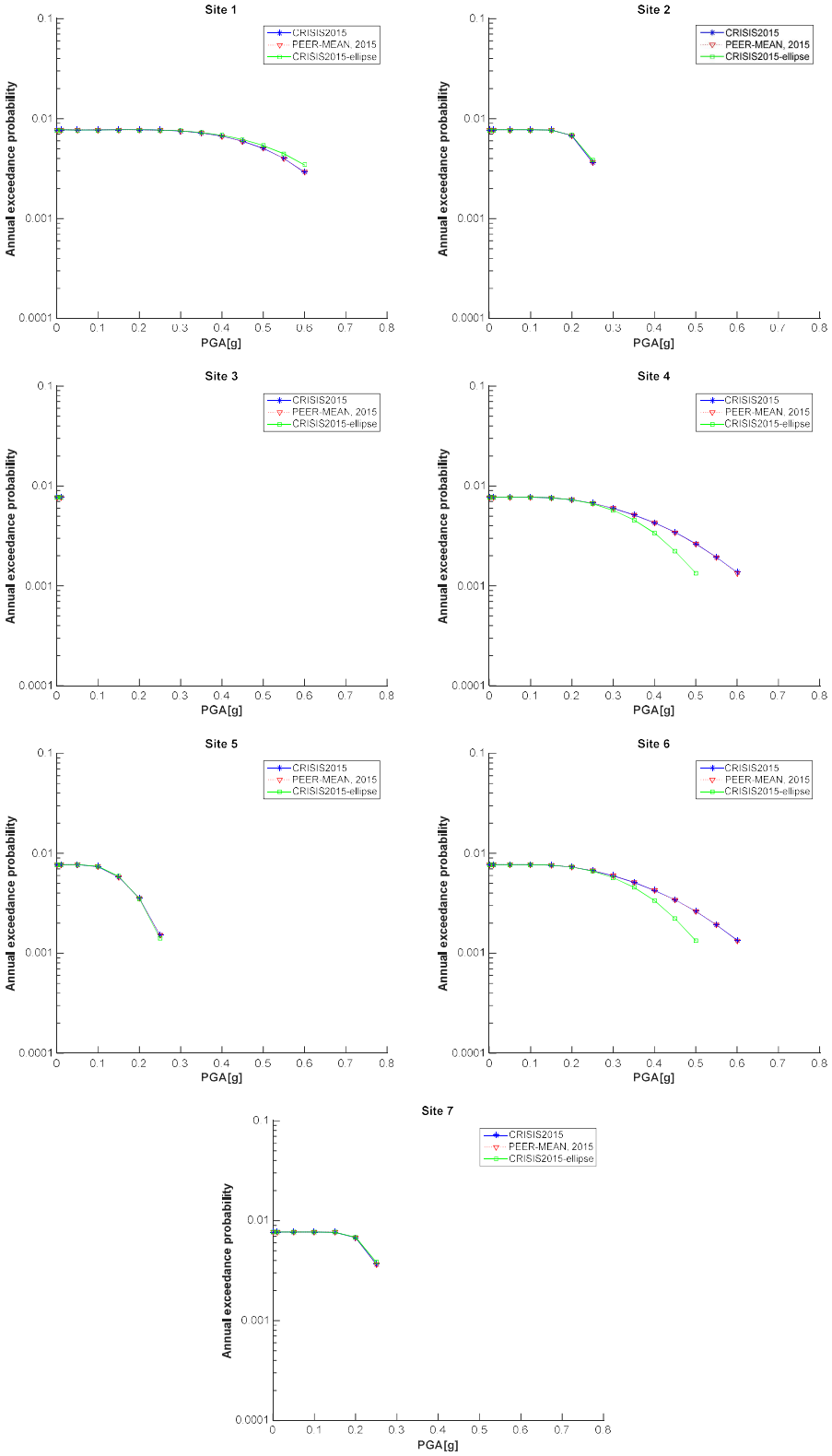

Figure 4-22 Comparison of elliptical and rectangular rupture shapes for PEER-2015 Set 1 Case 6

4.1.11 Set 1 case 7

Input parameters

The source adopted is fault 1 and Table 4-23 shows the seismicity input data provided for this case.

Table 4-23 Summary of input data for Set 1, case 7

Name	Description	Source	Mag-Density Function	Ground Motion Model[1,2]	Rupture Dimension Relationships[3,4,5,6]
Set 1 Case 7	Characteristic model (Youngs and Coppersmith, 1985)	Fault 1(vertical SS) b-value=0.9 Slip rate=2mm/yr.	Truncated normal model, Mmax=6.5, Mmin=5.0, Mchar=6.2, σ=0.25	Sadigh et al. (1997), rock. σ = 0	$Log(A) = M - 4; \sigma_A = 0$ $Log(W) = 0.5 * M - 2.15; \sigma_W = 0$ $Log(L) = 0.5 * M - 1.85; \sigma_L = 0$

[1] Integration over magnitude zero.
[2] Use magnitude integration step size as small as necessary to model the magnitude density function.
[3] For all cases, uniform slip with tapered slip at edges.
[4] No ruptures are to extend beyond the edge of the fault plane.
[5] Aspect ratio to be maintained until maximum width is reached, then increase length (maintain area at the expense of aspect ratio).
[6] Down-dip and along strike integration step size should be as small as necessary for uniform rupture location.

The seismicity for this case is described in R-CRISIS by means of the Youngs and Coppersmith (1985) characteristic model. That is:

- For low magnitude a G-R relation is assumed (between 5 and M_{max}^{GR})
- For hither magnitude a uniform density function describes the seismicity with the characteristic magnitude M_{CH}=6.2 and σM=0.25.

The probability density function is:

$$f(m) = f_1(m) + f_2(m) \quad \text{(Eq. 4-9)}$$

with:

$$f_1(m) = \frac{(\dot{N}(M_{\min}) - \dot{N}(M_{ch})) \cdot \beta \exp(-\beta(m - M_{\min}))}{1 - \exp(-\beta(M_{\max}^{GR} - M_{\min}))}, M_{\min} \le m \le M_{\max}^{GR} \quad \text{(Eq. 4-10)}$$

$$f_2(m) = \dot{n}(M_{ch}), M_{ch} - \frac{\Delta M_{ch}}{2} \le m \le M_{ch} + \frac{\Delta M_{ch}}{2} \quad \text{(Eq. 4-11)}$$

Where the term λ^{GR}=($N(M_{min})$-N(M_{CH})) represents the rate of the non-characteristic, exponentially distributed earthquakes on the fault and n(M_{CH}) is the rate density of the flat portion.

The two parameters needed for the description of the seismicity are the annual seismic rate λ and the mean recurrence time between characteristic earthquakes (T_{mean}). Following the original model of Youngs and Coppersmith (1985), we assume that:

1. Events of any magnitude are possible. this leads to $M_{max}^{GR} = M_{CH} - \Delta M_{ch}$=5.95, where M_{max}=6.45 (from PEER) and ΔM_{ch}=0.25x2=0.5. Thus, a uniform distribution is adopted between 5.95 and 6.45.
2. $n(M_{CH}) \approx n(M_{max}^{GR} - 1)$

replacing equation 4-9 in equation 4-6 and solving the integral one obtains:

$$\dot{M}_o = \mu A \dot{s} = \frac{\lambda^{GR} b \exp(-\beta(M_{\max}{}^{GR} - M_{\min}) \times M_o(M_{\max}{}^{GR})}{\left[1-\exp(-\beta(M_{\max}{}^{GR} - M_{\min})\right](1.5-b)} + \frac{\dot{N}(M_{ch}) M_o(M_{\max})(1-10^{-1.5\Delta M_{ch}})}{c \ln(10) \Delta M_{ch}} \qquad \text{(Eq. 4-12)}$$

The input values are the b-value=0.9 and the slip rate of 2 mm/yr. Hence, with hypotheses 1 and 2, λ^{GR}=0.0048 and T_{mean}=157 yr. Figures 4-23 and 4-24 show the seismicity screens of R-CRISIS for the modified G-R and the characteristic earthquake seismicity models, respectively.

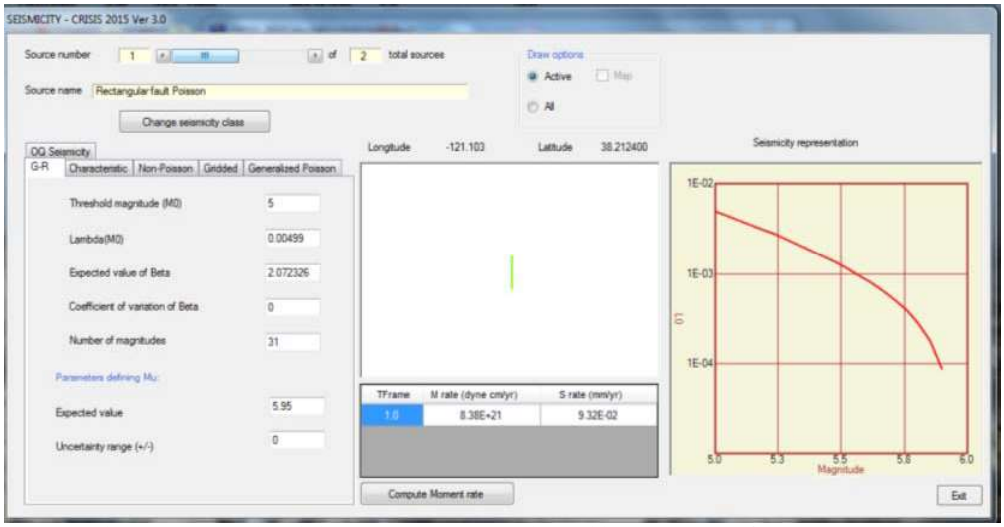

Figure 4-23 Seismicity parameters assigned in R-CRISIS for set 1, case 7 (modified G-R model)

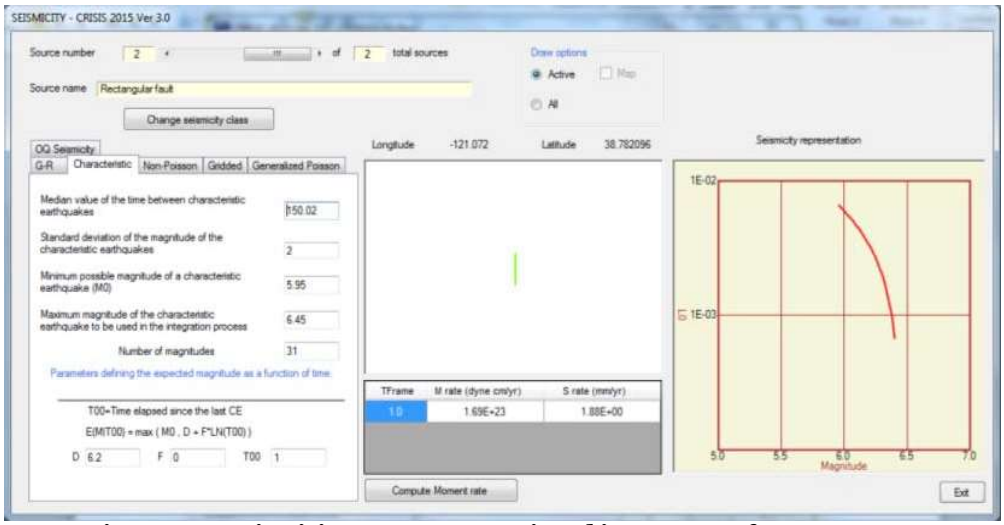

Figure 4-24 Seismicity parameters assigned in R-CRISIS for set 1, case 7 (characteristic earthquake model)

Results

Results computed in R-CRISIS for set 1, case 7 are shown in Table 4-24. Table 4-25 shows the results provided by the PEER-2015 project whereas Table 4-26 shows the analytical solution also provided by the coordinators of the PEER-2015 project. Figure 4-25 shows the hazard plots for the 7 computation sites. In all cases there is a full agreement between the results and therefore, it is possible to conclude that R-CRISIS fulfills all the requirements evaluated by the PEER-2015 project in set 1, case 7.

Figure 4-26 shows the hazard plots comparing the results obtained with R-CRISIS (elliptical and rectangular options) and the ones provided by the PEER-2015 project. Differences at computation sites 1, 4, 5 and 6 exist for exactly the same reasons explained in section 4.1.2.

Table 4-24 Annual exceedance probabilities obtained in R-CRISIS for Case 1, set 7

Peak Ground Acceleration (g)	Annual Exceedance Probability						
	Site 1	Site 2	Site 3	Site 4	Site 5	Site 6	Site 7
0.001	1.16E-02	1.16E-02	1.16E-02	1.16E-02	1.16E-02	1.16E-02	1.16E-02
0.01	1.16E-02	1.16E-02	1.16E-02	1.16E-02	1.16E-02	1.16E-02	1.16E-02
0.05	1.16E-02	1.16E-02	0.00E+00	1.16E-02	1.04E-02	1.16E-02	1.16E-02
0.10	1.16E-02	1.07E-02	0.00E+00	1.02E-02	7.74E-03	1.02E-02	1.07E-02
0.15	1.09E-02	7.77E-03	0.00E+00	8.83E-03	5.74E-03	8.82E-03	7.77E-03
0.20	9.68E-03	6.74E-03	0.00E+00	7.85E-03	3.56E-03	7.84E-03	6.74E-03
0.25	8.70E-03	3.58E-03	0.00E+00	6.94E-03	1.43E-03	6.93E-03	3.58E-03
0.30	7.97E-03	*	0.00E+00	6.03E-03	0.00E+00	6.02E-03	*
0.35	7.39E-03	0.00E+00	0.00E+00	5.14E-03	0.00E+00	5.13E-03	0.00E+00
0.40	6.68E-03	0.00E+00	0.00E+00	4.24E-03	0.00E+00	4.23E-03	0.00E+00
0.45	5.87E-03	0.00E+00	0.00E+00	3.40E-03	0.00E+00	3.38E-03	0.00E+00
0.50	4.98E-03	0.00E+00	0.00E+00	2.61E-03	0.00E+00	2.59E-03	0.00E+00
0.55	3.99E-03	0.00E+00	0.00E+00	1.89E-03	0.00E+00	1.86E-03	0.00E+00
0.60	2.88E-03	0.00E+00	0.00E+00	1.22E-03	0.00E+00	1.20E-03	0.00E+00
0.70	*	0.00E+00	0.00E+00	*	0.00E+00	*	0.00E+00
0.80	0.00E+00	0.00E+00	0.00E+00	0.00E+00	0.00E+00	0.00E+00	0.00E+00
0.90	0.00E+00	0.00E+00	0.00E+00	0.00E+00	0.00E+00	0.00E+00	0.00E+00
1.00	0.00E+00	0.00E+00	0.00E+00	0.00E+00	0.00E+00	0.00E+00	0.00E+00

* for these cases a value different than zero was computed, however, it was considered by the PEER coordinators as inappropriate for comparative purposes since there are significant differences between the values obtained by the 5 reference codes used to estimate the mean value.

Table 4-25 Annual exceedance probabilities reported as benchmarks by PEER project coordinators for Case 1, set 7

Peak Ground Acceleration (g)	Annual Exceedance Probability						
	Site 1	Site 2	Site 3	Site 4	Site 5	Site 6	Site 7
0.001	1.16E-02	1.16E-02	1.16E-02	1.16E-02	1.16E-02	1.16E-02	1.16E-02
0.01	1.16E-02	1.16E-02	1.16E-02	1.16E-02	1.16E-02	1.16E-02	1.16E-02
0.05	1.16E-02	1.16E-02	0.00E+00	1.16E-02	1.04E-02	1.16E-02	1.16E-02
0.10	1.16E-02	1.07E-02	0.00E+00	1.02E-02	7.74E-03	1.02E-02	1.07E-02
0.15	1.09E-02	7.76E-03	0.00E+00	8.83E-03	5.73E-03	8.83E-03	7.77E-03
0.20	9.67E-03	6.74E-03	0.00E+00	7.85E-03	3.55E-03	7.85E-03	6.75E-03
0.25	8.69E-03	3.57E-03	0.00E+00	6.93E-03	1.43E-03	6.93E-03	3.58E-03
0.30	7.97E-03	*	0.00E+00	6.02E-03	*	6.02E-03	*
0.35	7.38E-03	0.00E+00	0.00E+00	5.12E-03	0.00E+00	5.11E-03	0.00E+00
0.40	6.68E-03	0.00E+00	0.00E+00	4.23E-03	0.00E+00	4.22E-03	0.00E+00
0.45	5.87E-03	0.00E+00	0.00E+00	3.38E-03	0.00E+00	3.37E-03	0.00E+00
0.50	4.97E-03	0.00E+00	0.00E+00	2.59E-03	0.00E+00	2.59E-03	0.00E+00
0.55	3.98E-03	0.00E+00	0.00E+00	1.87E-03	0.00E+00	1.86E-03	0.00E+00
0.60	2.89E-03	0.00E+00	0.00E+00	1.21E-03	0.00E+00	1.21E-03	0.00E+00
0.70	*	0.00E+00	0.00E+00	*	0.00E+00	*	0.00E+00
0.80	0.00E+00	0.00E+00	0.00E+00	0.00E+00	0.00E+00	0.00E+00	0.00E+00
0.90	0.00E+00	0.00E+00	0.00E+00	0.00E+00	0.00E+00	0.00E+00	0.00E+00
1.00	0.00E+00	0.00E+00	0.00E+00	0.00E+00	0.00E+00	0.00E+00	0.00E+00

* for these cases a value different than zero was computed, however, it was considered by the PEER coordinators as inappropriate for comparative purposes since there are significant differences between the values obtained by the 5 reference codes used to estimate the mean value.

Table 4-26 Analytical annual exceedance probabilities obtained by PEER project coordinators for Case 1, set 7

Peak Ground Acceleration (g)	Annual Exceedance Probability						
	Site 1	Site 2	Site 3	Site 4	Site 5	Site 6	Site 7
0.001	**	**	**	1.14E-02	1.14E-02	1.14E-02	**
0.01	**	**	**	1.14E-02	1.14E-02	1.14E-02	**
0.05	**	**	**	1.14E-02	1.03E-02	1.14E-02	**
0.10	**	**	**	1.01E-02	7.65E-03	1.01E-02	**
0.15	**	**	**	8.72E-03	5.66E-03	8.72E-03	**
0.20	**	**	**	7.75E-03	3.50E-03	7.75E-03	**
0.25	**	**	**	6.84E-03	1.40E-03	6.84E-03	**
0.30	**	**	**	5.95E-03	**	5.95E-03	**
0.35	**	**	**	5.06E-03	**	5.06E-03	**
0.40	**	**	**	4.18E-03	**	4.18E-03	**
0.45	**	**	**	3.34E-03	**	3.34E-03	**
0.50	**	**	**	2.56E-03	**	2.56E-03	**
0.55	**	**	**	1.85E-03	**	1.85E-03	**
0.60	**	**	**	1.20E-03	**	1.20E-03	**
0.70	**	**	**	**	**	**	**
0.80	**	**	**	**	**	**	**
0.90	**	**	**	**	**	**	**
1.00	**	**	**	**	**	**	**

** There are no data available for these cases

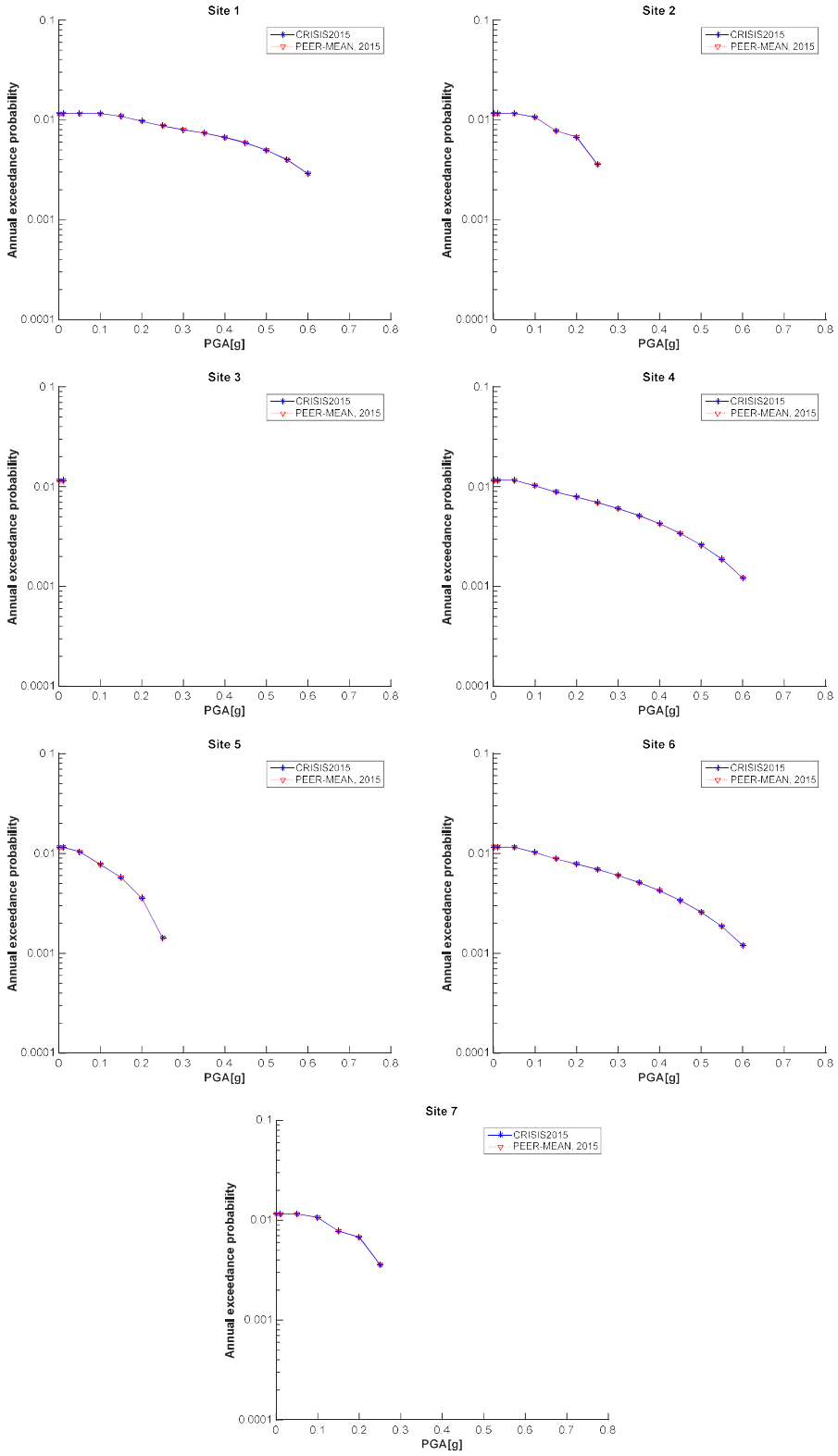

Figure 4-25 Comparison of the CRISIS and PEER-2015 results for Sites 1 to 7 (Set 1 Case 7)

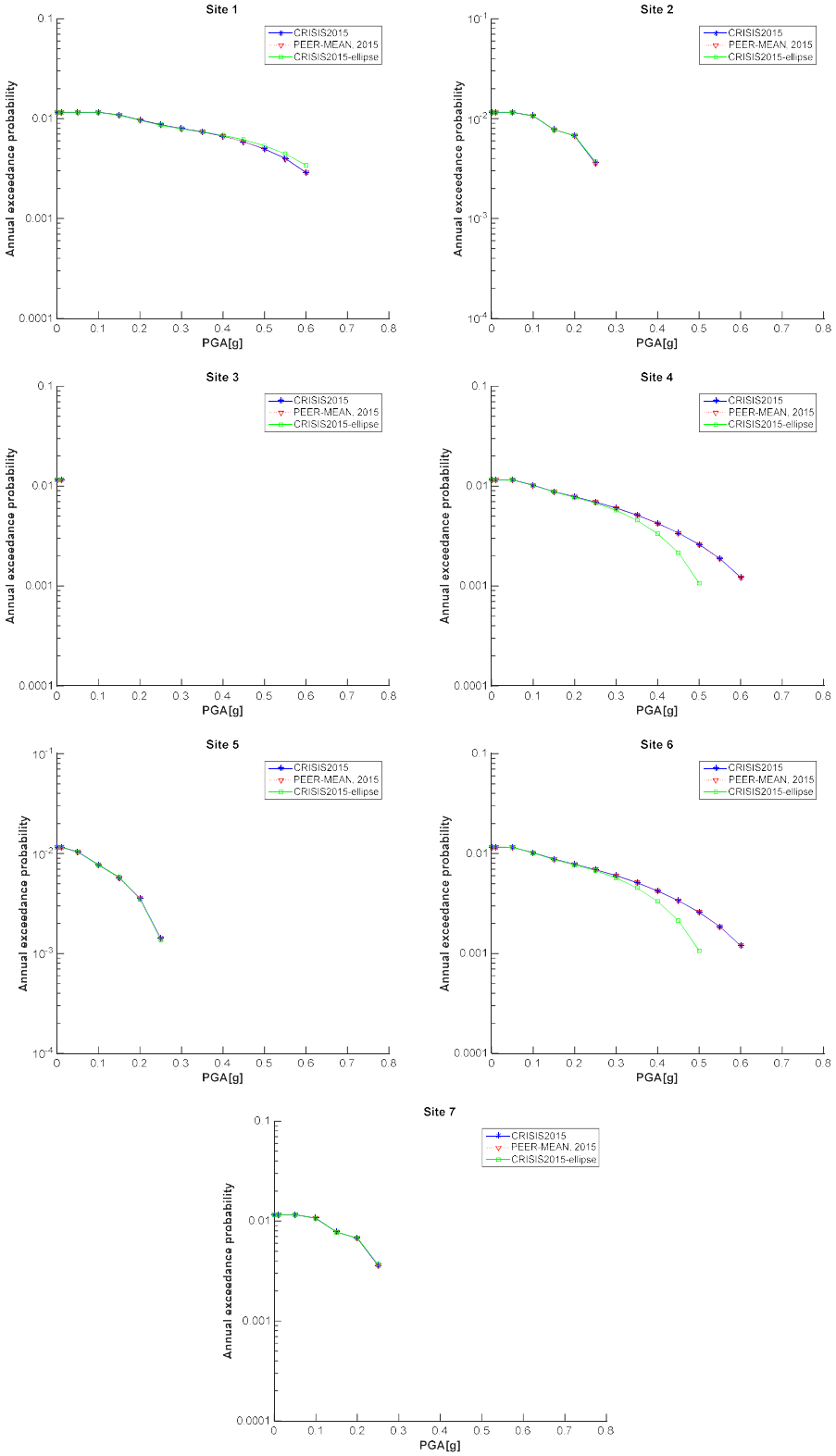

Figure 4-26 Comparison of elliptical and rectangular rupture shapes for PEER-2015 Set 1 Case 7

4.1.12 Set 1 case 8a

Input parameters

Table 4-27 summarizes the input data for case 8a. The computation sites are the same as in previous cases. Case 8a is similar to case 2 with the difference that the ground motion variability is considered as un-truncated herein.

Table 4-27 Summary of input data for Set 1, case 8a

Name	Description	Source	Mag-Density Function	Ground Motion Model[1,2]	Rupture Dimension Relationships[3,4,5,6]
Set 1 Case 8a	Single rupture smaller than fault plane. Untruncated ground motion variability	Fault 1(vertical SS) b-value=0.9 Slip rate=2mm/yr.	Delta function at M 6.0	Sadigh et al. (1997), rock. No σ truncation	$Log(A) = M - 4; \sigma_A = 0$ $Log(W) = 0.5 * M - 2.15; \sigma_W = 0$ $Log(L) = 0.5 * M - 1.85; \sigma_L = 0$

[1] Integration over magnitude zero.
[2] Use magnitude integration step size as small as necessary to model the magnitude density function.
[3] For all cases, uniform slip with tapered slip at edges.
[4] No ruptures are to extend beyond the edge of the fault plane.
[5] Aspect ratio to be maintained until maximum width is reached, then increase length (maintain area at the expense of aspect ratio).
[6] Down-dip and along strike integration step size should be as small as necessary for uniform rupture location.

Figure 4-27 shows the R-CRISIS attenuation data screen where the corresponding option has been chosen.

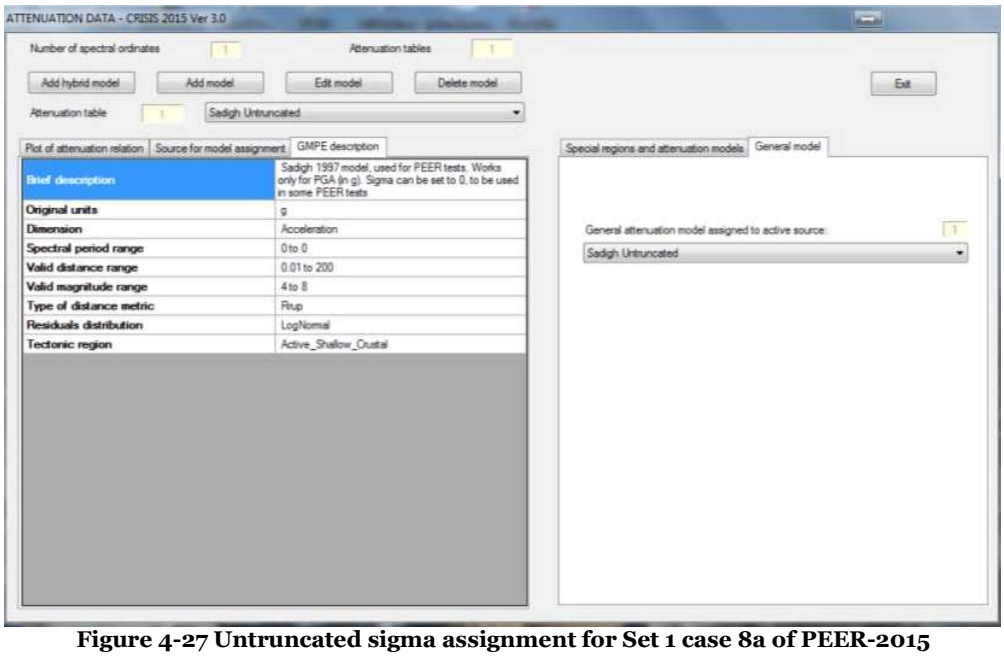

Figure 4-27 Untruncated sigma assignment for Set 1 case 8a of PEER-2015

Results

Results computed in R-CRISIS for set 1, case 8a are shown in Table 4-28 whereas Table 4-29 shows the results provided by the PEER-2015 project. Figure 4-28 shows the hazard plots for the 7 computation sites. In all cases there is a full agreement between the results and therefore, it is possible to conclude that R-CRISIS fulfills all the requirements evaluated by the PEER-2015 project in set 1, case 8a.

Figure 4-29 shows the hazard plots comparing the results obtained with R-CRISIS (elliptical and rectangular options) and the ones provided by the PEER-2015 project. Differences at computation sites 1, 4, 5 and 6 exist for exactly the same reasons explained in section 4.1.2.

Table 4-28 Annual exceedance probabilities obtained in R-CRISIS for Case 1, set 8a

Peak Ground Acceleration (g)	Annual Exceedance Probability						
	Site 1	Site 2	Site 3	Site 4	Site 5	Site 6	Site 7
0.001	1.59E-02	1.59E-02	1.59E-02	1.59E-02	1.59E-02	1.59E-02	1.59E-02
0.01	1.59E-02	1.57E-02	1.59E-02	1.59E-02	1.59E-02	1.59E-02	1.59E-02
0.05	1.59E-02	3.41E-03	1.59E-02	1.54E-02	1.59E-02	1.59E-02	1.59E-02
0.10	1.47E-02	3.18E-04	1.54E-02	1.20E-02	1.54E-02	1.47E-02	1.47E-02
0.15	1.20E-02	4.17E-05	1.41E-02	7.98E-03	1.41E-02	1.20E-02	1.20E-02
0.20	8.94E-03	7.28E-06	1.22E-02	4.99E-03	1.22E-02	8.94E-03	8.94E-03
0.25	6.39E-03	1.58E-06	1.02E-02	3.08E-03	1.02E-02	6.39E-03	6.39E-03
0.30	4.47E-03	4.02E-07	8.40E-03	1.91E-03	8.38E-03	4.47E-03	4.47E-03
0.35	3.10E-03	1.17E-07	6.81E-03	1.19E-03	6.79E-03	3.10E-03	3.10E-03
0.40	2.15E-03	3.77E-08	5.48E-03	7.59E-04	5.46E-03	2.15E-03	2.15E-03
0.45	1.49E-03	1.32E-08	4.40E-03	4.90E-04	4.39E-03	1.49E-03	1.49E-03
0.50	1.04E-03	*	3.53E-03	3.21E-04	3.52E-03	1.04E-03	1.04E-03
0.55	7.36E-04	*	2.84E-03	2.14E-04	2.83E-03	7.36E-04	7.36E-04
0.60	5.22E-04	*	2.29E-03	1.44E-04	2.28E-03	5.22E-04	5.22E-04
0.70	2.70E-04	*	1.50E-03	6.84E-05	1.49E-03	2.70E-04	2.70E-04
0.80	1.44E-04	*	9.91E-04	3.39E-05	9.86E-04	1.44E-04	1.44E-04
0.90	7.91E-05	*	6.66E-04	1.75E-05	6.62E-04	7.91E-05	7.91E-05
1.00	4.47E-05	*	4.54E-04	9.40E-06	4.51E-04	4.47E-05	4.47E-05

* for these cases a value different than zero was computed, however, it was considered by the PEER coordinators as inappropriate for comparative purposes since there are significant differences between the values obtained by the 5 reference codes used to estimate the mean value.

Table 4-29 Annual exceedance probabilities reported as benchmarks by PEER project coordinators for Case 1, set 8a

Peak Ground Acceleration (g)	Annual Exceedance Probability						
	Site 1	Site 2	Site 3	Site 4	Site 5	Site 6	Site 7
0.001	1.59E-02	1.59E-02	1.59E-02	1.59E-02	1.59E-02	1.59E-02	1.59E-02
0.01	1.59E-02	1.59E-02	1.57E-02	1.59E-02	1.59E-02	1.59E-02	1.59E-02
0.05	1.59E-02	1.59E-02	3.41E-03	1.59E-02	1.54E-02	1.59E-02	1.59E-02
0.10	1.59E-02	1.47E-02	3.20E-04	1.54E-02	1.20E-02	1.54E-02	1.47E-02
0.15	1.55E-02	1.20E-02	4.20E-05	1.41E-02	7.97E-03	1.41E-02	1.20E-02
0.20	1.47E-02	8.95E-03	7.34E-06	1.22E-02	4.98E-03	1.22E-02	8.95E-03
0.25	1.36E-02	6.40E-03	1.59E-06	1.02E-02	3.07E-03	1.02E-02	6.40E-03
0.30	1.22E-02	4.47E-03	4.07E-07	8.38E-03	1.90E-03	8.38E-03	4.47E-03
0.35	1.08E-02	3.10E-03	1.18E-07	6.79E-03	1.19E-03	6.79E-03	3.10E-03
0.40	9.43E-03	2.15E-03	3.82E-08	5.46E-03	7.57E-04	5.46E-03	2.15E-03
0.45	8.14E-03	1.50E-03	1.34E-08	4.39E-03	4.89E-04	4.39E-03	1.50E-03
0.50	6.97E-03	1.05E-03	*	3.52E-03	3.20E-04	3.52E-03	1.05E-03
0.55	5.95E-03	7.38E-04	*	2.83E-03	2.13E-04	2.83E-03	7.37E-04
0.60	5.06E-03	5.24E-04	*	2.28E-03	1.44E-04	2.28E-03	5.24E-04
0.70	3.64E-03	2.71E-04	*	1.49E-03	6.82E-05	1.49E-03	2.71E-04
0.80	2.62E-03	1.44E-04	*	9.89E-04	3.39E-05	9.87E-04	1.44E-04
0.90	1.89E-03	7.94E-05	*	6.65E-04	1.75E-05	6.63E-04	7.94E-05
1.00	1.37E-03	4.49E-05	*	4.53E-04	9.38E-06	4.52E-04	4.49E-05

* for these cases a value different than zero was computed, however, it was considered by the PEER coordinators as inappropriate for comparative purposes since there are significant differences between the values obtained by the 5 reference codes used to estimate the mean value.

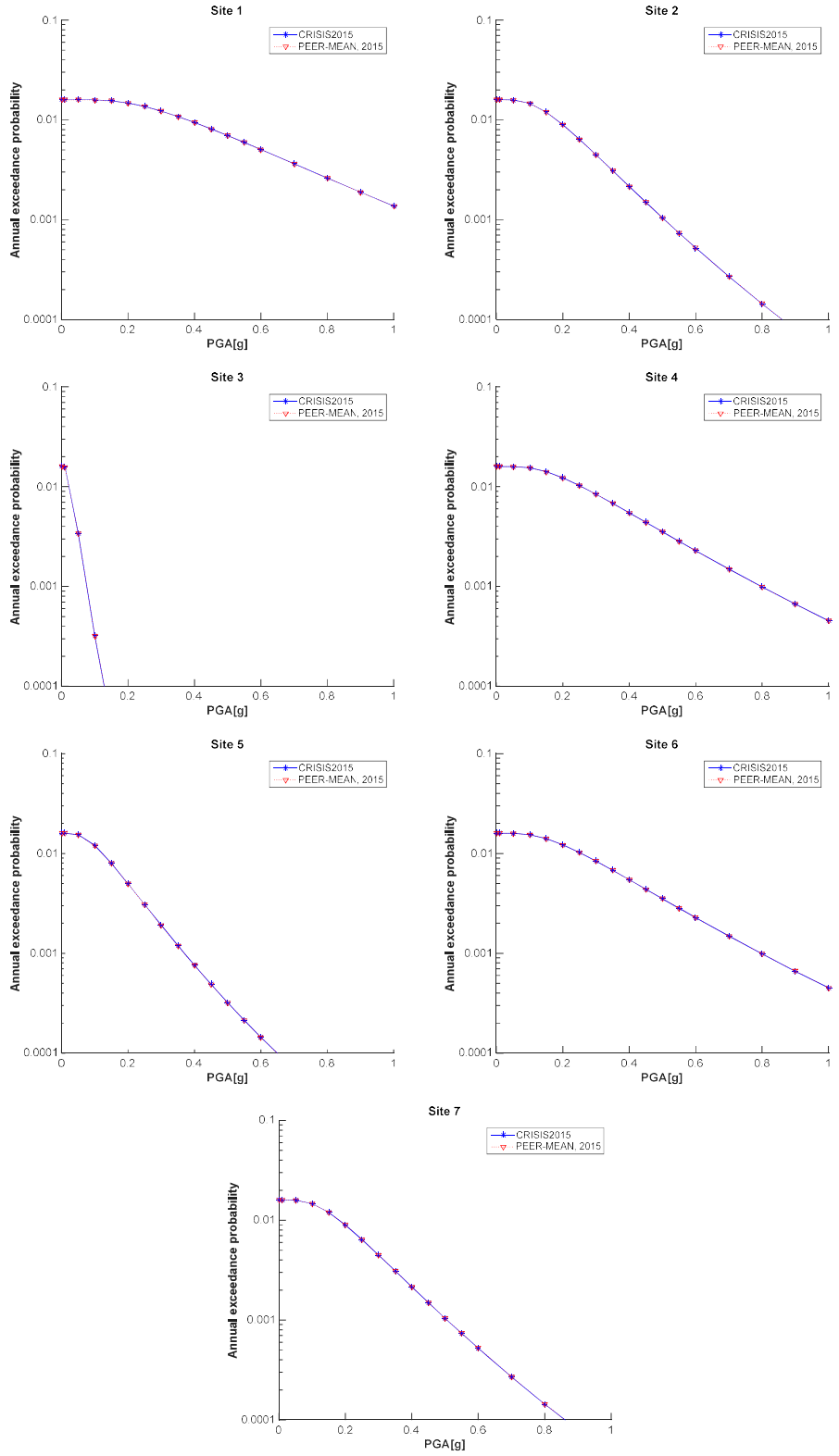

Figure 4-28 Comparison of the CRISIS and PEER-2015 results for Sites 1 to 7 (Set 1 Case 8a)

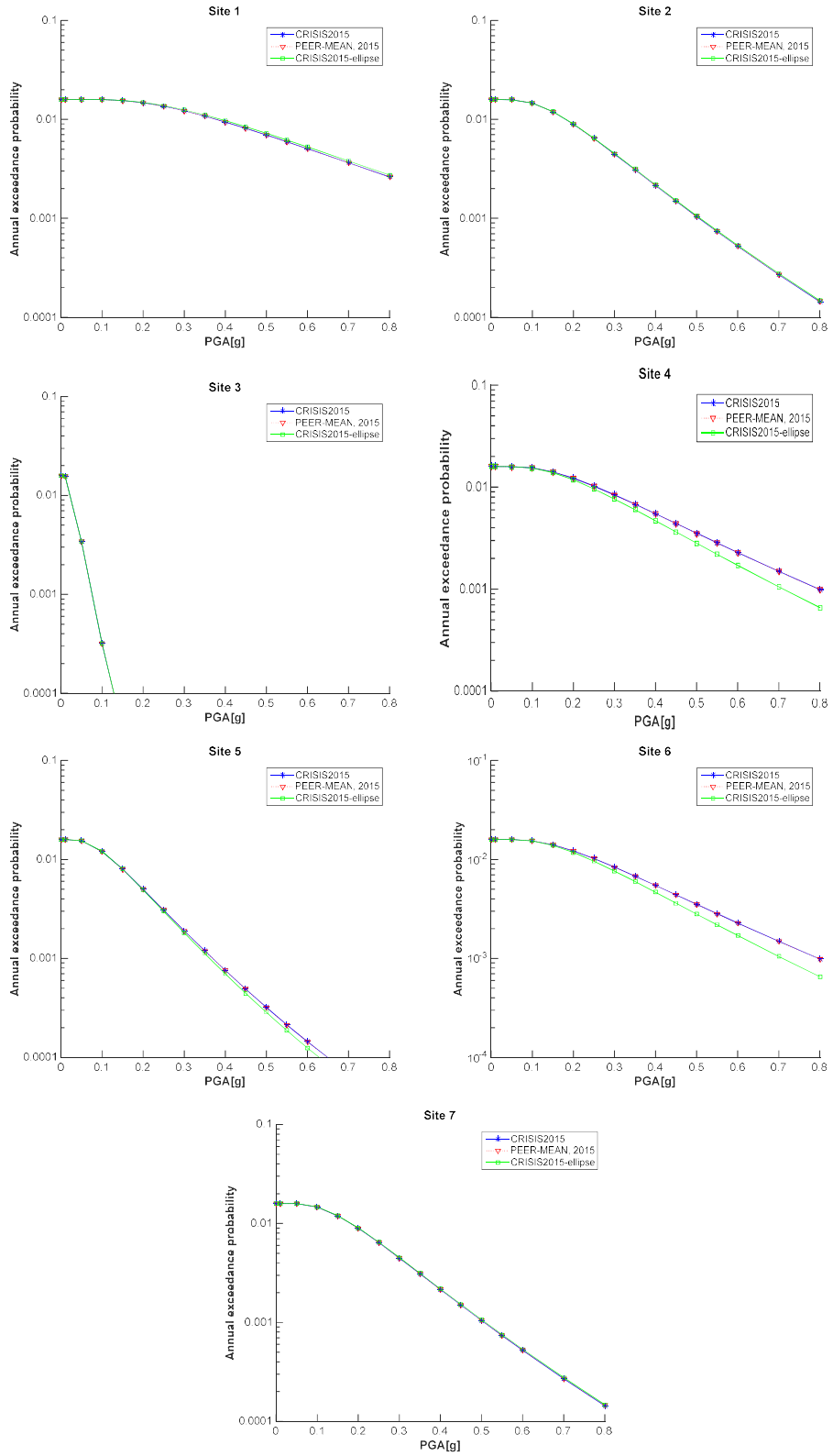

Figure 4-29 Comparison of elliptical and rectangular rupture shapes for PEER-2015 Set 1 Case 8a

4.1.13 Set 1 case 8b

Input parameters

Table 4.30 summarizes the input data for case 8b. The computation sites are the same as in previous cases. Case 8b is similar to case 2 with the difference that the ground motion variability is truncated to 2σ herein.

Table 4-30 Summary of input data for Set 1, case 8b

Name	Description	Source	Mag-Density Function	Ground Motion Model[1,2]	Rupture Dimension Relationships[3,4,5,6]
Set 1 Case 8b	Single rupture smaller than fault plane. Ground motion variability truncated at 2 sigma	Fault 1(vertical SS) b-value=0.9 Slip rate=2mm/yr.	Delta function at M 6.0	Sadigh et al. (1997), rock. Truncate σ at two standard deviations	$Log(A) = M - 4; \sigma_A = 0$ $Log(W) = 0.5 * M - 2.15; \sigma_W = 0$ $Log(L) = 0.5 * M - 1.85; \sigma_L = 0$

[1] Integration over magnitude zero.
[2] Use magnitude integration step size as small as necessary to model the magnitude density function.
[3] For all cases, uniform slip with tapered slip at edges.
[4] No ruptures are to extend beyond the edge of the fault plane.
[5] Aspect ratio to be maintained until maximum width is reached, then increase length (maintain area at the expense of aspect ratio).
[6] Down-dip and along strike integration step size should be as small as necessary for uniform rupture location.

Results

Results computed in R-CRISIS for set 1, case 8b are shown in Table 4-31 whereas Table 4-32 shows the results provided by the PEER-2015 project. Figure 4-30 shows the hazard plots for the 7 computation sites. In all cases there is a full agreement between the results and therefore, it is possible to conclude that R-CRISIS fulfills all the requirements evaluated by the PEER-2015 project in set 1, case 8b.

Figure 4-31 shows the hazard plots comparing the results obtained with R-CRISIS (elliptical and rectangular options) and the ones provided by the PEER-2015 project. Differences at computation sites 1, 4, 5 and 6 exist for the same reasons explained in section 4.1.2.

Table 4-31 Annual exceedance probabilities obtained in R-CRISIS for Case 1, set 8b

Peak Ground Acceleration (g)	Annual Exceedance Probability						
	Site 1	Site 2	Site 3	Site 4	Site 5	Site 6	Site 7
0.001	1.59E-02	1.59E-02	1.59E-02	1.59E-02	1.59E-02	1.59E-02	1.59E-02
0.01	1.59E-02	1.59E-02	1.56E-02	1.59E-02	1.59E-02	1.59E-02	1.59E-02
0.05	1.59E-02	1.59E-02	3.11E-03	1.59E-02	1.54E-02	1.59E-02	1.59E-02
0.10	1.59E-02	1.46E-02	0.00E+00	1.54E-02	1.19E-02	1.54E-02	1.46E-02
0.15	1.55E-02	1.19E-02	0.00E+00	1.41E-02	7.80E-03	1.41E-02	1.19E-02
0.20	1.47E-02	8.78E-03	0.00E+00	1.22E-02	4.74E-03	1.21E-02	8.78E-03
0.25	1.35E-02	6.17E-03	0.00E+00	1.01E-02	2.78E-03	1.01E-02	6.17E-03
0.30	1.22E-02	4.20E-03	0.00E+00	8.22E-03	1.58E-03	8.21E-03	4.20E-03
0.35	1.07E-02	2.80E-03	0.00E+00	6.59E-03	8.56E-04	6.58E-03	2.80E-03
0.40	9.28E-03	1.82E-03	0.00E+00	5.24E-03	4.49E-04	5.22E-03	1.82E-03
0.45	7.96E-03	1.15E-03	0.00E+00	4.13E-03	2.23E-04	4.12E-03	1.15E-03
0.50	6.77E-03	6.95E-04	0.00E+00	3.24E-03	9.99E-05	3.23E-03	6.95E-04
0.55	5.72E-03	3.79E-04	0.00E+00	2.53E-03	3.65E-05	2.52E-03	3.79E-04
0.60	4.81E-03	1.61E-04	0.00E+00	1.97E-03	8.29E-06	1.96E-03	1.61E-04
0.70	3.35E-03	0.00E+00	0.00E+00	1.17E-03	0.00E+00	1.17E-03	0.00E+00
0.80	2.31E-03	0.00E+00	0.00E+00	6.93E-04	0.00E+00	6.88E-04	0.00E+00
0.90	1.56E-03	0.00E+00	0.00E+00	4.00E-04	0.00E+00	3.97E-04	0.00E+00
1.00	1.03E-03	0.00E+00	0.00E+00	2.24E-04	0.00E+00	2.22E-04	0.00E+00

Table 4-32 Annual exceedance probabilities reported as benchmarks by PEER project coordinators for Case 1, set 8b

Peak Ground Acceleration (g)	Annual Exceedance Probability						
	Site 1	Site 2	Site 3	Site 4	Site 5	Site 6	Site 7
0.001	1.59E-02	1.59E-02	1.59E-02	1.59E-02	1.59E-02	1.59E-02	1.59E-02
0.01	1.59E-02	1.59E-02	1.58E-02	1.59E-02	1.59E-02	1.59E-02	1.59E-02
0.05	1.59E-02	1.59E-02	3.14E-03	1.59E-02	1.56E-02	1.59E-02	1.59E-02
0.10	1.59E-02	1.48E-02	0.00E+00	1.55E-02	1.21E-02	1.55E-02	1.48E-02
0.15	1.56E-02	1.20E-02	0.00E+00	1.42E-02	7.88E-03	1.42E-02	1.20E-02
0.20	1.49E-02	8.89E-03	0.00E+00	1.23E-02	4.78E-03	1.23E-02	8.88E-03
0.25	1.37E-02	6.24E-03	0.00E+00	1.02E-02	2.80E-03	1.02E-02	6.24E-03
0.30	1.23E-02	4.25E-03	0.00E+00	8.31E-03	1.59E-03	8.30E-03	4.25E-03
0.35	1.08E-02	2.83E-03	0.00E+00	6.66E-03	8.64E-04	6.65E-03	2.83E-03
0.40	9.40E-03	1.85E-03	0.00E+00	5.29E-03	4.54E-04	5.28E-03	1.84E-03
0.45	8.06E-03	1.17E-03	0.00E+00	4.17E-03	2.25E-04	4.17E-03	1.17E-03
0.50	6.85E-03	7.04E-04	0.00E+00	3.27E-03	1.01E-04	3.27E-03	7.02E-04
0.55	5.79E-03	3.85E-04	0.00E+00	2.56E-03	3.70E-05	2.55E-03	3.83E-04
0.60	4.87E-03	1.64E-04	0.00E+00	1.99E-03	*	1.98E-03	1.62E-04
0.70	3.40E-03	0.00E+00	0.00E+00	1.19E-03	0.00E+00	1.18E-03	0.00E+00
0.80	2.34E-03	0.00E+00	0.00E+00	7.00E-04	0.00E+00	6.99E-04	0.00E+00
0.90	1.58E-03	0.00E+00	0.00E+00	4.05E-04	0.00E+00	4.05E-04	0.00E+00
1.00	1.04E-03	0.00E+00	0.00E+00	2.27E-04	0.00E+00	2.26E-04	0.00E+00

* for these cases a value different than zero was computed, however, it was considered by the PEER coordinators as inappropriate for comparative purposes since there are significant differences between the values obtained by the 5 reference codes used to estimate the mean value.

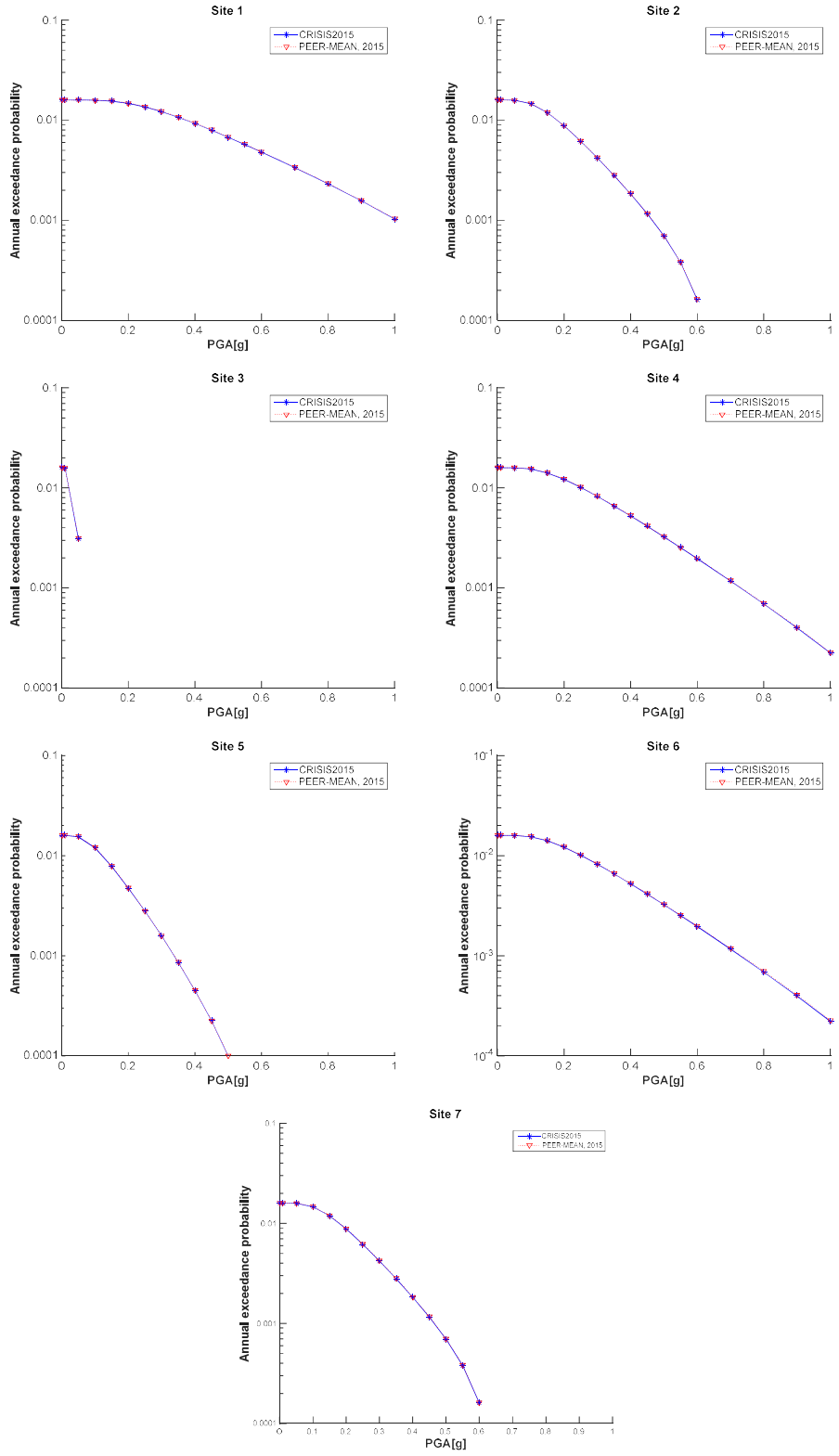

Figure 4-30 Comparison of the CRISIS and PEER-2015 results for Sites 1 to 7 (Set 1 Case 8b)

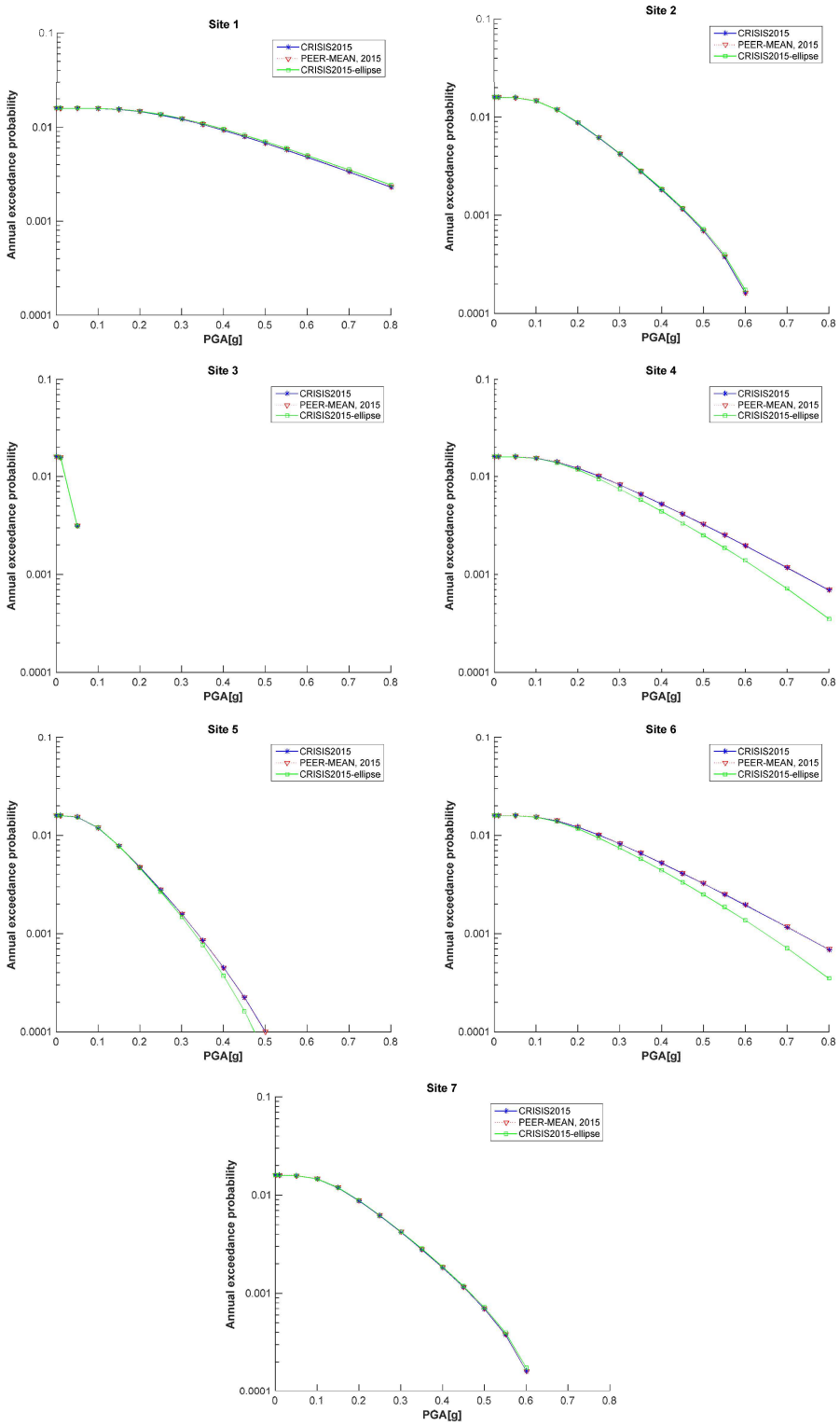

Figure 4-31 Comparison of elliptical and rectangular rupture shapes for PEER-2015 Set 1 Case 8b

4.1.14 Set 1 case 8c

Input parameters

Table 4-33 summarizes the input data for set 1, case 8c. The computation sites are the same as in previous cases. Case 8c is similar to case 2 with the difference that the ground motion variability is truncated to 3σ herein.

Table 4-33 Summary of input data for Set 1, case 8c

Name	Description	Source	Mag-Density Function	Ground Motion Model[1,2]	Rupture Dimension Relationships[3,4,5,6]
Set 1 Case 8c	Single rupture smaller than fault plane. Ground motion variability truncated at 3 sigma	Fault 1(vertical SS) b-value=0.9 Slip rate=2mm/yr.	Delta function at M 6.0	Sadigh et al. (1997), rock. Truncate σ at three standard deviations	$Log(A) = M - 4; \sigma_A = 0$ $Log(W) = 0.5 * M - 2.15; \sigma_W = 0$ $Log(L) = 0.5 * M - 1.85; \sigma_L = 0$

[1] Integration over magnitude zero.
[2] Use magnitude integration step size as small as necessary to model the magnitude density function.
[3] For all cases, uniform slip with tapered slip at edges.
[4] No ruptures are to extend beyond the edge of the fault plane.
[5] Aspect ratio to be maintained until maximum width is reached, then increase length (maintain area at the expense of aspect ratio).
[6] Down-dip and along strike integration step size should be as small as necessary for uniform rupture location.

Results

Results computed in R-CRISIS for set 1, case 8c are shown in Table 4-34 whereas Table 4-35 shows the results provided by the PEER-2015 project. Figure 4-32 shows the hazard plots for the 7 computation sites. In all cases there is a full agreement between the results and therefore, it is possible to conclude that R-CRISIS fulfills all the requirements evaluated by the PEER-2015 project in set 1, case 8c.

Figure 4-33 shows the hazard plots comparing the results obtained with R-CRISIS (elliptical and rectangular options) and the ones provided by the PEER-2015 project. Differences at computation sites 1, 4, 5 and 6 exist for exactly the same reasons explained in section 4.1.2.

Table 4-34 Annual exceedance probabilities obtained in R-CRISIS for Case 1, set 8c

Peak Ground Acceleration (g)	Annual Exceedance Probability						
	Site 1	Site 2	Site 3	Site 4	Site 5	Site 6	Site 7
0.001	1.59E-02	1.59E-02	1.59E-02	1.59E-02	1.59E-02	1.59E-02	1.59E-02
0.01	1.59E-02	1.59E-02	1.57E-02	1.59E-02	1.59E-02	1.59E-02	1.59E-02
0.05	1.59E-02	1.59E-02	3.39E-03	1.59E-02	1.54E-02	1.59E-02	1.59E-02
0.10	1.59E-02	1.47E-02	2.97E-04	1.54E-02	1.20E-02	1.54E-02	1.47E-02
0.15	1.55E-02	1.19E-02	2.00E-05	1.41E-02	7.97E-03	1.41E-02	1.19E-02
0.20	1.47E-02	8.93E-03	0.00E+00	1.22E-02	4.98E-03	1.22E-02	8.93E-03
0.25	1.36E-02	6.38E-03	0.00E+00	1.02E-02	3.06E-03	1.02E-02	6.38E-03
0.30	1.22E-02	4.45E-03	0.00E+00	8.39E-03	1.89E-03	8.37E-03	4.45E-03
0.35	1.08E-02	3.08E-03	0.00E+00	6.79E-03	1.17E-03	6.78E-03	3.08E-03
0.40	9.42E-03	2.13E-03	0.00E+00	5.47E-03	7.38E-04	5.45E-03	2.13E-03
0.45	8.13E-03	1.47E-03	0.00E+00	4.38E-03	4.69E-04	4.37E-03	1.47E-03
0.50	6.96E-03	1.02E-03	0.00E+00	3.52E-03	3.00E-04	3.50E-03	1.02E-03
0.55	5.94E-03	7.15E-04	0.00E+00	2.82E-03	1.92E-04	2.81E-03	7.15E-04
0.60	5.05E-03	5.01E-04	0.00E+00	2.27E-03	1.23E-04	2.26E-03	5.01E-04
0.70	3.63E-03	2.49E-04	0.00E+00	1.48E-03	5.03E-05	1.47E-03	2.49E-04
0.80	2.60E-03	1.22E-04	0.00E+00	9.71E-04	1.96E-05	9.66E-04	1.22E-04
0.90	1.87E-03	5.75E-05	0.00E+00	6.45E-04	6.64E-06	6.42E-04	5.75E-05
1.00	1.35E-03	2.31E-05	0.00E+00	4.33E-04	1.58E-06	4.30E-04	2.31E-05

Table 4-35 Annual exceedance probabilities reported as benchmarks by PEER project coordinators for Case 1, set 8c

Peak Ground Acceleration (g)	Annual Exceedance Probability						
	Site 1	Site 2	Site 3	Site 4	Site 5	Site 6	Site 7
0.001	1.59E-02	1.59E-02	1.59E-02	1.59E-02	1.59E-02	1.59E-02	1.59E-02
0.01	1.59E-02	1.59E-02	1.57E-02	1.59E-02	1.59E-02	1.59E-02	1.59E-02
0.05	1.59E-02	1.59E-02	3.40E-03	1.59E-02	1.54E-02	1.59E-02	1.59E-02
0.10	1.59E-02	1.47E-02	2.99E-04	1.54E-02	1.20E-02	1.54E-02	1.47E-02
0.15	1.55E-02	1.20E-02	2.03E-05	1.41E-02	7.96E-03	1.41E-02	1.20E-02
0.20	1.47E-02	8.95E-03	0.00E+00	1.22E-02	4.97E-03	1.22E-02	8.95E-03
0.25	1.36E-02	6.39E-03	0.00E+00	1.02E-02	3.05E-03	1.02E-02	6.39E-03
0.30	1.22E-02	4.46E-03	0.00E+00	8.38E-03	1.88E-03	8.37E-03	4.46E-03
0.35	1.08E-02	3.09E-03	0.00E+00	6.78E-03	1.17E-03	6.78E-03	3.09E-03
0.40	9.43E-03	2.13E-03	0.00E+00	5.46E-03	7.37E-04	5.45E-03	2.13E-03
0.45	8.13E-03	1.48E-03	0.00E+00	4.38E-03	4.68E-04	4.37E-03	1.48E-03
0.50	6.97E-03	1.03E-03	0.00E+00	3.51E-03	2.99E-04	3.50E-03	1.03E-03
0.55	5.94E-03	7.17E-04	0.00E+00	2.82E-03	1.92E-04	2.81E-03	7.17E-04
0.60	5.05E-03	5.03E-04	0.00E+00	2.26E-03	1.23E-04	2.26E-03	5.03E-04
0.70	3.63E-03	2.50E-04	0.00E+00	1.47E-03	5.02E-05	1.47E-03	2.50E-04
0.80	2.60E-03	1.23E-04	0.00E+00	9.69E-04	1.95E-05	9.67E-04	1.23E-04
0.90	1.87E-03	5.78E-05	0.00E+00	6.44E-04	6.62E-06	6.43E-04	5.78E-05
1.00	1.35E-03	2.32E-05	0.00E+00	4.32E-04	1.58E-06	4.31E-04	2.32E-05

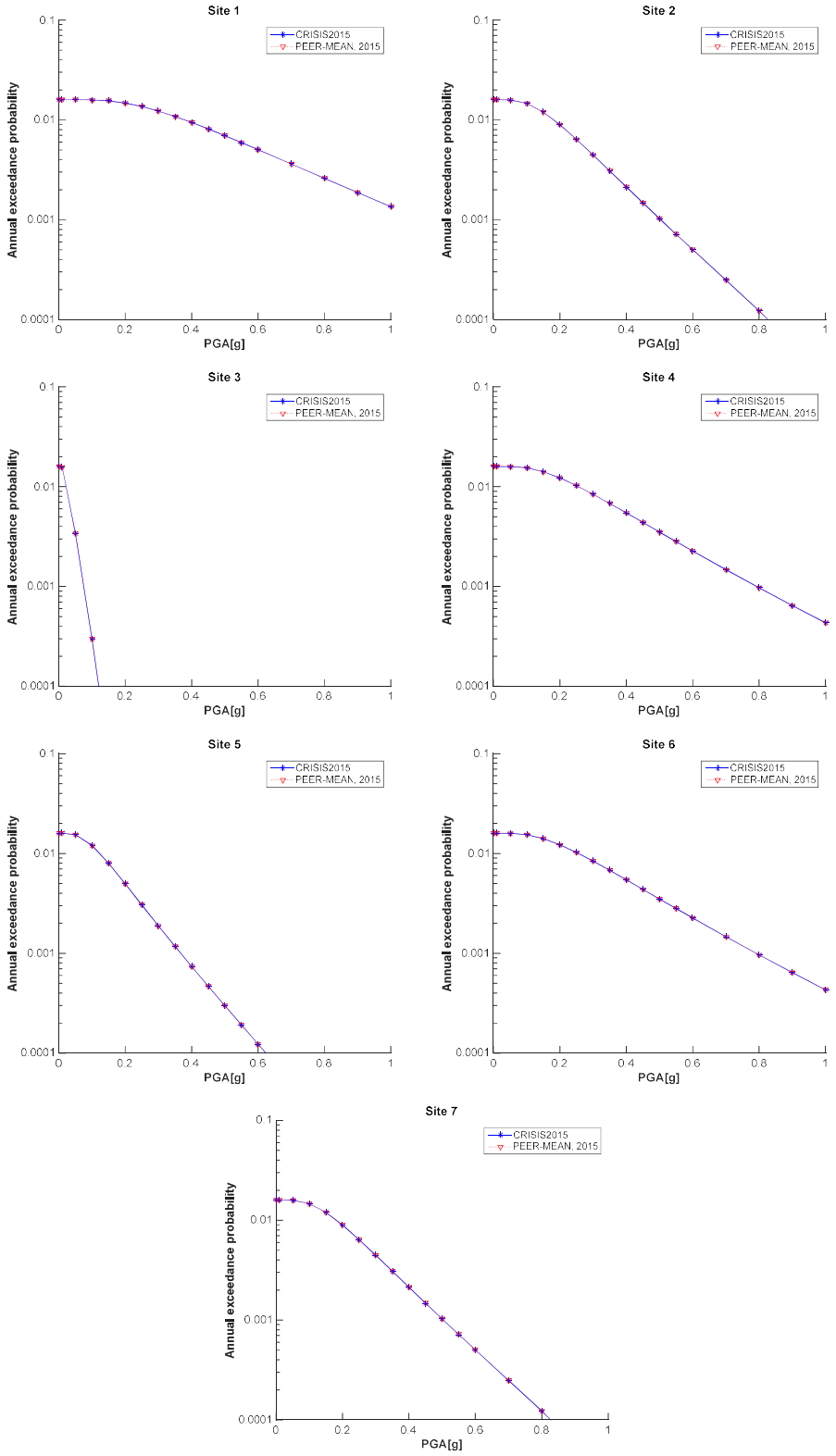

Figure 4-32 Comparison of the CRISIS and PEER-2015 results for Sites 1 to 7 (Set 1 Case 8c)

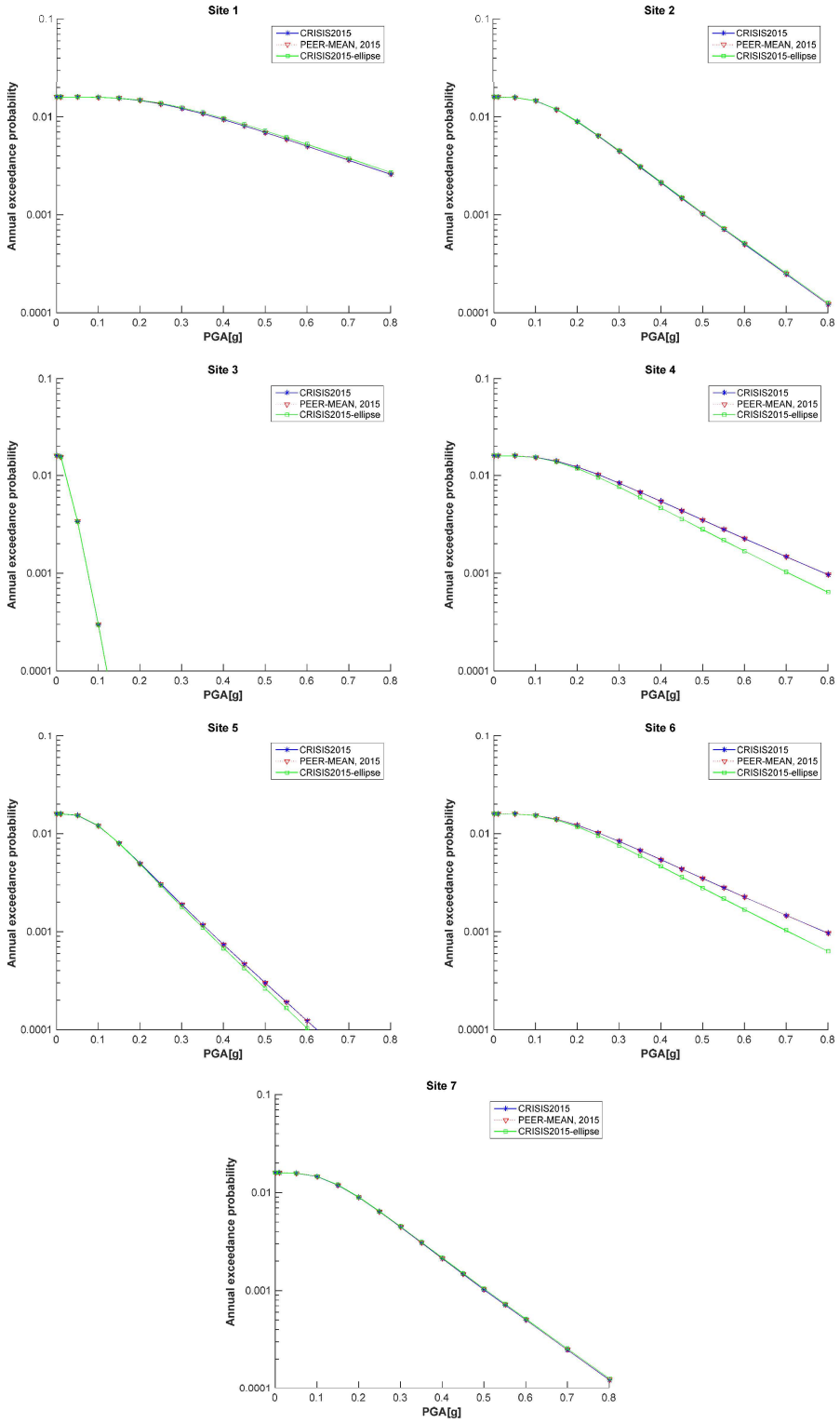

Figure 4-33 Comparison of elliptical and rectangular rupture shapes for PEER-2015 Set 1 Case 8c

4.1.15 Set 1 case 9

As for the three variations of case 8, the tests of case 9 aim at evaluating the computation of ground motion attenuation in the code. In these cases a dipping fault is used instead of a vertical fault and different GMPM are used. This test has not been performed since the handling of ground motion relations and their variability by the R-CRISIS code has already been shown to be satisfactory.

4.1.16 Set 1 case 10

Input parameters

The source adopted is the circular area source (Figure 4-2) with a constant depth of 5km. The seismicity was modeled assuming a *b*-value=0.9 and a seismicity rate, λ, (i.e. the annual number of earthquakes with magnitude $M \geq Mmin$) of 0.0395. The magnitude density function is a truncated exponential with *Mmin*=5.0 and *Mmax*=6.5. For this test, PEER suggests adopting point sub-sources as shown in Table 4-36.

Figure 4-34 shows the geometry data screen of R-CRISIS with the parameters that were used herein, whereas, Figure 4-35 shows the seismicity data screen of R-CRISIS with the assigned parameters for this particular case.

Table 4-36 Summary of input data for Set 1, case 10

Name	Description	Source	Mag-Density Function	Ground Motion Model[1,2]	Rupture Dimension Relationships[3,4,5,6]
Set 1 Case 10	Area source with fixed depth of 5km	Area 1 N(M≥5)=0.0395, b-value=0.9	Truncated exponential, Mmax=6.5, Mmin=5.0	Sadigh et al. (1997), rock	Use 1km grid spacing of point sources or small faults to simulate a uniform distribution

[1] Integration over magnitude zero.

[2] Use magnitude integration step size as small as necessary to model the magnitude density function.

[3] For all cases, uniform slip with tapered slip at edges.

[4] No ruptures are to extend beyond the edge of the fault plane.

[5] Aspect ratio to be maintained until maximum width is reached, then increase length (maintain area at the expense of aspect ratio).

[6] Down-dip and along strike integration step size should be as small as necessary for uniform rupture location.

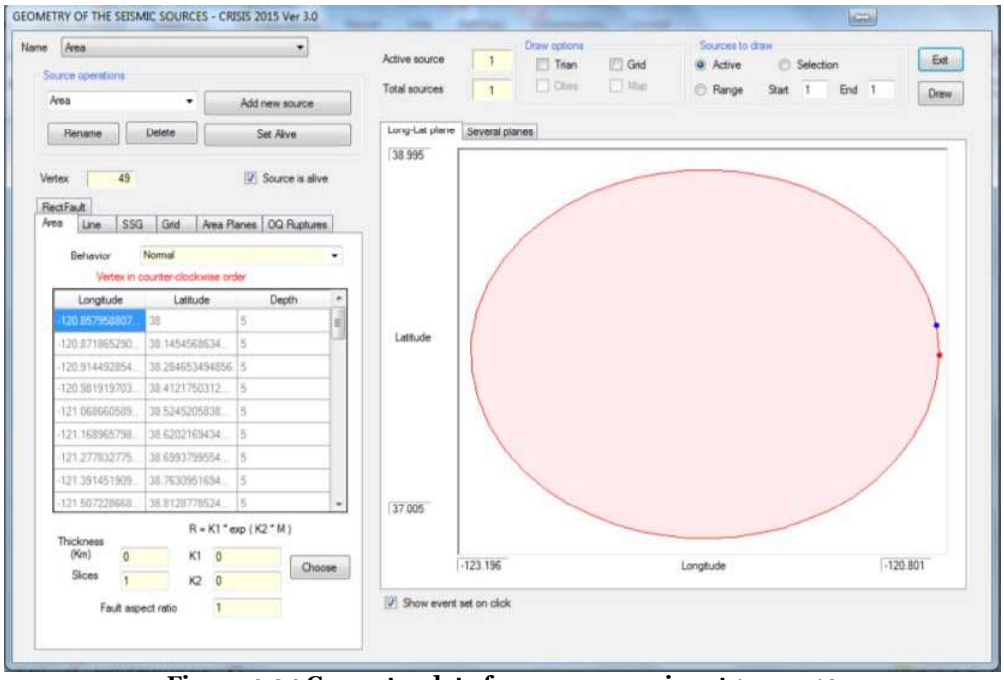

Figure 4-34 Geometry data for area source in set 1, case 10

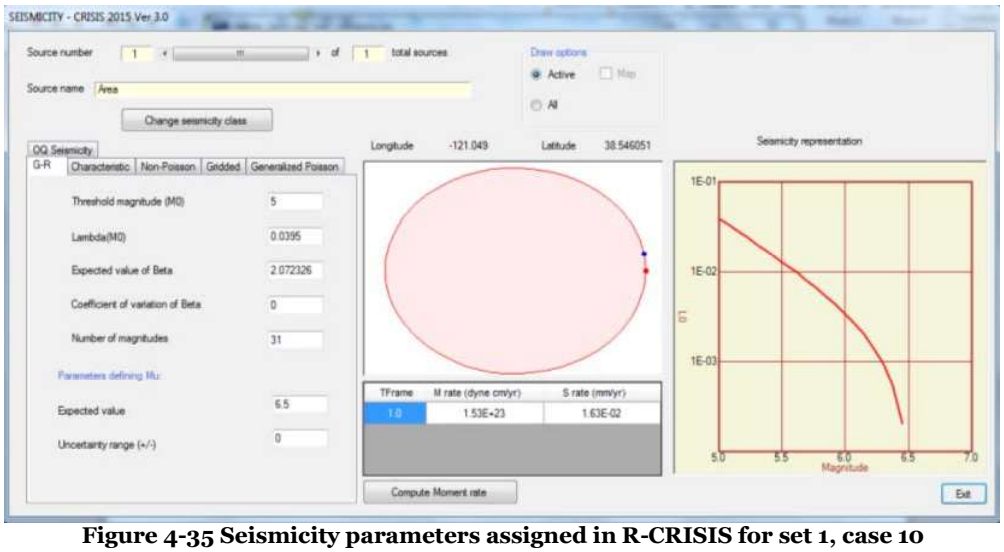

Figure 4-35 Seismicity parameters assigned in R-CRISIS for set 1, case 10

Note: the area source for this case is circular although, due to its location and the datum R-CRISIS uses, is displayed as elliptical.

The coordinates for the computation sites are shown in Table 4-37.

Table 4-37 Coordinates and comments of the computation sites for the area source

Site	Latitude	Longitude	Comment
1	38.000	-122.000	At center of area
2	37.550	-122.000	50 km from center (radially)
3	37.099	-122.000	On area boundary
4	36.874	-122.000	25 km from boundary

Results

Results computed in R-CRISIS for Set 1-Case 10 are shown in Table 4-38 whereas Table 4-39 shows the results provided by the PEER-2015 project. Figure 4-36 shows the hazard plots for the 4 computation sites. In all cases there is a full agreement between the results and therefore, it is possible to conclude that CRISIS fulfills all the requirements evaluated by the PEER-2015 project in Set 1-Case 10.

Table 4-38 Annual exceedance probabilities obtained in R-CRISIS for Case 1, set 10

Peak Ground Acceleration (g)	Annual Exceedance Probability			
	Site 1	Site 2	Site 3	Site 4
0.001	3.87E-02	3.87E-02	3.87E-02	3.82E-02
0.01	2.19E-02	1.82E-02	9.33E-03	5.33E-03
0.05	2.96E-03	2.96E-03	1.37E-03	1.21E-04
0.10	9.20E-04	9.20E-04	4.35E-04	1.40E-06
0.15	3.60E-04	3.60E-04	1.71E-04	0.00E+00
0.20	1.32E-04	1.32E-04	6.23E-05	0.00E+00
0.25	4.71E-05	4.71E-05	2.22E-05	0.00E+00
0.30	1.68E-05	1.69E-05	7.91E-06	0.00E+00
0.35	5.38E-06	5.38E-06	2.50E-06	0.00E+00
0.40	1.21E-06	1.21E-06	5.48E-07	0.00E+00
0.45	*	*	2.33E-08	0.00E+00
0.50	0.00E+00	0.00E+00	0.00E+00	0.00E+00
0.55	0.00E+00	0.00E+00	0.00E+00	0.00E+00
0.60	0.00E+00	0.00E+00	0.00E+00	0.00E+00
0.70	0.00E+00	0.00E+00	0.00E+00	0.00E+00
0.80	0.00E+00	0.00E+00	0.00E+00	0.00E+00
0.90	0.00E+00	0.00E+00	0.00E+00	0.00E+00
1.00	0.00E+00	0.00E+00	0.00E+00	0.00E+00

* for these cases a value different than zero was computed, however, it was considered by the PEER coordinators as inappropriate for comparative purposes since there are significant differences between the values obtained by the 5 reference codes used to estimate the mean value.

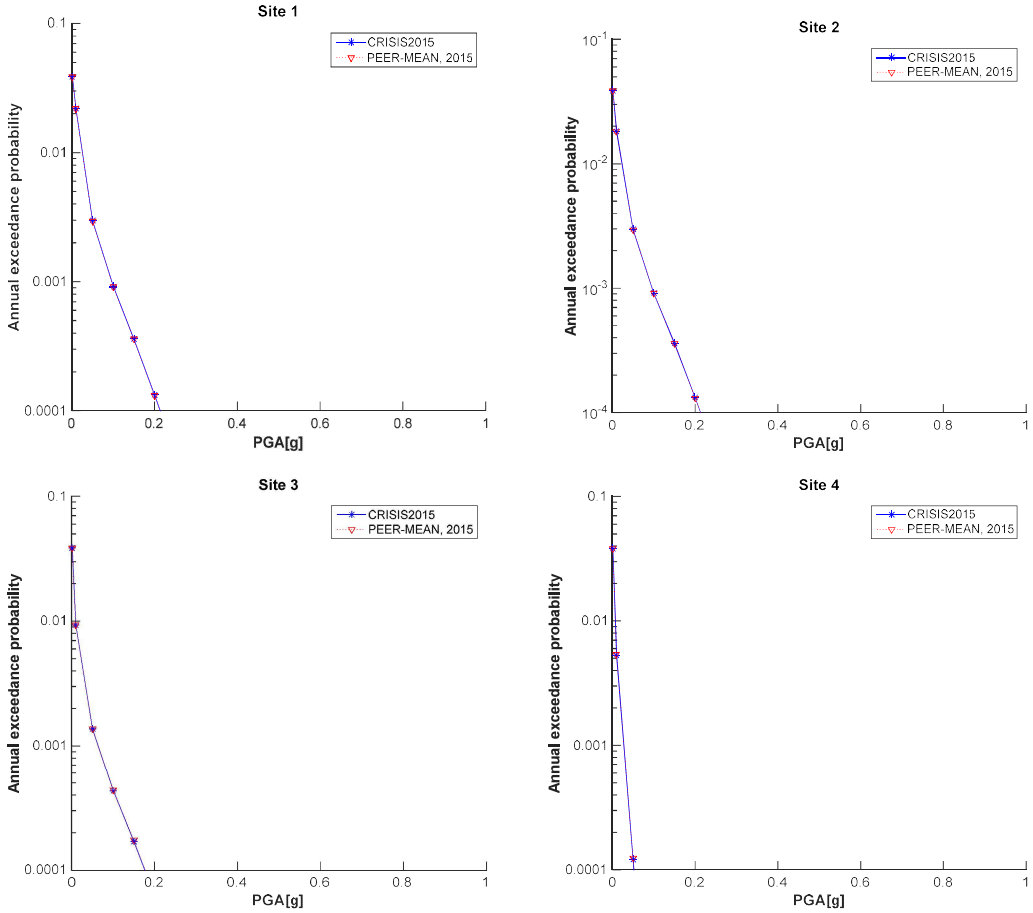

Figure 4-36 Comparison of the CRISIS and PEER-2015 results for Sites 1 to 4 (Set 1 Case 10)

4.1.17 Set 1 case 11

Input parameters

The source adopted is volume source with the shape of the area source of case 10 and a depth between 5 and 10km. In CRISIS the volume source was modelled by 6 area sources with the same coordinates of the original area source and at different depths (spaced at 1km, coherently with the prescriptions of PEER described in Table 4-39).

Figure 4-37 shows the geometry data screen of R-CRISIS with the parameters that were used herein (slices).

Table 4-39 Summary of input data for Set 1, case 11

Name	Description	Source	Mag-Density Function	Ground Motion Model[1,2]	Rupture Dimension Relationships[3,4,5,6]
Set 1 Case 11	Volume source with depth of 5km to 10km	Area 1 N(M≥5)=0.0395, b-value=0.9	Truncated exponential, Mmax=6.5, Mmin=5.0	Sadigh et al. (1997), rock	Use 1km grid spacing of point sources or small faults to simulate a uniform distribution. For the depth distribution a 1km spacing was used including 5 and 10km

[1] Integration over magnitude zero.
[2] Use magnitude integration step size as small as necessary to model the magnitude density function.
[3] For all cases, uniform slip with tapered slip at edges.
[4] No ruptures are to extend beyond the edge of the fault plane.
[5] Aspect ratio to be maintained until maximum width is reached, then increase length (maintain area at the expense of aspect ratio).
[6] Down-dip and along strike integration step size should be as small as necessary for uniform rupture location.

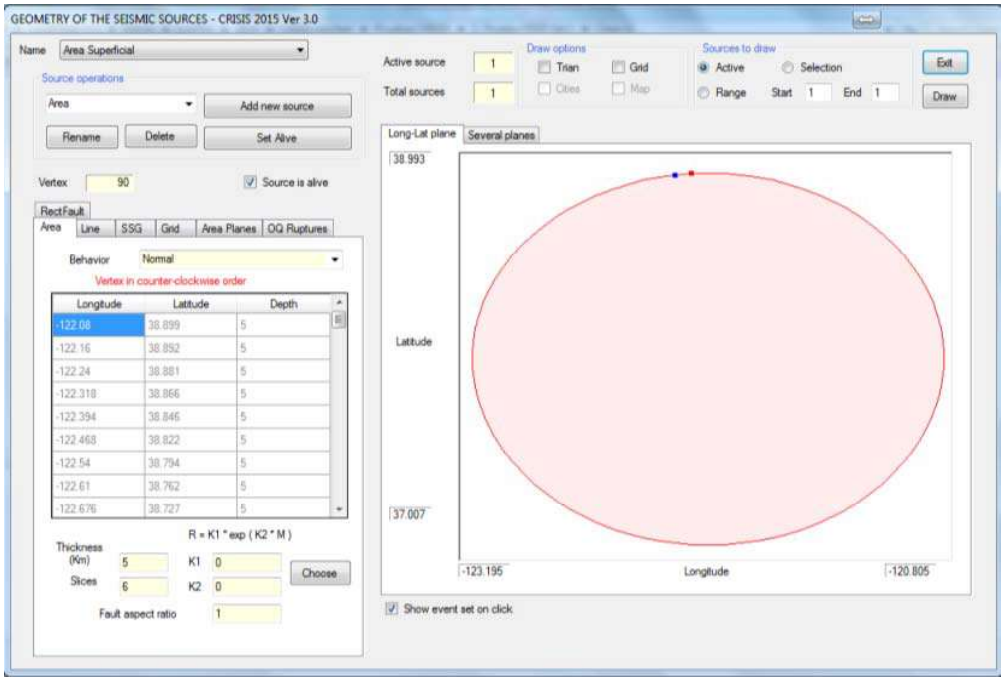

Figure 4-37 Geometry data for area source in set 1, case 11

Each slice is considered as an individual source and is modelled in R-CRISIS with a modified G-R seismicity model with *b*-value=0.9 and a seismicity rate λ=0.0395/6. As in set 1, case 10, the magnitude density function is a truncated exponential with Mmin=5.0 and Mmax=6.5.

Results

Results computed in R-CRISIS for Set 1-Case 11 are shown in Table 4-40 whereas Table 4-41 shows the results provided by the PEER-2015 project. Figure 4-38 shows the hazard plots for the 4 computation sites. In all cases there is a full agreement between the results and

therefore, it is possible to conclude that CRISIS fulfills all the requirements evaluated by the PEER-2015 project in set 1, case 11.

Table 4-40 Annual exceedance probabilities obtained in R-CRISIS for Case 1, set 11

Peak Ground Acceleration (g)	Annual Exceedance Probability			
	Site 1	Site 2	Site 3	Site 4
0.001	3.87E-02	3.83E-02	3.66E-02	3.50E-02
0.01	2.28E-02	1.91E-02	1.08E-02	6.81E-03
0.05	3.97E-03	3.86E-03	1.79E-03	4.50E-04
0.10	1.35E-03	1.35E-03	6.32E-04	6.44E-05
0.15	6.29E-04	6.29E-04	2.98E-04	1.44E-05
0.20	3.34E-04	3.34E-04	1.59E-04	4.04E-06
0.25	1.91E-04	1.91E-04	9.17E-05	1.33E-06
0.30	1.16E-04	1.16E-04	5.56E-05	4.90E-07
0.35	7.28E-05	7.28E-05	3.51E-05	1.98E-07
0.40	4.73E-05	4.73E-05	2.28E-05	8.59E-08
0.45	0.0000315	0.0000315	1.52E-05	3.97E-08
0.50	2.14E-05	2.14E-05	1.04E-05	1.93E-08
0.55	1.49E-05	1.49E-05	7.20E-06	9.83E-09
0.60	1.05E-05	1.05E-05	5.09E-06	5.20E-09
0.70	5.45E-06	5.45E-06	2.64E-06	1.61E-09
0.80	2.97E-06	2.97E-06	1.44E-06	5.58E-10
0.90	1.69E-06	1.69E-06	8.20E-07	2.10E-10
1.00	9.91E-07	9.91E-07	4.82E-07	8.54E-11

Table 4-41 Annual exceedance probabilities reported as benchmarks by PEER project coordinators for Case 1, set 11

Peak Ground Acceleration (g)	Annual Exceedance Probability			
	Site 1	Site 2	Site 3	Site 4
0.001	3.87E-02	3.83E-02	3.66E-02	3.49E-02
0.01	2.26E-02	1.90E-02	1.08E-02	6.79E-03
0.05	3.92E-03	3.82E-03	1.78E-03	4.49E-04
0.10	1.34E-03	1.33E-03	6.26E-04	6.46E-05
0.15	6.22E-04	6.21E-04	2.95E-04	1.44E-05
0.20	3.30E-04	3.30E-04	1.58E-04	4.08E-06
0.25	1.89E-04	1.89E-04	9.08E-05	1.35E-06
0.30	1.14E-04	1.14E-04	5.51E-05	4.98E-07
0.35	7.20E-05	7.20E-05	3.47E-05	2.02E-07
0.40	4.67E-05	4.67E-05	2.26E-05	8.79E-08
0.45	0.0000311	0.0000311	1.51E-05	4.07E-08
0.50	2.12E-05	2.12E-05	1.03E-05	1.98E-08
0.55	1.47E-05	1.47E-05	7.13E-06	1.01E-08
0.60	1.04E-05	1.04E-05	5.03E-06	5.36E-09
0.70	5.38E-06	5.38E-06	2.62E-06	1.66E-09
0.80	2.93E-06	2.93E-06	1.43E-06	5.74E-10
0.90	1.67E-06	1.67E-06	8.11E-07	2.15E-10
1.00	9.79E-07	9.79E-07	4.77E-07	8.56E-11

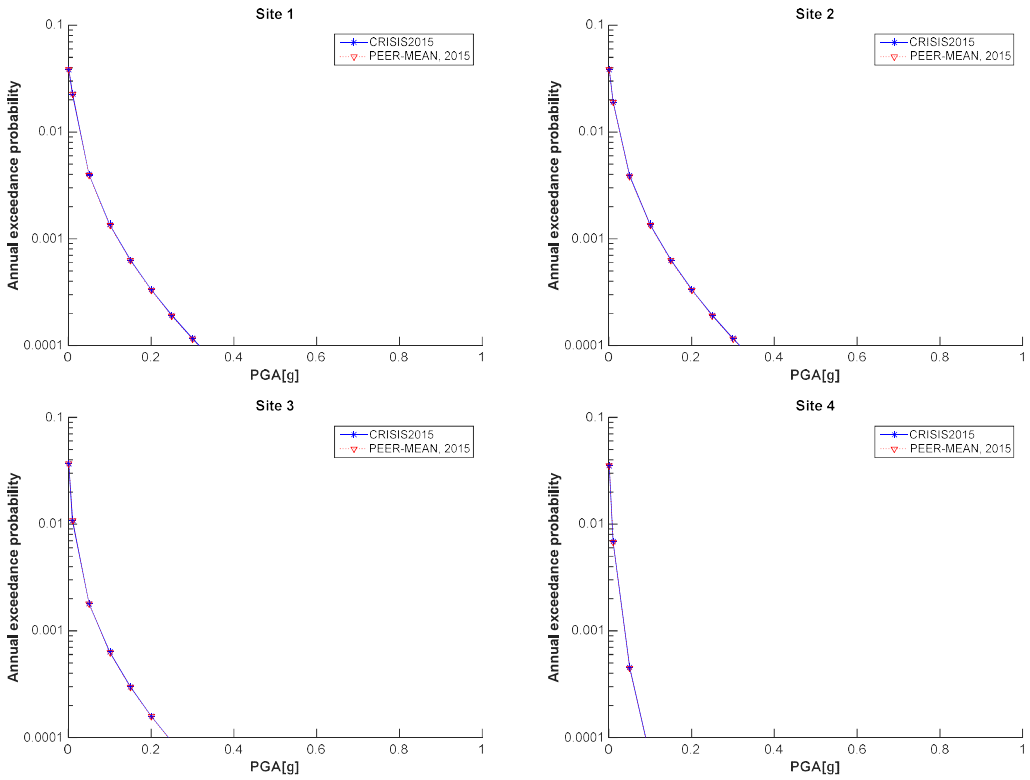

Figure 4-38 Comparison of the CRISIS and PEER-2015 results for Sites 1 to 4 (Set 1 Case 11)

4.1.18 Comments about the computation of distances

In the instructions provided by the PEER-2015 project the coordinates to generate each fault were included together with those of each computation site. Before showing the results of the validation and verification process, it is important to check the way in which R-CRISIS calculates the distance between two points and how it compares with the benchmark. Table 4-42 shows the distance computed by R-CRISIS for computation sites 1 and 2 of the Set 1 from where a slight difference can be seen.

Table 4-42 Real distance computed by R-CRISIS with the PEER project coordinates

Site	Latitude (degrees)	Longitude (degrees)	Distance between sites 1 and 2	
			Considered by PEER-2015 project	Computed by CRISIS2015
1	38.000*	-122.000*	25 km*	24.9798 km**
2	38.2248*	-122.000*		

To reach the same 25km distance between the two sites in R-CRISIS, small differences in the coordinates are needed as shown in Table 4-43.

Table 4-43 Adjustment on coordinates to estimate the same real distance in R-CRISIS

Site	Latitude (degrees)	Longitude (degrees)	Distance between sites 1 and 2
			Computed by CRISIS2015
1	38.000	-122.000	25.002 km
2	38.225	-122.000	

Seismic hazard calculations were made using both coordinates' values and no differences were obtained in the final results.

4.2 PEER validation tests (set 2)

A second phase of the PEER validation project was finished in 2018 (Hale et al., 2018). Among the PSHA tools, R-CRISIS was included. This second phase considered more complicated cases (e.g. multiple sources, the handling of state-of-the-art GMPMs – NGA West2 – and the modelling of complex intraslab sources) and again, the results obtained by R-CRISIS were compared against those provided as benchmark. As can be seen with detail in this section, the results obtained in R-CRISIS are highly satisfactory.

4.2.1 Set 2 case 1

Input parameters

Three different sources are used in this case, being two of them fault sources and the other an area source with constant depth as shown in Figure 4-39. The objective of this test is to review the estimation of hazard from multiple sources and to perform a disaggregation on the magnitude, distance and epsilon values. GMPE is set to Sadigh et al. (1997) for rock

conditions and untruncated σ. Details of the characteristics of the faults together with the magnitude density functions parameters are shown in Table 4-44.

Tables 4-45 and 4-46 show the geometry data associated to the fault sources whereas Table 4-47 includes the coordinates of the computation site together with the explanation of its relevance for the validation and verification purposes.

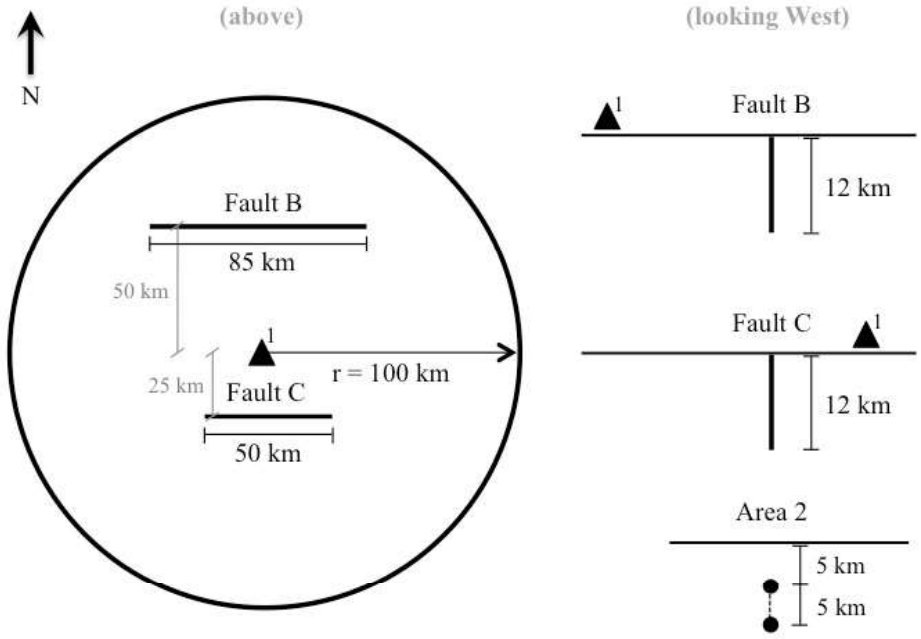

Figure 4-39 Geometry of the fault sources, the area source and the location of the observation size for Set 2, case 1

Table 4-44 Summary of input data for Set 2, case 1

Name	Description	Source	Mag-Density Function	Ground Motion Model	Rupture Dimension Relationships
Set 2 Case 1	Two faults and area source. Computation of hazard from multiple sources and M, R, ε dissagreggation. Ground motion variability, untruncated σ	Area 2 b-value=0.9	Truncated exponential, Mmax=6.5, Mmin=5.0	Sadigh et al. (1997), rock, untruncated σ	$Log(A) = M - 4; \sigma_A = 0$ $Log(W) = 0.5 * M - 2.15; \sigma_W = 0$ $Log(L) = 0.5 * M - 1.85; \sigma_L = 0$
		Fault B (vertical SS) b-value=0.9 slip-rate 2mm/yr	Y&C Model. Mmax=7.0, Mmin=5.0, Mchar=6.75		
		Fault C (vertical SS) b-value=0.9 slip-rate 1 mm/yr	Y&C Model. Mmax=6.75, Mmin=5.0, Mchar=6.5		

Table 4-45 Coordinates of the fault source B

Latitude	Longitude	Comment
0.44966	-65.3822	West end of fault
0.44966	-64.6178	East end of fault

Table 4-46 Coordinates of the fault source C

Latitude	Longitude	Comment
-0.22483	-65.2248	West end of fault
-0.22483	-64.7752	East end of fault

Table 4-47 Coordinates and comments of the computation site for set 2 case 1

Site	Latitude	Longitude	Comment
1	0.00000	-65.00000	In center of area source

Results

Results obtained in R-CRISIS for the estimation of seismic hazard from multiple sources at Site 1 are shown in Figure 4-40 together with the comparison against the benchmark values provided by PEER. From the plot it can be seen a complete agreement between the results obtained by R-CRISIS and those provided by PEER. Because of that, it can be concluded that R-CRISIS fulfills all the requirements evaluated by the PEER project in Set2-Case1.

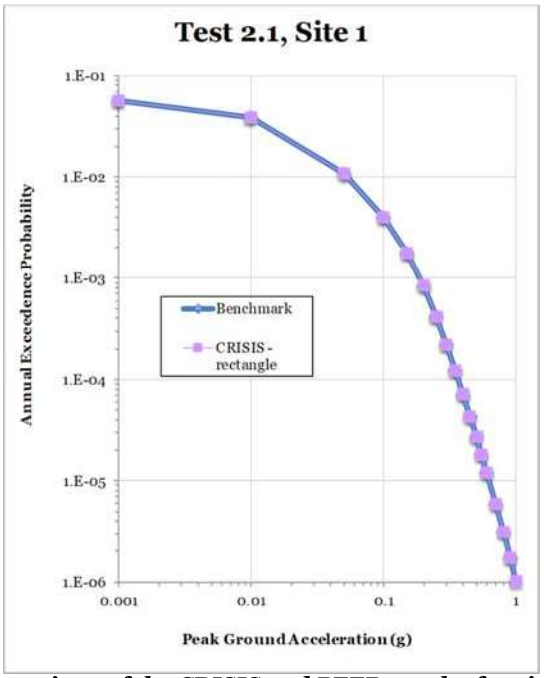

Figure 4-40 Comparison of the CRISIS and PEER results for site 1 (set 2 case 1)

In addition, Figures 4-41 to 4-43 show the comparison of the disaggregation results obtained by R-CRISIS and those provided as benchmark by PEER. The disaggregation was made for the following cases:

a) PGA 0.05g
b) PGA corresponding to a hazard of 0.001
c) PGA 0.35g

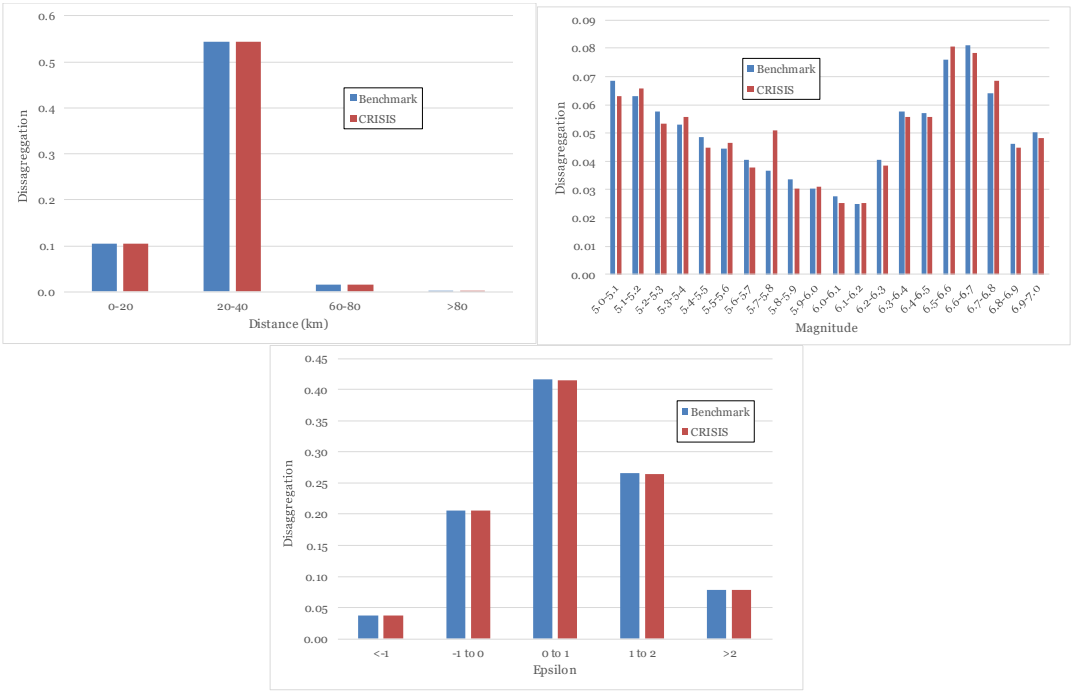

Figure 4-41 Comparison of the disaggregation results of CRISIS and PEER by distance (top left), magnitude (top right) and epsilon (bottom). PGA – 0.05g

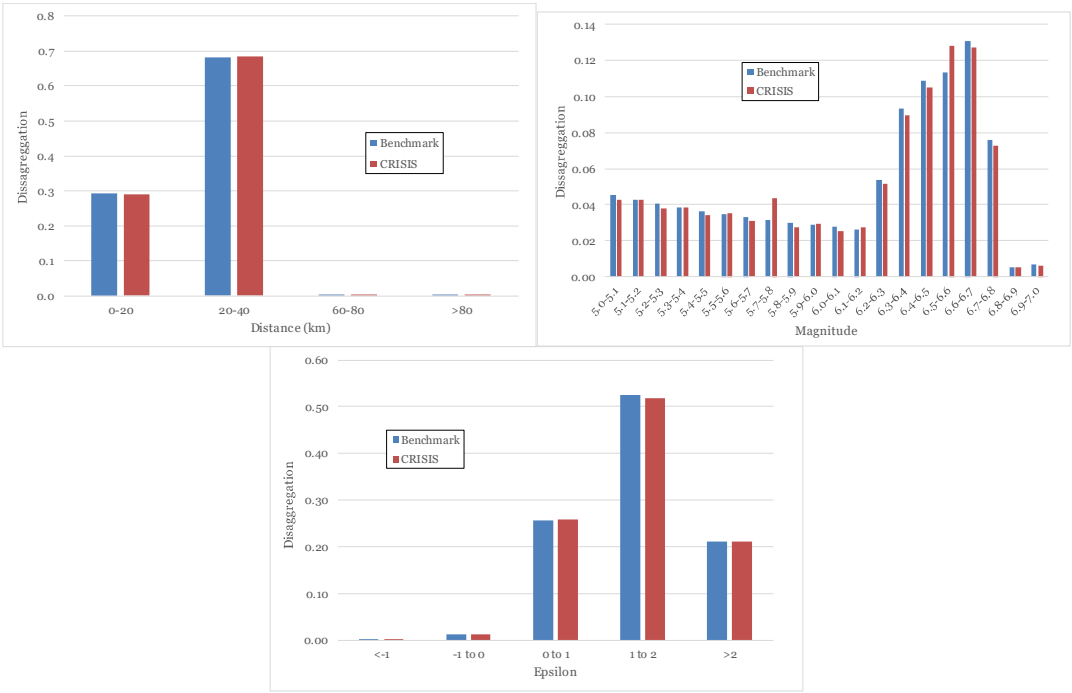

Figure 4-42 Comparison of the disaggregation results of CRISIS and PEER by distance (top left), magnitude (top right) and epsilon (bottom). PGA corresponding to a hazard of 0.001

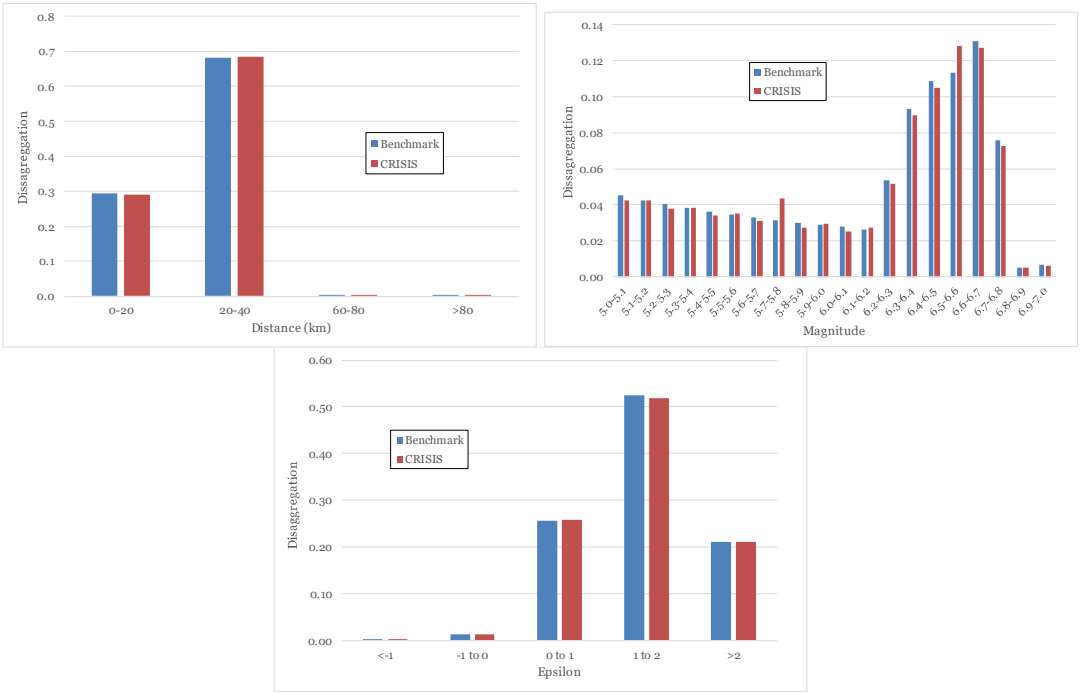

Figure 4-43 Comparison of the disaggregation results of CRISIS and PEER by distance (top left), magnitude (top right) and epsilon (bottom). PGA – 0.35g

4.2.2 Set 2 case 2

Input parameters

The source adopted for this case corresponds to fault 3 (see Figure 4-44). Seismicity input is specified through a b-value of 0.9, a slip rate of 2mm/yr and a magnitude density function in the form of a truncated exponential relationship with the minimum and magnitude values shown in Table 4-48. The objective of this test is to evaluate the handling of NGA-West2 ground-motion models (considering variability) for a source with strike-slip faulting mechanism.

Table 4-49 shows the data associated to the geometry of the fault source whereas Table 4-50 includes the coordinates of the computation sites together with an explanation about its relevance for validation and verification purposes.

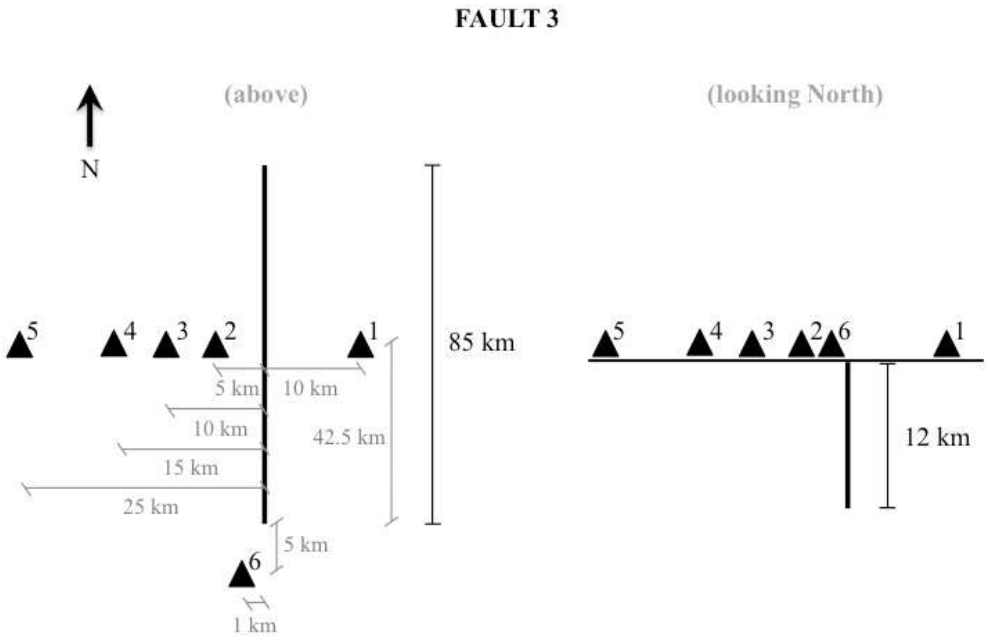

Figure 4-44 Geometry of the fault source and the location of the observation size for set 2, case 2

Table 4-48 Summary of input data for Set 2, case 2 (a,b,c,d)

Name	Description	Source	Mag-Density Function	Ground Motion Model[1,2,3,4]	Rupture Dimension Relationships
Set 2 Case 2	Single fault, NGA-West2 ground-motion models	Fault 3 (vertical SS) b-value=0.9 slip-rate 2mm/yr	Truncated exponential, Mmax=7.0, Mmin=5.0	NGA-West2; Damping ratio=5%; Vs30=760 m/s (measured); Z1.0=0.048 km; Z2.5=0.607 km; Region=California	$Log(A) = M - 4; \sigma_A = 0$ $Log(W) = 0.5 * M - 2.15; \sigma_W = 0$ $Log(L) = 0.5 * M - 1.85; \sigma_L = 0$

[1] Abrahamson et al. (2014) – σ untruncated

[2] Boore et al. (2014) – σ untruncated

[3] Campbell and Bozorgnia (2014) – σ untruncated
[4] Chiou and Youngs (2014) – σ untruncated

Note: These four GMPMs are included as built-in models in R-CRISIS

Table 4-49 Coordinates of the fault source 3

Latitude	Longitude	Comment
0.38221	-65.0000	North end of fault
-0.38221	-65.0000	South end of fault

Table 4-50 Coordinates and comments of the computation sites for set 2 case 2

Site	Latitude	Longitude	Comment
1	0.00000	-64.91005	10 km east of fault, at midpoint along strike
2	0.00000	-65.04497	5 km west of fault, at midpoint along strike
3	0.00000	-65.08995	10 km west of fault, at midpoint along strike
4	0.00000	-65.13490	15 km west of fault, at midpoint along strike
5	0.00000	-65.22483	25 km west of fault, at midpoint along strike
7	-0.42718	-65.00900	5 km south of southern end, 1 km west

Results for case 2a: Abrahamson et al. (2014)

Results obtained in R-CRISIS are shown in Figure 4-45 where the plots of the seismic hazard results obtained are compared against those provided as benchmark by PEER. In all the plots there is a complete agreement between the obtained results by R-CRISIS and the latter for the six computation sites.

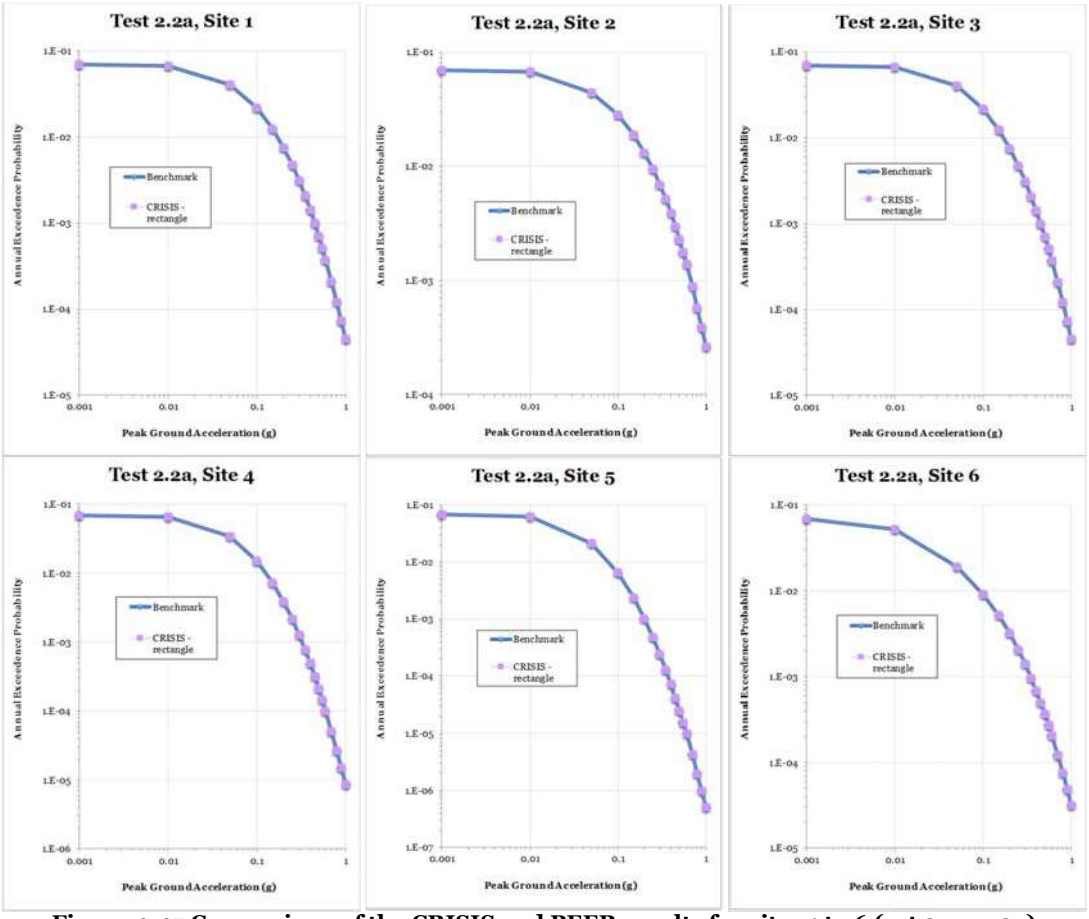

Figure 4-45 Comparison of the CRISIS and PEER results for sites 1 to 6 (set 2 case 2a)

Results for case 2b: Boore et al. (2014)

Results obtained in R-CRISIS are shown in Figure 4-46 where the plots of the seismic hazard results obtained are compared against those provided as benchmark by PEER. In all the plots there is a complete agreement between the obtained results by R-CRISIS and the latter for the six computation sites.

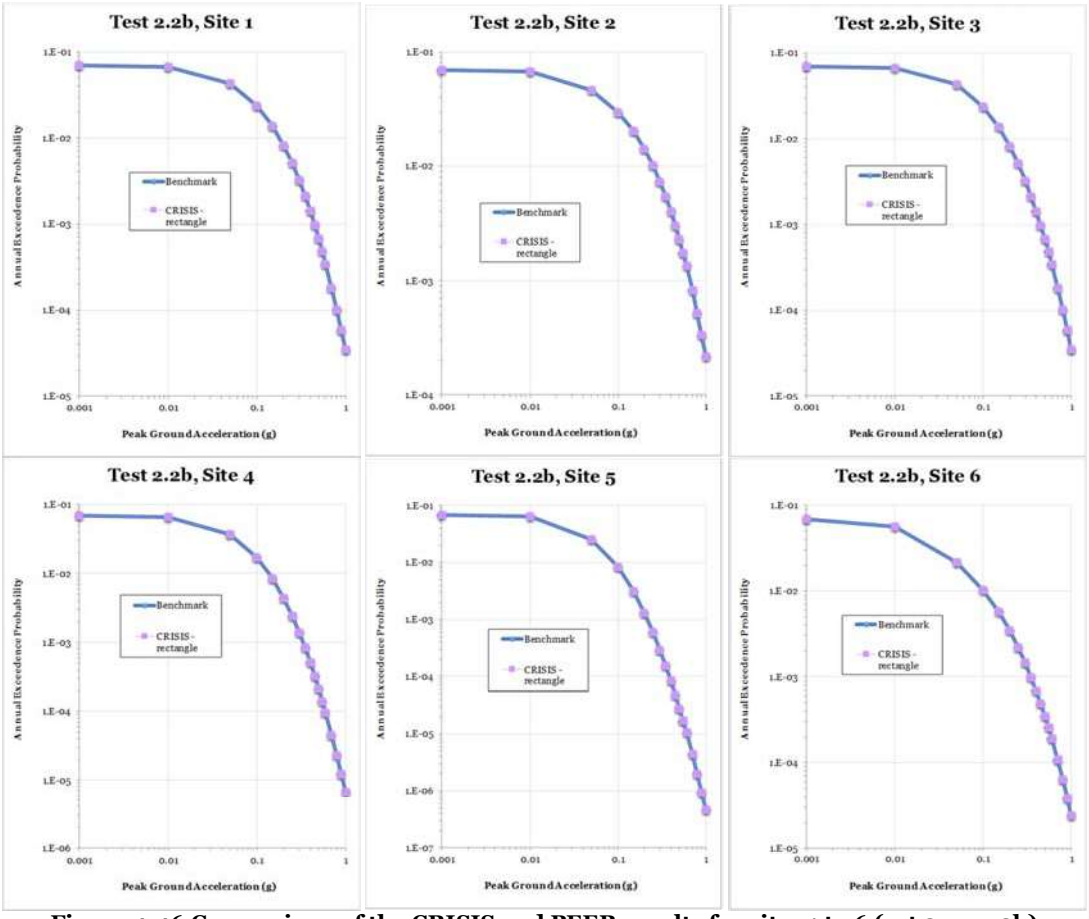

Figure 4-46 Comparison of the CRISIS and PEER results for sites 1 to 6 (set 2 case 2b)

Results for case 2c: Campbell and Bozorgnia (2014)

Results obtained in R-CRISIS are shown in Figure 4-47 where the plots of the seismic hazard results obtained are compared against those provided as benchmark by PEER. In all the plots there is a complete agreement between the obtained results by R-CRISIS and the latter for the six computation sites.

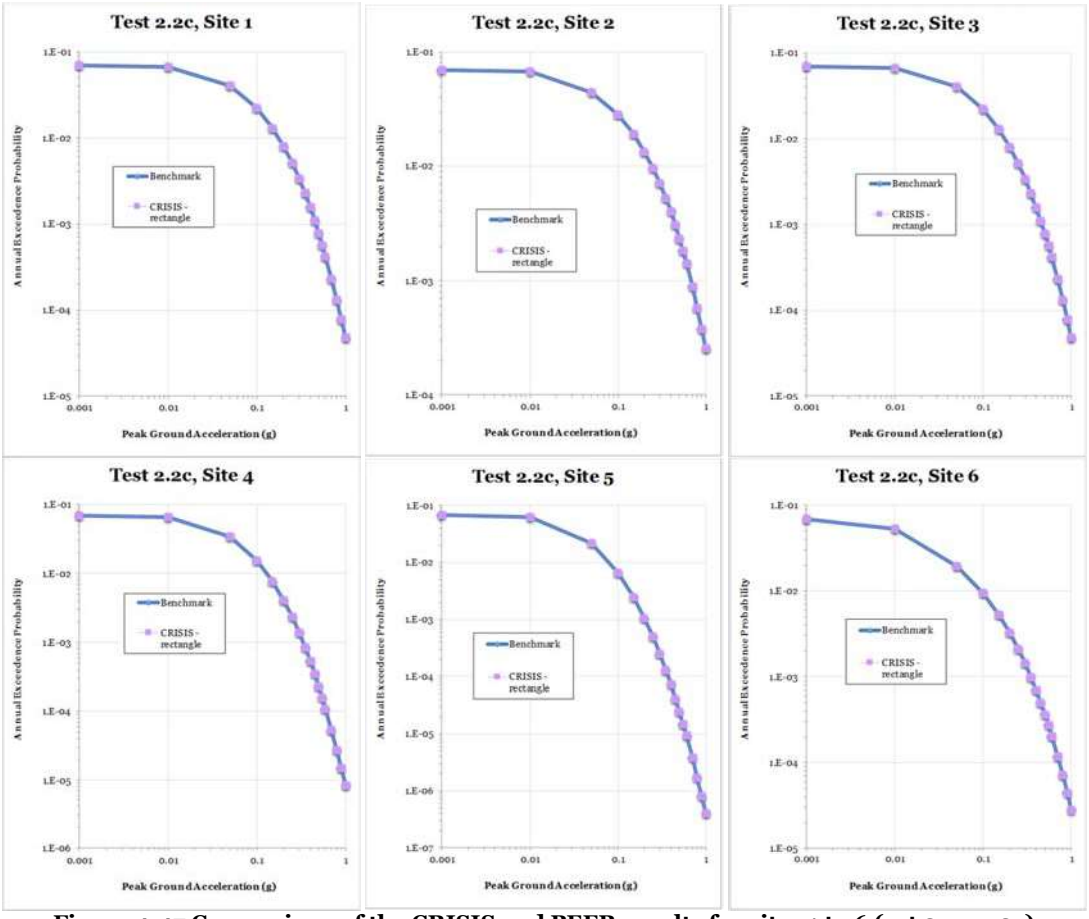

Figure 4-47 Comparison of the CRISIS and PEER results for sites 1 to 6 (set 2 case 2c)

Results for case 2d: Chiou and Youngs (2014)

Results obtained in R-CRISIS are shown in Figure 4-48 where the plots of the seismic hazard results obtained are compared against those provided as benchmark by PEER. In all the plots there is a complete agreement between the obtained results by R-CRISIS and the latter for the six computation sites.

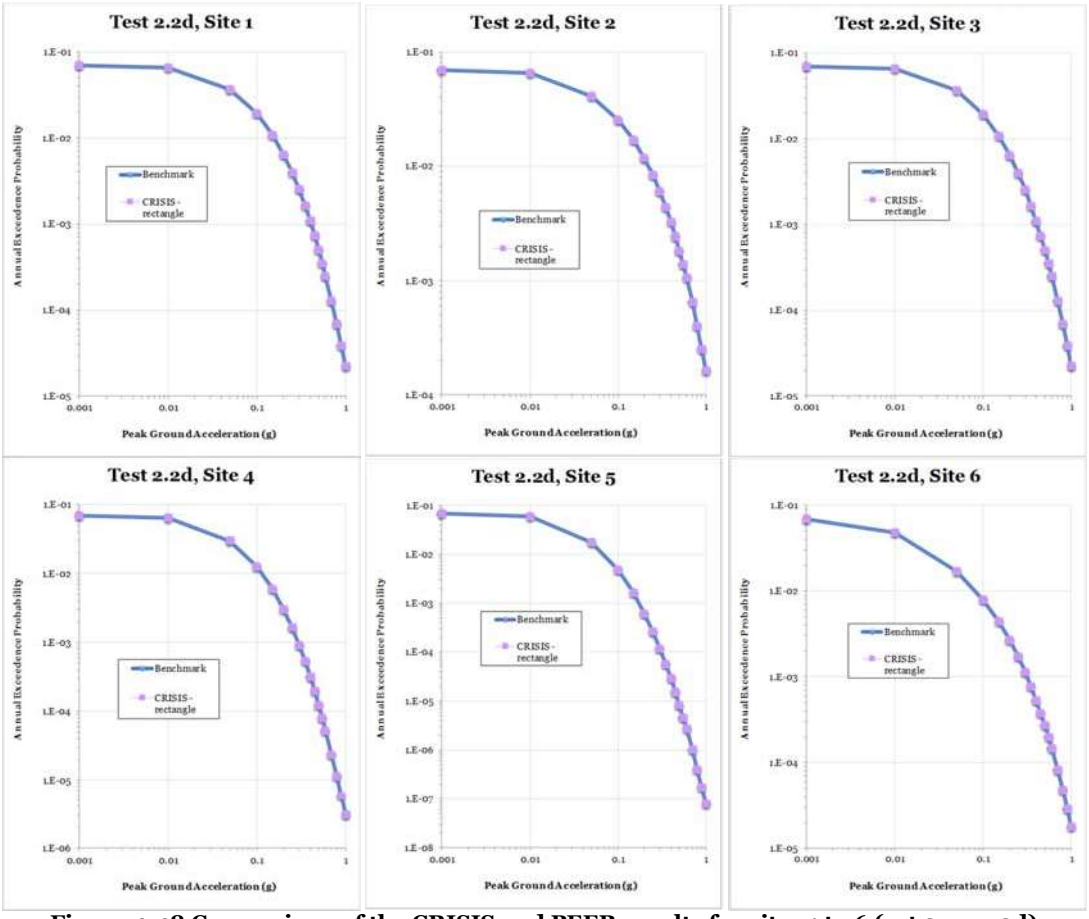

Figure 4-48 Comparison of the CRISIS and PEER results for sites 1 to 6 (set 2 case 2d)

4.2.3 Set 2 case 3

Input parameters

The source adopted for this case corresponds to fault 4 (see Figure 4-49), with reverse mechanism and 45° dip. Seismicity input is specified through a b-value of 0.9, a slip rate of 2mm/yr and a magnitude density function in the form of a delta function at M7.0 (see Table 4-51). The objective of this test is to evaluate the handling of NGA-West2 ground-motion models (considering variability) for a source with reverse faulting mechanism.

Table 4-52 shows the data associated to the geometry of the fault source whereas Table 4-53 includes the coordinates of the computation sites together with an explanation about its relevance for validation and verification purposes.

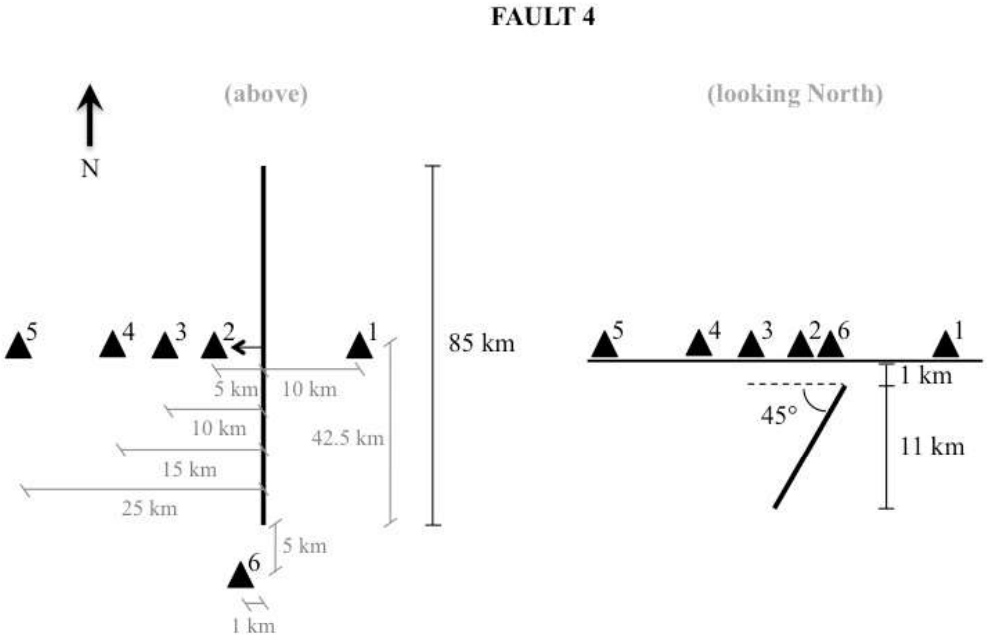

Figure 4-49 Geometry of the fault source and the location of the observation size for set 2, case 3

Table 4-51 Summary of input data for set 2, case 3 (a,b,c,d)

Name	Description	Source	Mag-Density Function	Ground Motion Model[1,2,3,4]	Rupture Dimension Relationships
Set 2 Case 3	Single fault, NGA-West2 ground-motion models	Fault 4 (reverse, 45°dip) b-value=0.9 slip-rate 2mm/yr	Delta function at M7.0	NGA-West2; Damping ratio=5%; Vs30=760 m/s (measured); Z1.0=0.048 km; Z2.5=0.607 km; Region=California	$Log(A) = M - 4; \sigma_A = 0$ $Log(W) = 0.5 * M - 2.15; \sigma_W = 0$ $Log(L) = 0.5 * M - 1.85; \sigma_L = 0$

[1] Abrahamson et al. (2014) – σ untruncated
[2] Boore et al. (2014) – σ untruncated
[3] Campbell and Bozorgnia (2014) – σ untruncated
[4] Chiou and Youngs (2014) – σ untruncated

Note: These four GMPMs are included as built-in models in R-CRISIS

Table 4-52 Coordinates of the fault source 4

Latitude	Longitude	Comment
0.38221	-65.0000	North end of fault
-0.38221	-65.0000	South end of fault

Table 4-53 Coordinates and comments of the computation sites for set 2 case 3

Site	Latitude	Longitude	Comment
1	0.00000	-64.91005	10 km east of fault, at midpoint along strike
2	0.00000	-65.04497	5 km west of fault, at midpoint along strike
3	0.00000	-65.08995	10 km west of fault, at midpoint along strike
4	0.00000	-65.13490	15 km west of fault, at midpoint along strike
5	0.00000	-65.22483	25 km west of fault, at midpoint along strike
7	-0.42718	-65.00900	5 km south of southern end, 1 km west

Results for case 3a: Abrahamson et al. (2014)

Results obtained in R-CRISIS are shown in Figure 4-50 where the plots of the seismic hazard results obtained are compared against those provided as benchmark by PEER. In all the plots there is a complete agreement between the obtained results by R-CRISIS and the latter for the six computation sites.

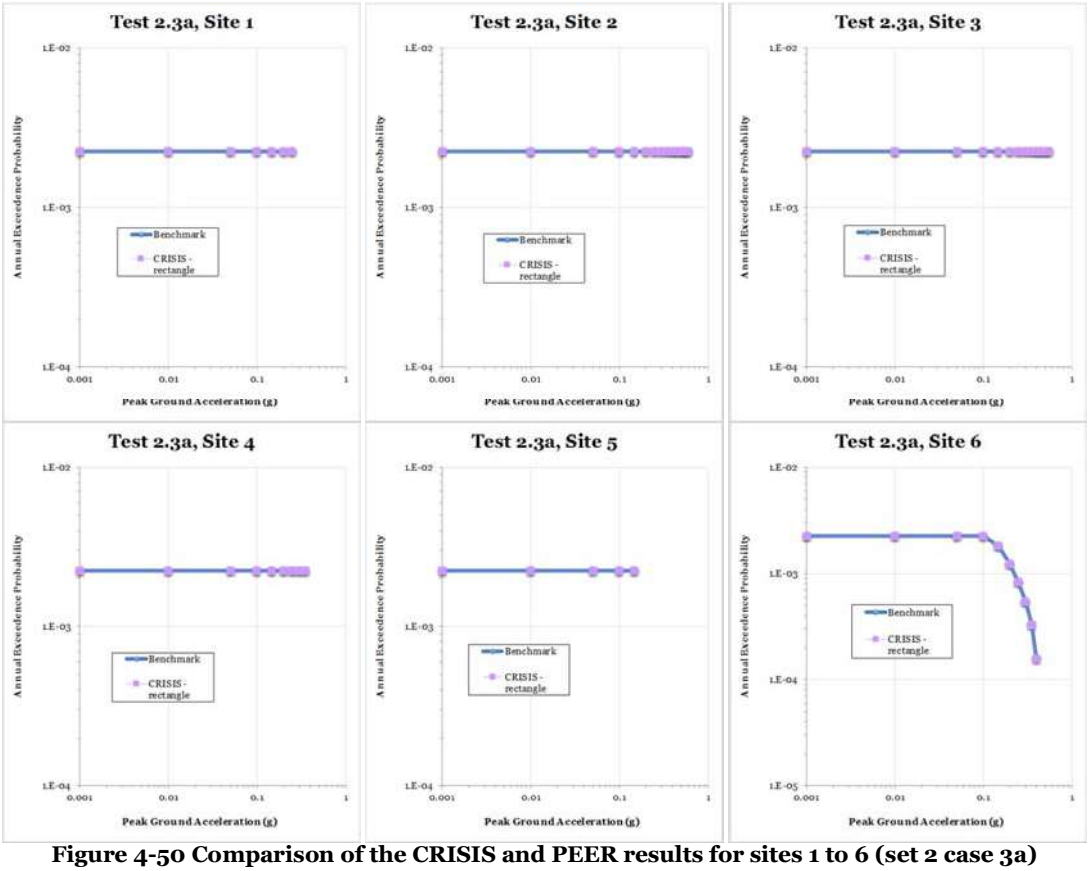

Figure 4-50 Comparison of the CRISIS and PEER results for sites 1 to 6 (set 2 case 3a)

Results for case 3b: Boore et al. (2014)

Results obtained in R-CRISIS are shown in Figure 4-51 where the plots of the seismic hazard results obtained are compared against those provided as benchmark by PEER. In all the plots

there is a complete agreement between the obtained results by R-CRISIS and the latter for the six computation sites.

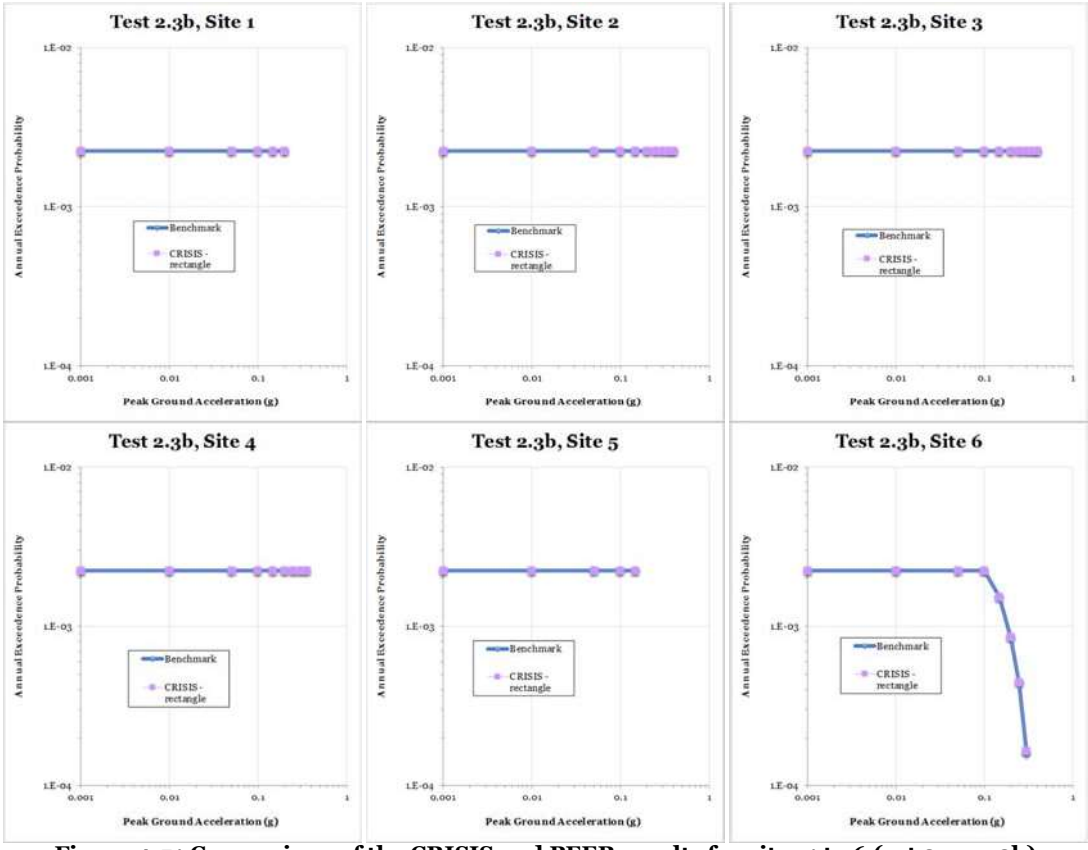

Figure 4-51 Comparison of the CRISIS and PEER results for sites 1 to 6 (set 2 case 3b)

Results for case 3c: Campbell and Bozorgnia (2014)

Results obtained in R-CRISIS are shown in Figure 4-52 where the plots of the seismic hazard results obtained are compared against those provided as benchmark by PEER. In all the plots there is a complete agreement between the obtained results by R-CRISIS and the latter for the six computation sites.

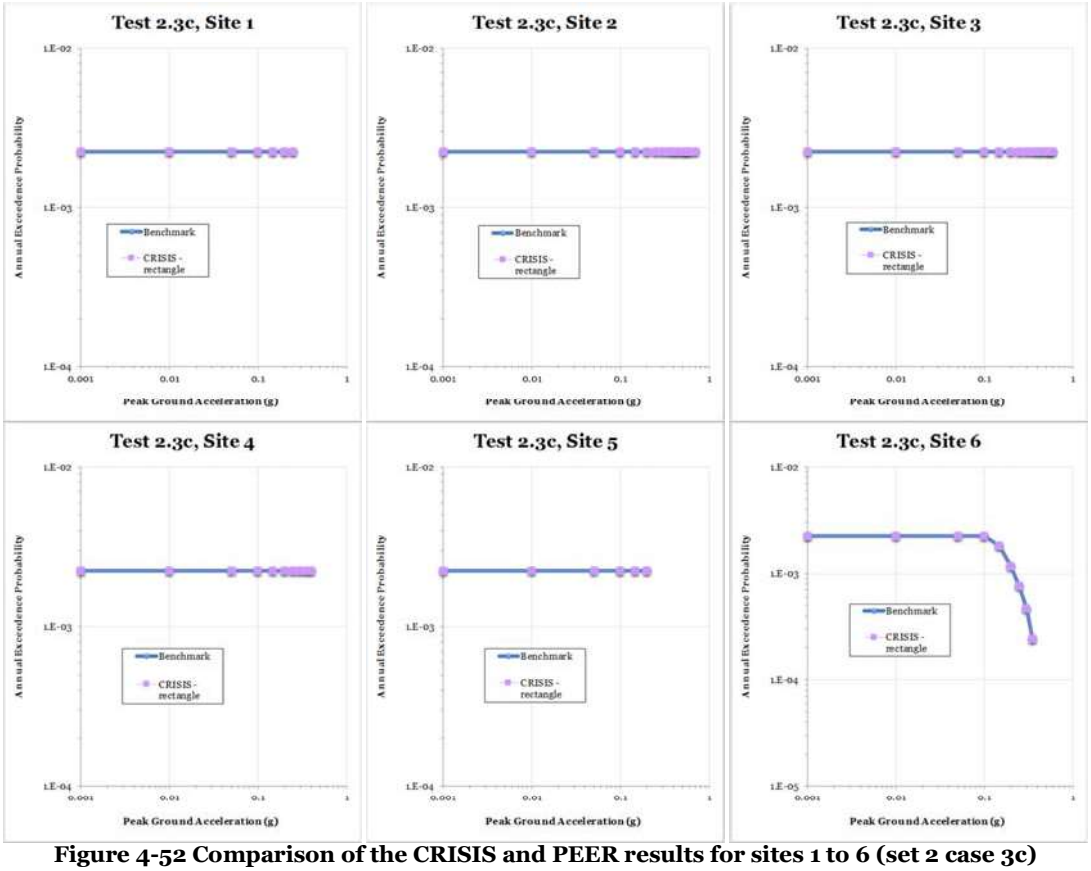

Figure 4-52 Comparison of the CRISIS and PEER results for sites 1 to 6 (set 2 case 3c)

Results for case 3d: Chiou and Youngs (2014)

Results obtained in R-CRISIS are shown in Figure 4-53 where the plots of the seismic hazard results obtained are compared against those provided as benchmark by PEER. In all the plots there is a complete agreement between the obtained results by R-CRISIS and the latter for the six computation sites.

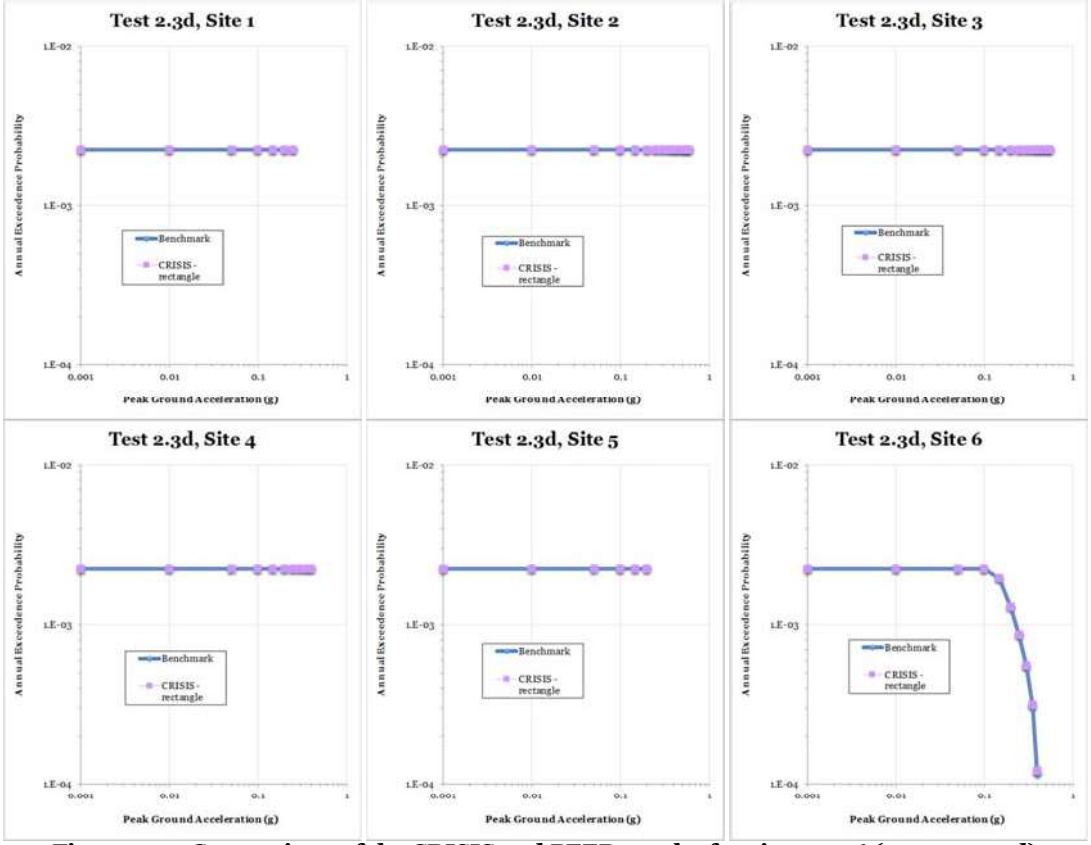

Figure 4-53 Comparison of the CRISIS and PEER results for sites 1 to 6 (set 2 case 3d)

4.2.4 Set 2 case 4a

Input parameters

The source adopted for this case corresponds to fault 5 (see Figure 4-54), with strike-slip mechanism and 90° dip. Seismicity input is specified through a b-value of 0.9, a slip rate of 2mm/yr and a magnitude density function in the form of a delta function at M6.0 (see Table 4-54). The objective of this test is to evaluate the results when using an uniform distribution down dip of the epicenters.

Table 4-55 shows the data associated to the geometry of the fault source whereas Table 4-56 includes the coordinates of the computation site together with an explanation about its relevance for validation and verification purposes.

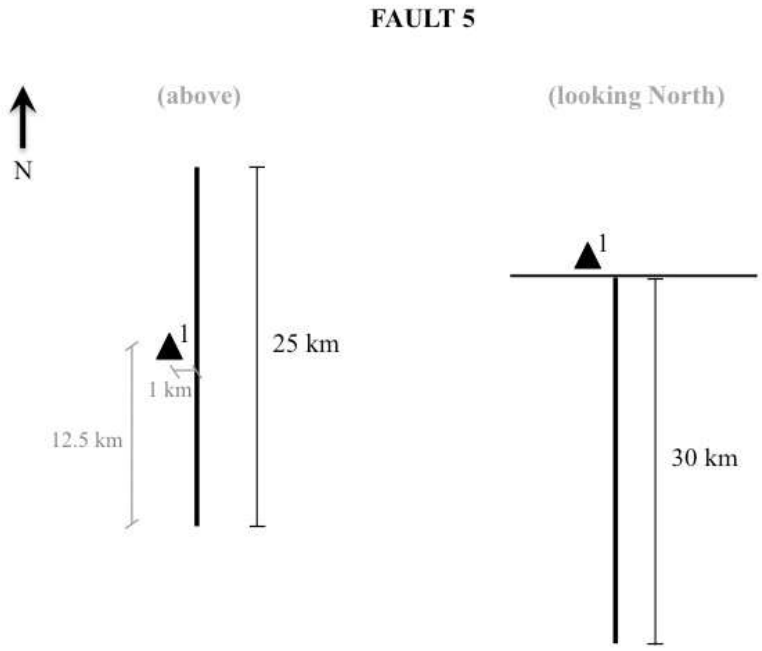

Figure 4-54 Geometry of the fault source and the location of the observation size for set 2, case 4a

Table 4-54 Summary of input data for Set 2, case 4a

Name	Description	Source	Mag-Density Function	Ground Motion Model	Rupture Dimension Relationships
Set 2 Case 4a	Single fault, NGA-West2 ground motion model, uniform distribution down dip	Fault 5 (vertical SS) b-value=0.9 slip-rate 2mm/yr	Delta function at M6.0	Chiou and Youngs (2014); σ=0; Damping ratio=5%; Vs30=760 m/s (measured); Z1.0=0.048 km; Z2.5=0.607 km; Region=California	$Log(A) = M - 4; \sigma_A = 0$ $Log(W) = 0.5 * M - 2.15; \sigma_W = 0$ $Log(L) = 0.5 * M - 1.85; \sigma_L = 0$

Table 4-55 Coordinates of the fault source 5

Latitude	Longitude	Comment
0.11240	-65.0000	North end of fault
-0.11240	-65.0000	South end of fault

Table 4-56 Coordinates and comments of the computation site for set 2 case 4a

Site	Latitude	Longitude	Comment
1	0.00000	-65.00900	1 km west of fault, at midpoint along strike

Results

Results obtained in R-CRISIS for the estimation of seismic hazard at Site 1 are shown in Figure 4-55 together with the comparison against the benchmark values provided by PEER. In all the plots, it can be seen a complete agreement between the results obtained by R-CRISIS and those provided by PEER. Because of that, it can be concluded that R-CRISIS fulfills all the requirements evaluated by the PEER project in Set2-Case4a.

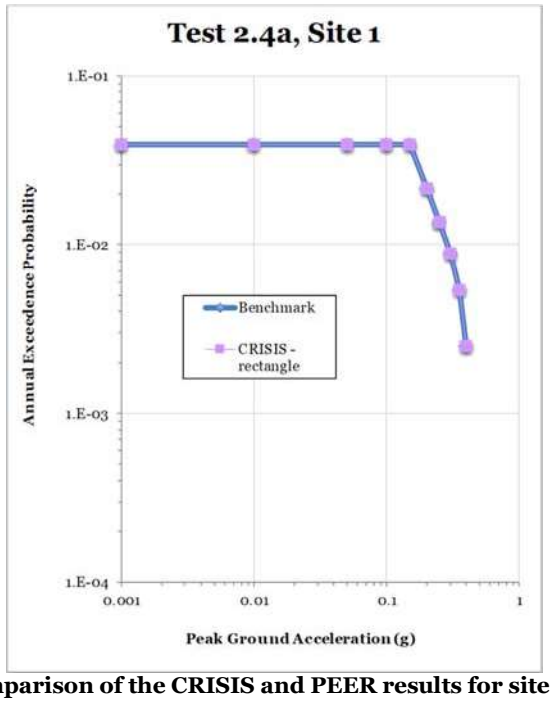

Figure 4-55 Comparison of the CRISIS and PEER results for site 1 (set 2 case 4a)

Note: The implementation of non-uniform hypocenter distributions (set 2 case 4b) is not yet implemented in R-CRISIS.

4.2.5 Set 2 case 5a

Input parameters

The source adopted for this case corresponds to fault 5 (see Figure 4-56), with strike-slip mechanism and 90° dip. Seismicity input is specified through a b-value of 0.9, a slip rate of 2mm/yr and a magnitude density function in the form of a delta function at M6.0 (see Table 4-57). The objective of this test is to evaluate the capability of R-CRISIS to model a normal distribution out to high epsilon values.

Table 4-58 shows the data associated to the geometry of the fault source whereas Table 4-59 includes the coordinates of the computation sites together with an explanation about its relevance for validation and verification purposes.

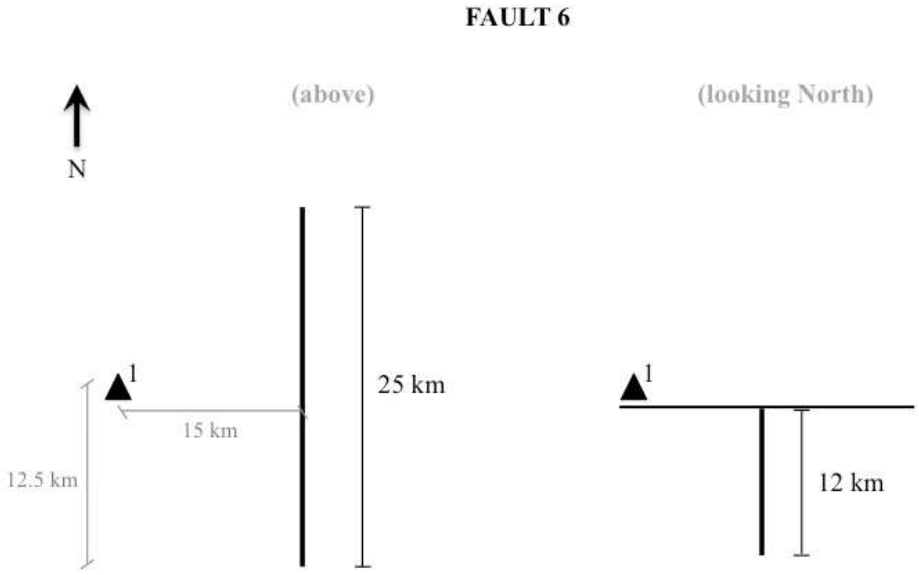

Figure 4-56 Geometry of the fault source and the location of the observation size for set 2, cases 5a-5b

Table 4-57 Summary of input data for Set 2, case 5a

Name	Description	Source	Mag-Density Function	Ground Motion Model	Rupture Dimension Relationships
Set 2 Case 5a	Single fault, NGA-West2 ground motion model, extreme tails	Fault 6 (vertical SS) b-value=0.9 slip-rate 2mm/yr	Delta function at M6.0	Chiou and Youngs (2014); σ=0.65 (untruncated); Damping ratio=5%; Vs30=760 m/s (measured); Z1.0=0.048 km; Z2.5=0.607 km; Region=California	$Log(A) = M - 4; \sigma_A = 0$ $Log(W) = 0.5 * M - 2.15; \sigma_W = 0$ $Log(L) = 0.5 * M - 1.85; \sigma_L = 0$

Table 4-58 Coordinates of the fault source 6

Latitude	Longitude	Comment
0.11240	-65.0000	North end of fault
-0.11240	-65.0000	South end of fault

Table 4-59 Coordinates and comments of the computation site for set 2 cases 5a-5b

Site	Latitude	Longitude	Comment
1	0.00000	-65.13490	15 km west of fault, at midpoint along strike

Results

Results obtained in R-CRISIS for the estimation of seismic hazard at Site 1 are shown in Figure 4-57 together with the comparison against the benchmark values provided by PEER. In all the plots, it can be seen a complete agreement between the results obtained by R-CRISIS

and those provided by PEER. Because of that, it can be concluded that R-CRISIS fulfills all the requirements evaluated by the PEER project in Set2-Case5a.

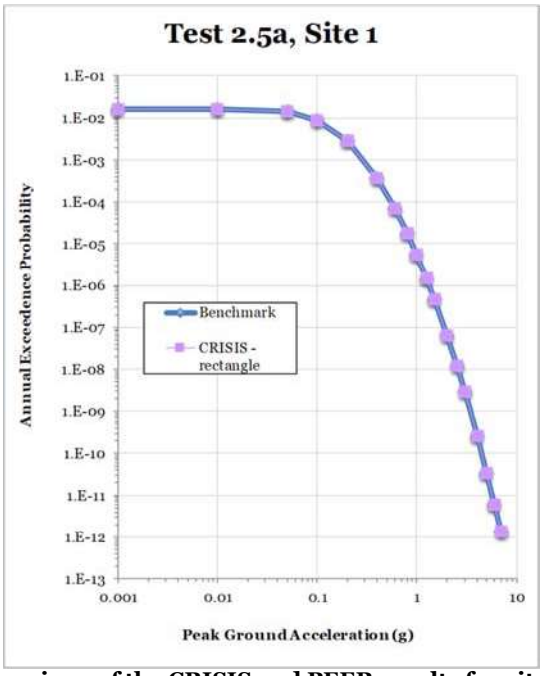

Figure 4-57 Comparison of the CRISIS and PEER results for site 1 (set 2 case 5a)

4.2.6 Set 2 case 5b

Input parameters

The source adopted for this case corresponds again to fault 6 (see Figure 4-56), with strike-slip mechanism and 90° dip. Seismicity input is specified through a b-value of 0.9, a slip rate of 2mm/yr and a magnitude density function in the form of a delta function at M6.0 (see Table 4-60). The objective of this test is to evaluate the consideration of mixture models (combination of two log-normal distribution).

The geometry of the source as well as the computation site are the same as in set 2 case 5a (Tables 4-58 and 4-59).

Table 4-60 Summary of input data for Set 2, case 5b

Name	Description	Source	Mag-Density Function	Ground Motion Model	Rupture Dimension Relationships
Set 2 Case 5b	Single fault, NGA-West2 ground motion model, mixture model, wmix1=0.5; wmix2=0.5; σmix1= 1.2σ; σmix2= 0.8σ	Fault 6 (vertical SS) b-value=0.9 slip-rate 2mm/yr	Delta function at M6.0	Chiou and Youngs (2014); σ=0.65 (untruncated); Damping ratio=5%; Vs30=760 m/s (measured); Z1.0=0.048 km; Z2.5=0.607 km; Region=California	$Log(A) = M - 4; \sigma_A = 0$ $Log(W) = 0.5 * M - 2.15; \sigma_W = 0$ $Log(L) = 0.5 * M - 1.85; \sigma_L = 0$

Results

Results obtained in R-CRISIS for the estimation of seismic hazard at Site 1 are shown in Figure 4-58 together with the comparison against the benchmark values provided by PEER. In all the plots, it can be seen a complete agreement between the results obtained by R-CRISIS and those provided by PEER. Because of that, it can be concluded that R-CRISIS fulfills all the requirements evaluated by the PEER project in Set2-Case5b.

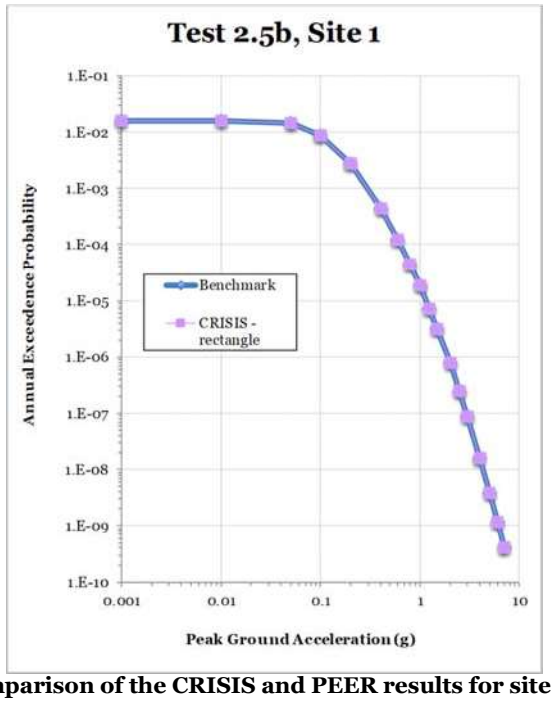

Figure 4-58 Comparison of the CRISIS and PEER results for site 1 (set 2 case 5b)

4.3 PEER validation tests (set 3)

Set 3 of the PEER validation tests aimed to verify the most complex elements of the PSHA codes. For example, the consideration of a bending fault, how the mean hazard and fractiles from logic trees, the modeling of intraslab sources at a subduction source and also the consideration of finite ruptures within area sources. Because there is not a single approach for the solution of any of these cases, no benchmark results were provided, reason why the reader is referred to the original reference (Hale et al., 2018) for reviewing the obtained results.

4.4 Validation against some analytical solutions

PSHA is, essentially, an integration process with respect to two variables, distance and magnitude. Said integration process is performed numerically by R-CRISIS, which is capable of solving general cases that involve geographic source layouts and GMPM. Since complex cases can only be solved numerically, the accuracy of the program can be tested by comparing the numerical solutions obtained in simple cases against their analytical solutions.

This section includes the comparison of the numerical and analytical solutions of the three cases proposed by Ordaz (2004) which although simple, are useful as canonical ones against which to calibrate the numerical code of R-CRISIS. The three cases have the following characteristics:

- Case 1: Point source with deterministic GMPM
- Case 2: Point source with probabilistic GMPM
- Case 3: Area source with probabilistic GMPM

In all cases the modified G-R seismicity model is used with the values of the parameters shown in Table 4-61.

Table 4-61 Seismicity parameters for the comparison against the analytical solution

M_o	4.0
λ_o	1.0
β	2.0
M_U	8.0

Also, a GMPM with the form:

$$E(\ln a) = a_1 + a_2 M + a_3 \ln R + a_4 R \qquad \text{(Eq. 4-13)}$$

with the coefficients proposed by Ordaz et al. (1989) is used.

4.4.1 Case 1: Point source with deterministic GMPM

This is the simplest case that considers a point source located at R=30 km from the computation site which seismicity is characterized by means of a modified G-R model with the parameters shown in Table 4-61. The GMPM shown in equation 4-13 with σ=0 is used. Figure 4-59 shows the comparison between the analytical and the numerical solutions for the simplest of the three cases.

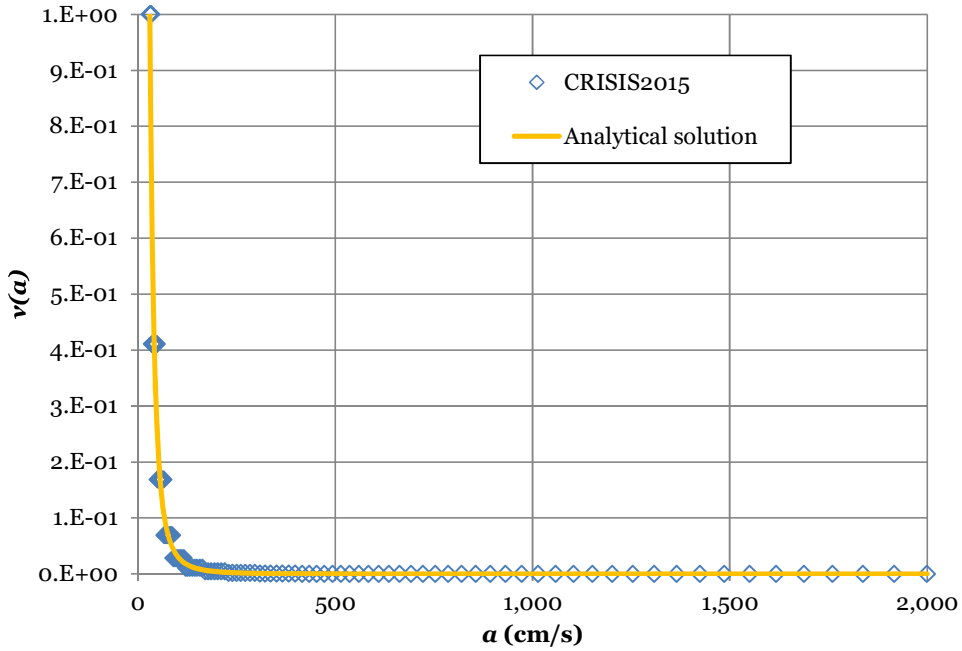

Figure 4-59 Comparison of analytical and numerical solutions for Case 1 of Ordaz (2004)

4.4.2 Case 2: Point source with probabilistic GMPM

This case is similar as the previous one with the difference that now the uncertainty in the GMPM is accounted for during the calculation process. For this purpose, different values of σ are used (0.3, 0.5 and 0.7). Figures 4-60 to 4-62 show the comparison between the analytical and the numerical solutions for this case considering different sigma values.

Note: no truncation has been considered in this case.

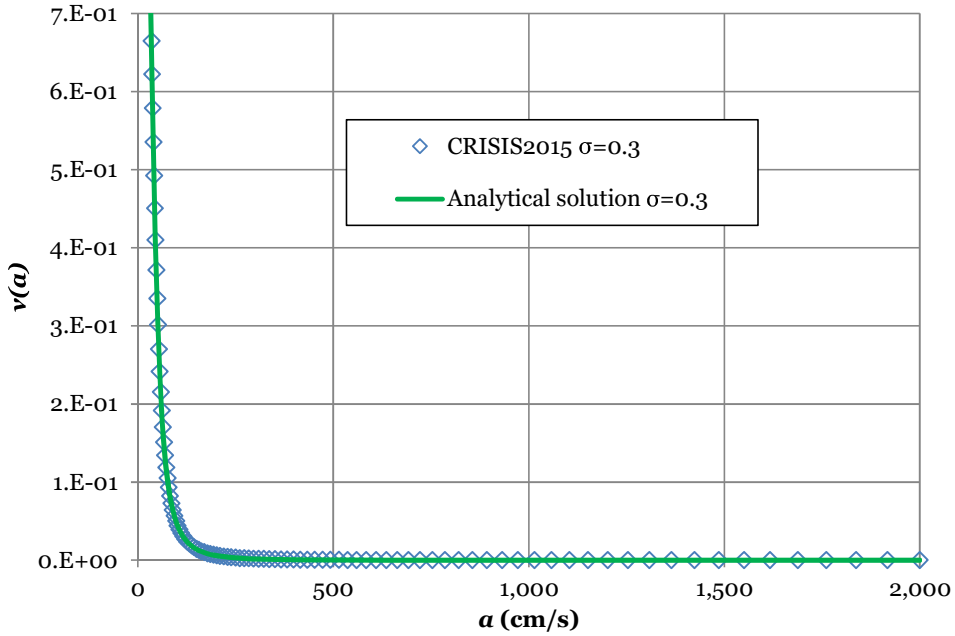

Figure 4-60 Comparison of analytical and numerical solutions for Case 2 of Ordaz (2004); σ=0.3

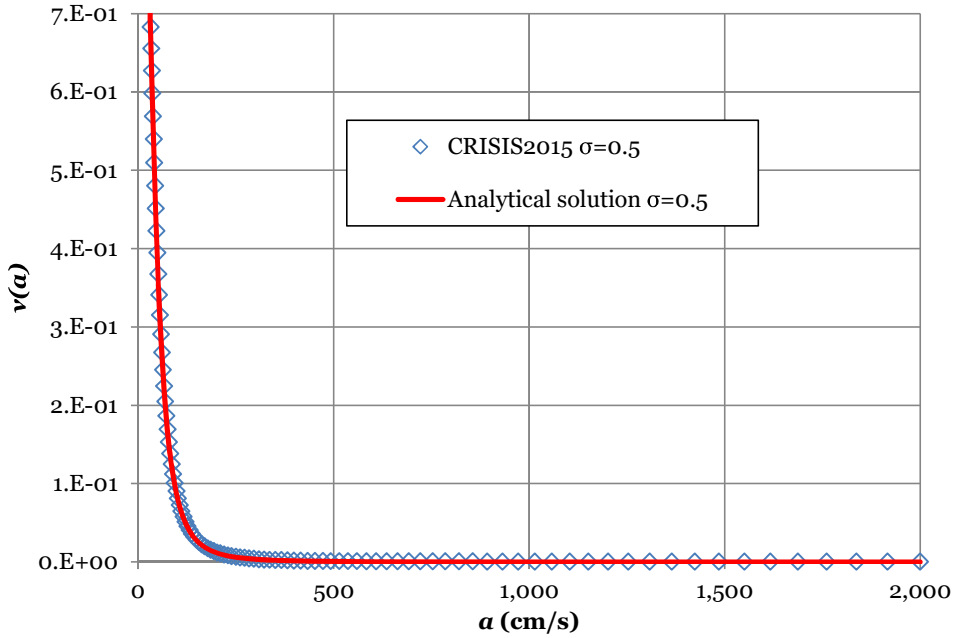

Figure 4-61 Comparison of analytical and numerical solutions for Case 2 of Ordaz (2004); σ=0.5

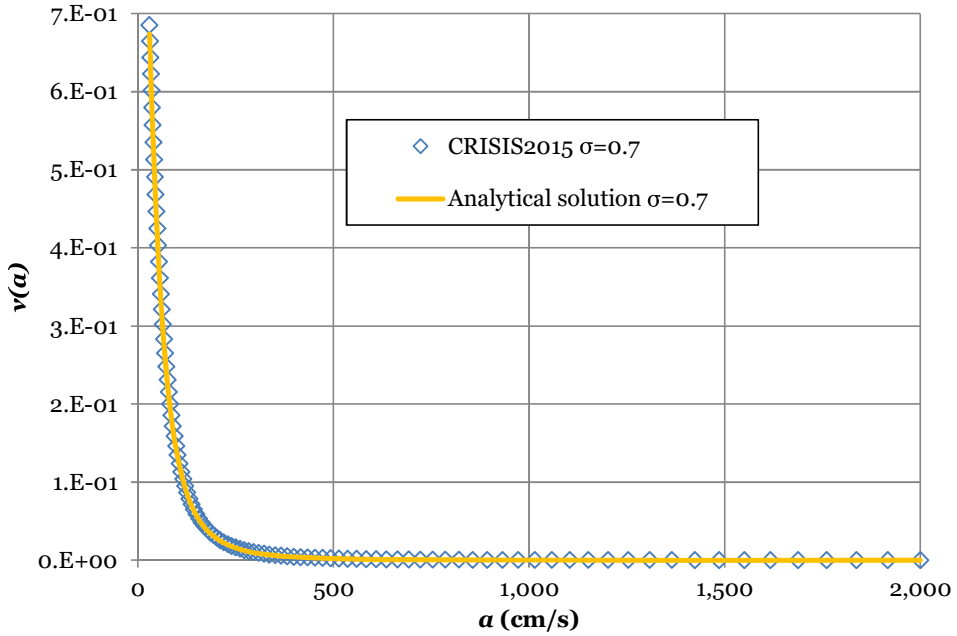

Figure 4-62 Comparison of analytical and numerical solutions for Case 2 of Ordaz (2004); σ=0.7

4.4.3 Case 3: Area source with probabilistic GMPM

For this case which corresponds to an area source, the latter is represented by means of a disc with uniform seismicity with a radius of 50 km, located at a depth equal to 10 km. The GMPM with σ=0.7 is used herein. Figure 4-63 shows the comparison between the analytical and numerical solutions.

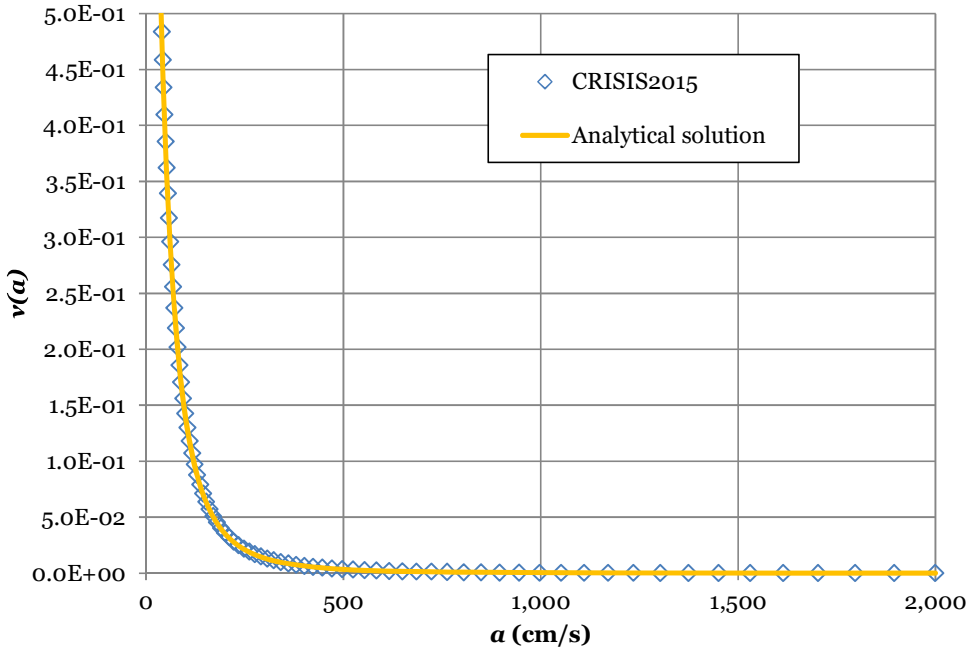

Figure 4-63 Comparison of analytical and numerical solutions for Case 3 of Ordaz (2004)

4.5 GMPM validation tests

Some of the built-in GMPM available in R-CRISIS have been validated (see Table 2-20) by means of different procedures based on the raw data availability for performing comparisons, verifications and validations. Those range from direct comparison against data published by the GMPM developers, direct contact with the authors in order to access to some information and graphical comparisons with the figures published in the dissemination reports and/or academic journals. Also, some authors of R-CRISIS have participated in the development of GMPM included in the built-in set and for those cases, even if no formal validation process has been applied, they are assumed to be properly implemented in the program.

The following sections summarize this process considering the different selected approaches with the aim of showing in a transparent way how said procedure has been developed.

4.5.1 Comparison against published raw data

For some of the GMPM developed under the NGA-West2 framework, the raw data for different magnitudes, distances, spectral ordinates and other characteristics (e.g. dip, V_{s30}, etc.) was published by the authors. Using those and the results obtained after the implementation of said GMPM as built-in models in R-CRISIS, different comparisons were performed to validate the latter.

Abrahamson et al. (2014)

Figures 4-64 and 4-65 show the comparison between the authors' values (median and percentile 84 respectively) and those obtained in R-CRISIS for the Abrahamson et al. (2014) GMPM with:

- M=7
- R_{RUP}=10 km
- V_{s30}=760 m/s
- Frv=1
- FHW=1
- Dip=90º

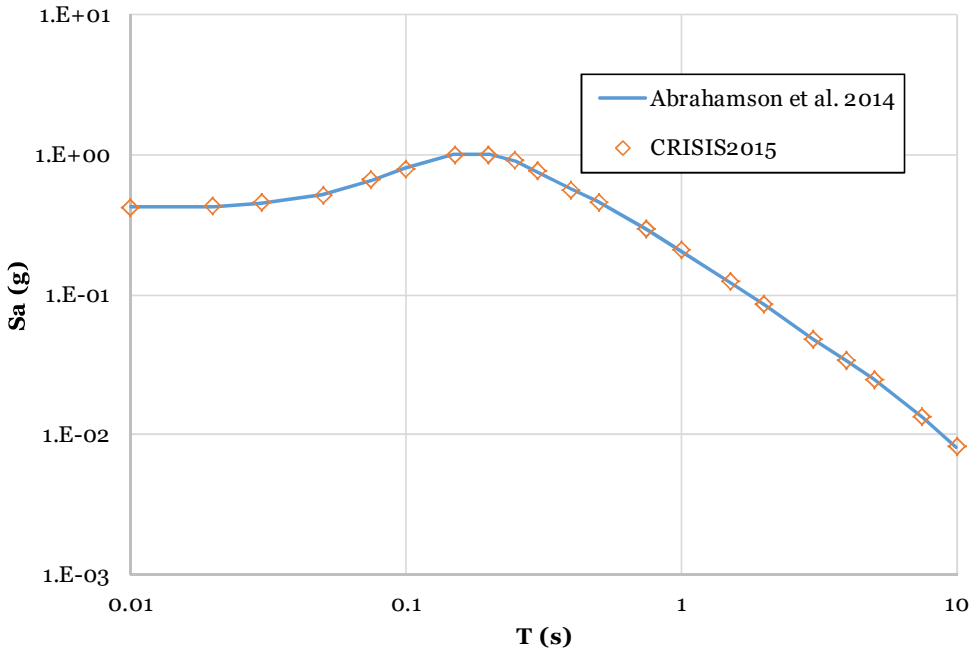

Figure 4-64 Comparison of median values between original and built-in Abrahamson et al. (2014) GMPM

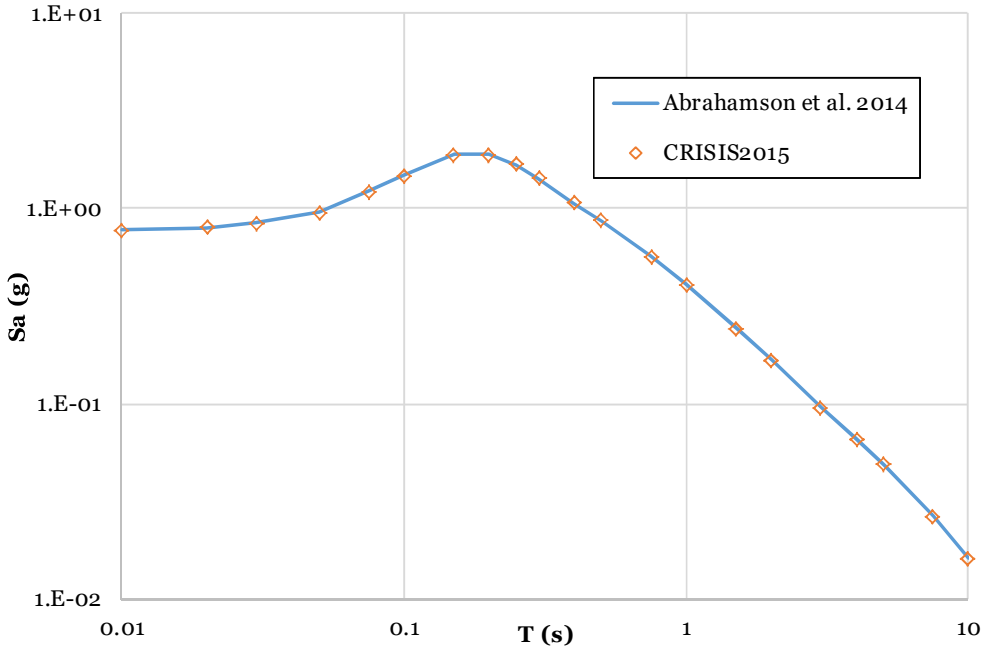

Figure 4-65 Comparison of percentile 84 values between original and built-in Abrahamson et al. (2014) GMPM

From both figures, the total congruence along the spectral range can be found. Results of the same type were obtained for other magnitude, V_{s30}, dip and distance values.

Chiou and Youngs (2014)

Figures 4-66 and 4-67 show the comparison between the author's values (median) and those obtained in R-CRISIS for the Chiou and Youngs (2014) GMPM for four magnitudes (5.5, 6.5, 7.5 and 8.5) with Rx=1 and Rx=10 km respectively. From both figures, the total congruence along the spectral range can be found.

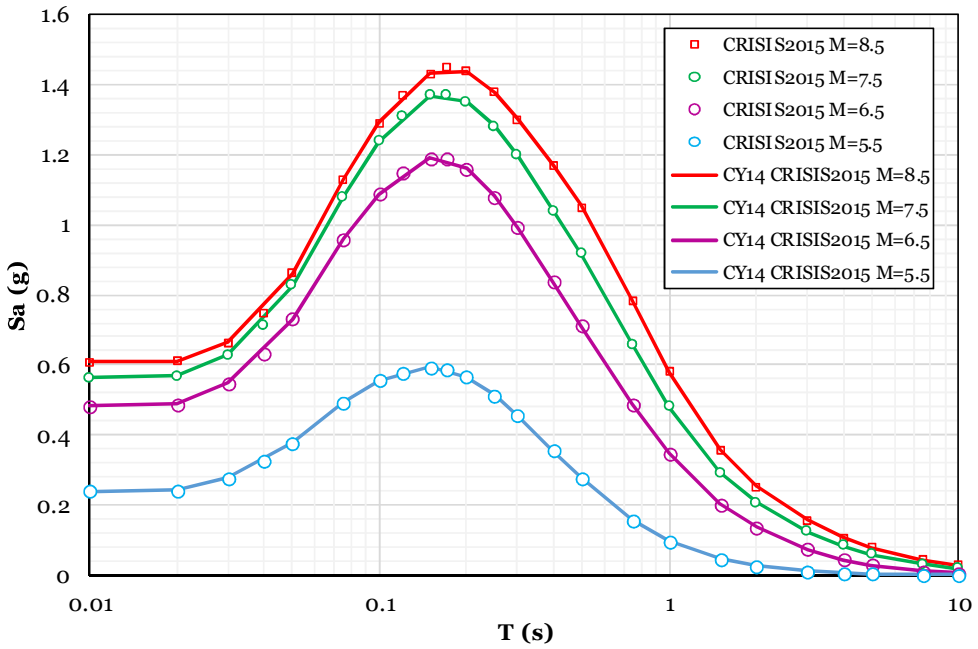

Figure 4-66 Comparison of median values between original and built-in Chiou and Youngs (2014) GMPM with Rx=1 km

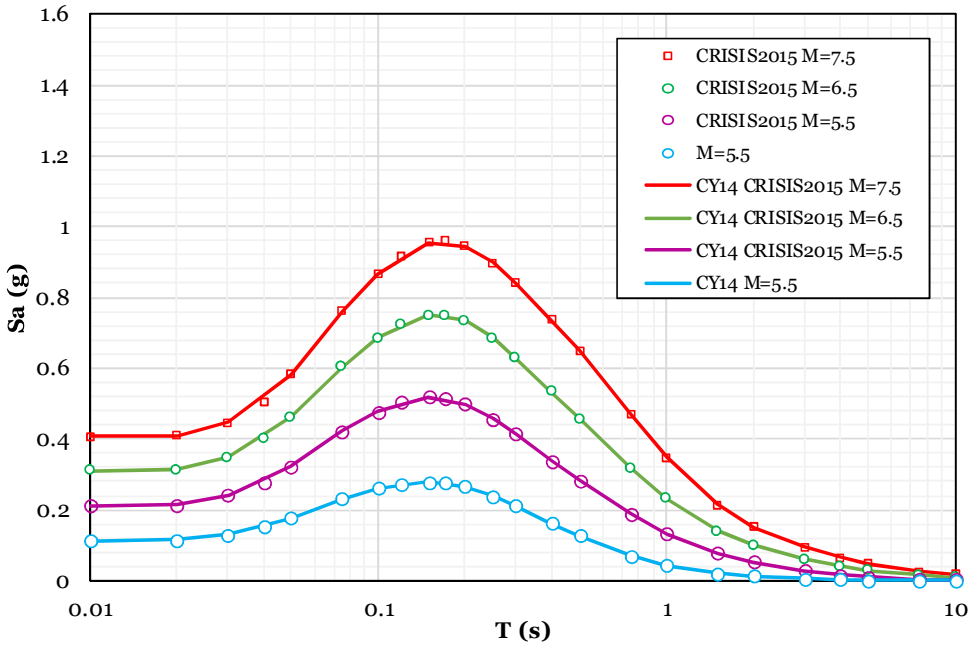

Figure 4-67 Comparison of median values between original and built-in Chiou and Youngs (2014) GMPM with Rx=10 km

Campbell and Bozorgnia (2014)

The validation of the built-in GMPM has been done for the Campbell and Bozorgnia (2014) case by means of five cases which characteristics are summarized in Table 4-62.

Table 4-62 Characteristics of the 5 validation cases of the Campbell-Bozorgnia (2014) GMPM

Case	1	2	3	4	5
Mechanism	Strike Slip	Strike Slip	Normal	Normal	Strike Slip
Region	California	California	California	California	California
Vs30	760	760	760	400	760
Z2.5	0.61	2.00	2.00	2.00	2.00
M	7.0	7.0	7.0	7.0	7.0
Rrup	5.0	100.1	5.0	5.0	5.0
Ztor	5.0	5.0	5.0	5.0	5.0
RJB	0	100	0	0	0
Rx	0	100	0	0	0
Rfoc	5.0	100.1	5.0	5.0	5.0
Dip	90	45	45	45	45
Frv	0	0	0	0	0
Fnm	0	0	1	1	0
FHW	1	1	1	1	0

Figures 4-68 to 4-70 show the graphical comparison of the author's values (median) and those obtained in R-CRISIS.

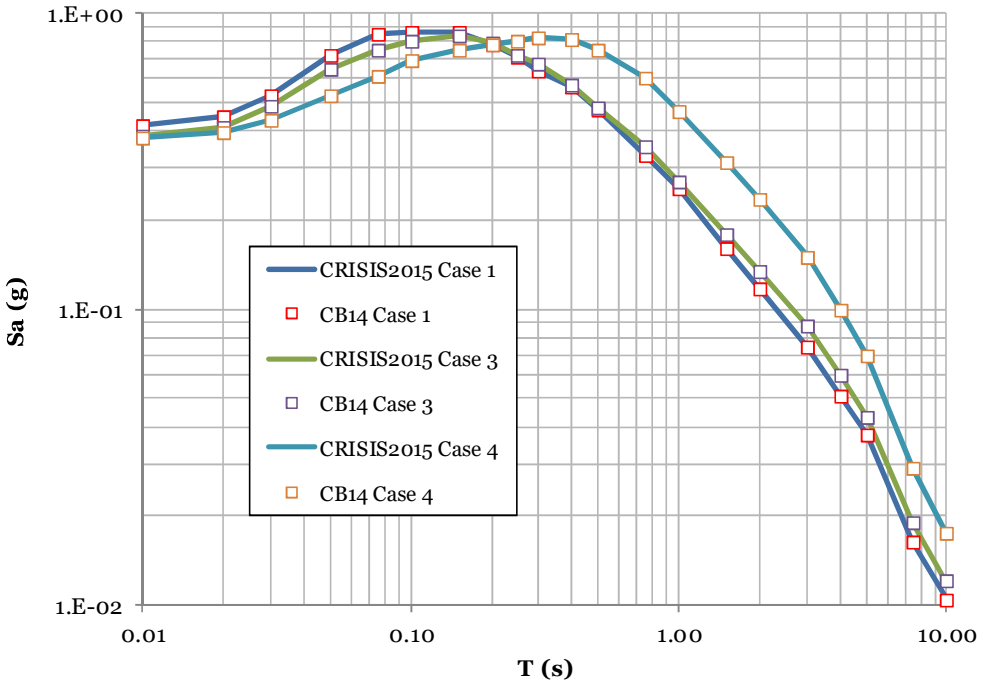

Figure 4-68 Comparison of median values between original and built-in Campbell and Bozorgnia (2014) GMPM. Cases 1, 3 and 4

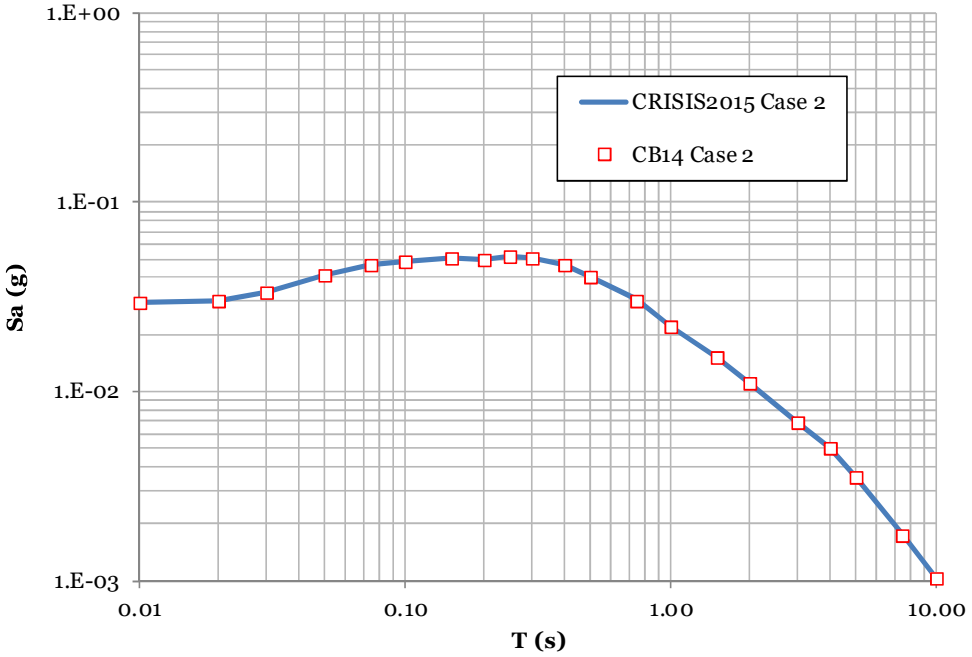

Figure 4-69 Comparison of median values between original and built-in Campbell and Bozorgnia (2014) GMPM. Case2

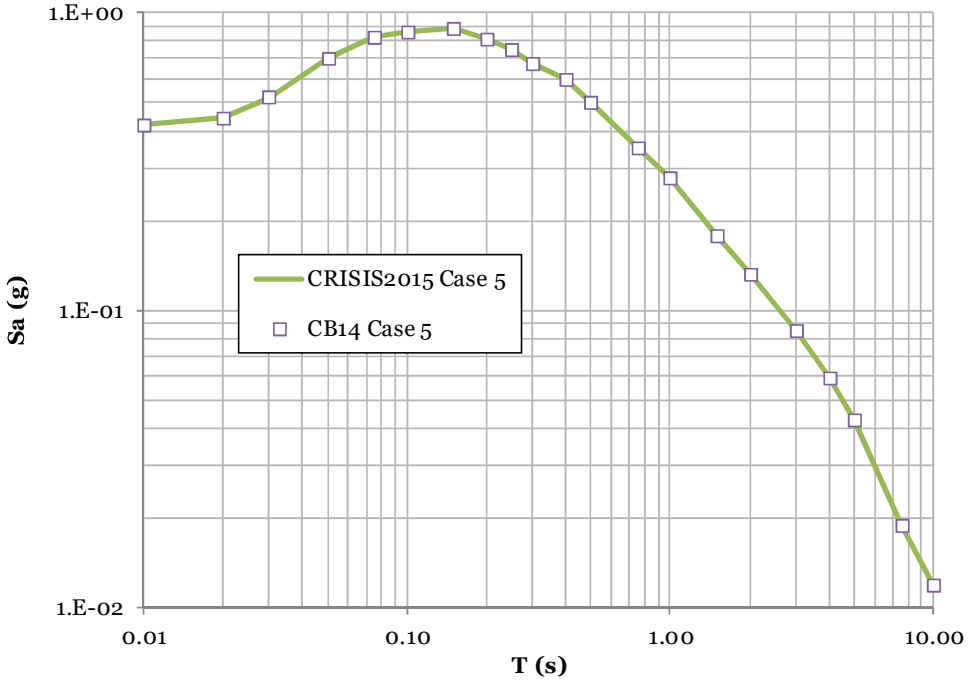

Figure 4-70 Comparison of median values between original and built-in Campbell and Bozorgnia (2014) GMPM. Case5

Akkar et al. (2014)

Figures 4-71 to 4-73 show the comparison of the attenuation plots obtained using the supplemental material from the Akkar et al. (2014) GMPM and those obtained from CRISIS. In all cases there is an exact agreement between the provided and programmed results.

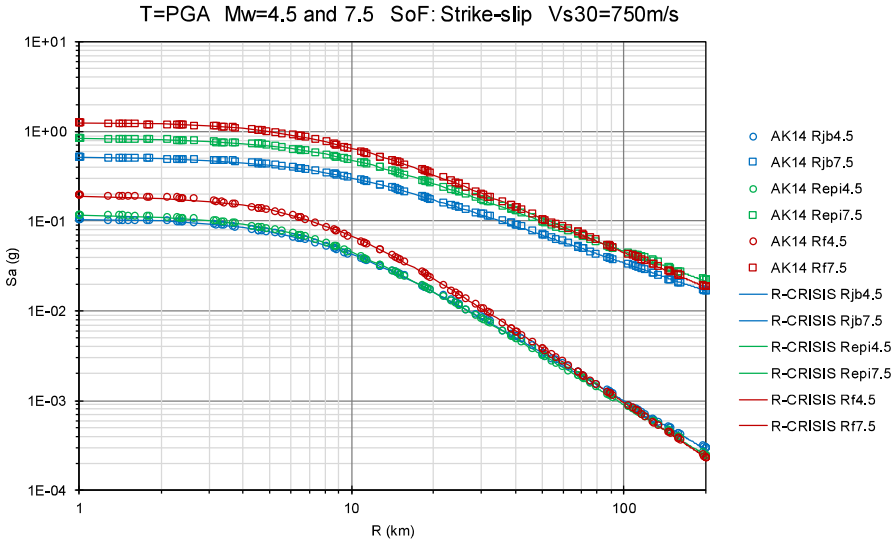

Figure 4-71 Comparison of distance scaling of the Akkar et al. (2014) model for different magnitudes and distances

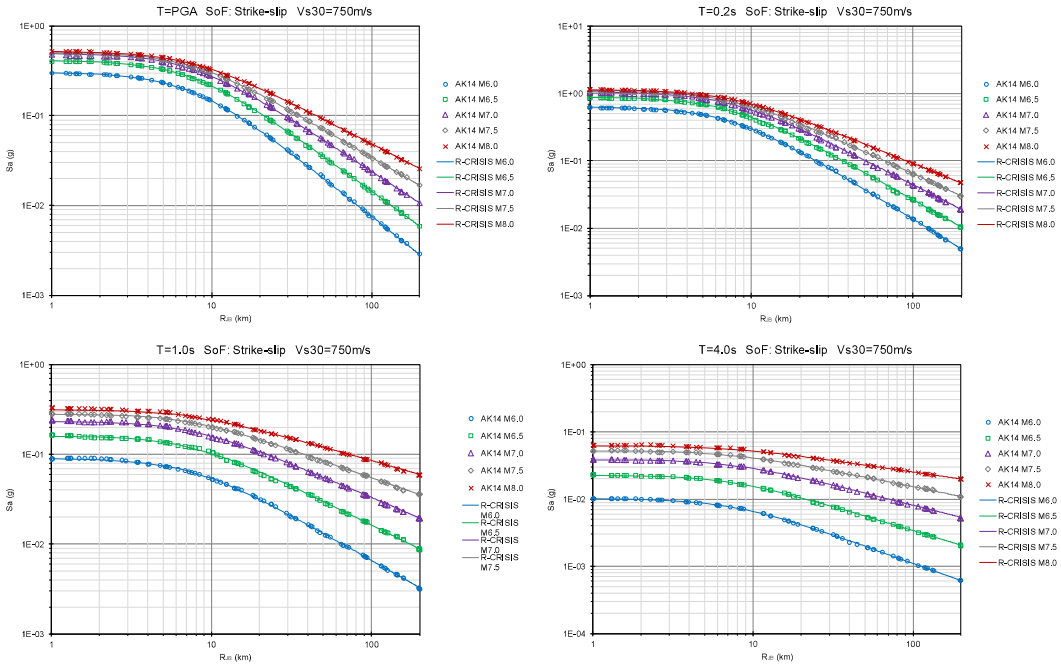

Figure 4-72 Comparison of distance scaling of R_{JB} model for different spectral ordinates. Top left: PGA; top right: 0.2s; bottom left: 1.0s; bottom right: 4.0s

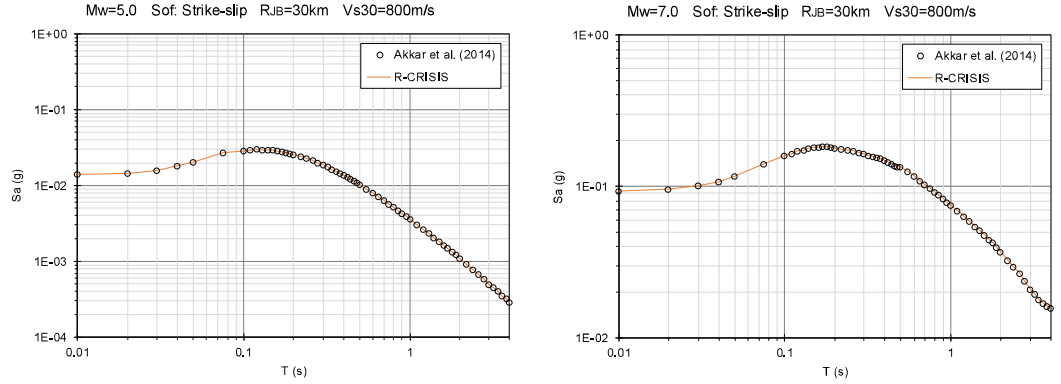

Figure 4-73 Comparison of median estimations of the predicted spectra for strike-slip mechanism, R_{JB}=30km, Vs30=800m/s and M_W=5 (left) and M_W=7 (right)

4.5.2 Graphical comparisons

For the GMPM included in this section, a graphical comparison was performed between the figures included in the original publications of the authors and the built-in GMPM in R-CRISIS. This process required the scale adjustments of both, ordinates and abscises in order to guarantee consistency in the plots.

Zhao et al. (2006)

The graphical comparison for the Zhao et al. (2006) GMPM was made against the figures included in the original paper published in the Bulletin of the Seismological Society of America. Figure 4-74 shows the comparison using the data of Figure 3 (PGA) of the original publication from where it can be seen a total congruency between the original and the built-in models.

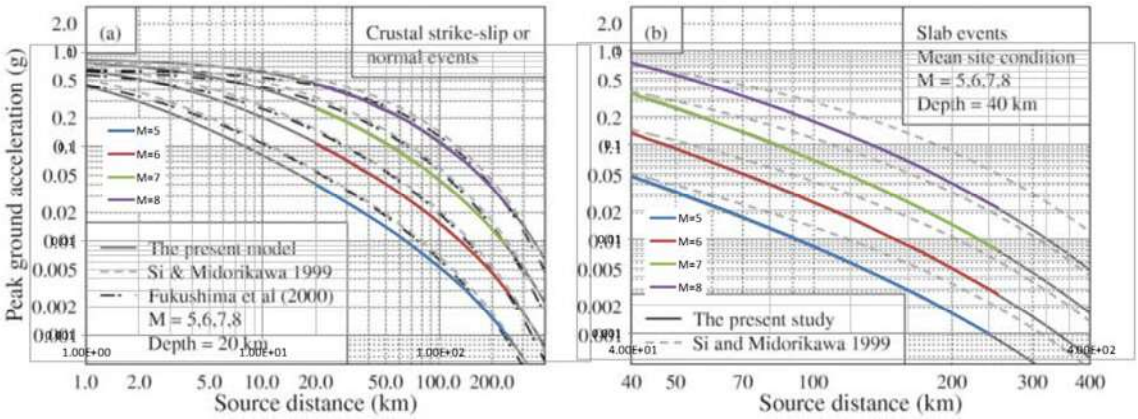

Figure 4-74 Comparison of median values between original and built-in Zhao et al. (2006) data. PGA and 4 magnitudes

Figure 4-75 shows the comparison for the complete spectral range for M=7, source distance=30 km, focal depth=20km and the four site classes. The base plot corresponds to Figure 6b of the original publication.

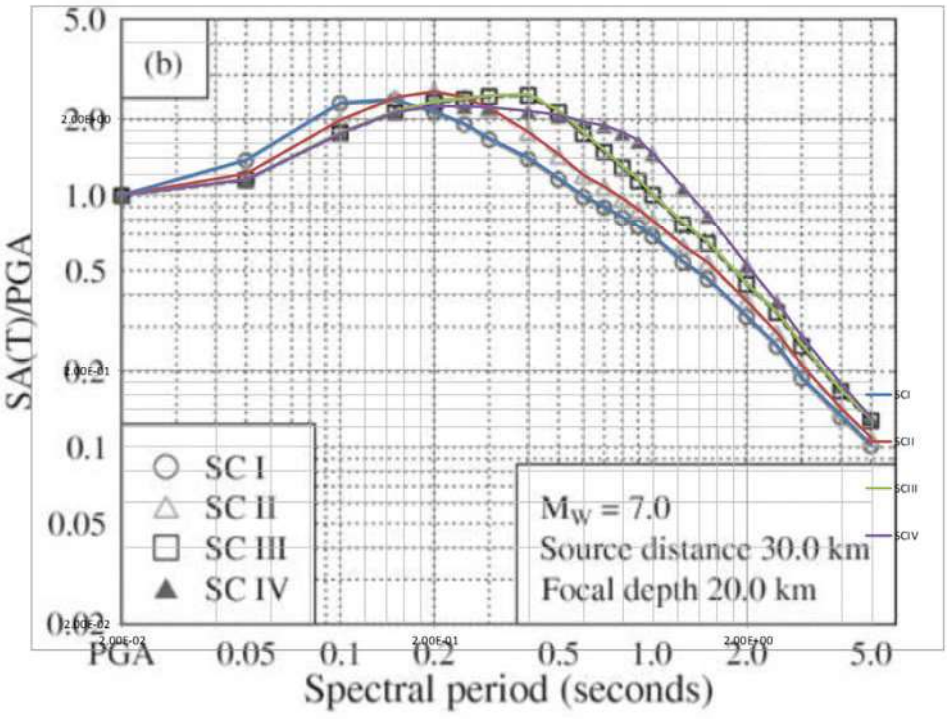

Figure 4-75 Comparison of median values between original and built-in Zhao et al. (2006) data. Full spectral range and 4 site classes

Figure 4-76 shows the comparison again for the complete spectral range, now in terms of pseudo-velocity (cm/s) for M=7, source distance=40 km, focal depth=20 km, site class II and crustal, interface and slab depths of 20 and 40 km. The base plot corresponds to Figure 7a of the original publication.

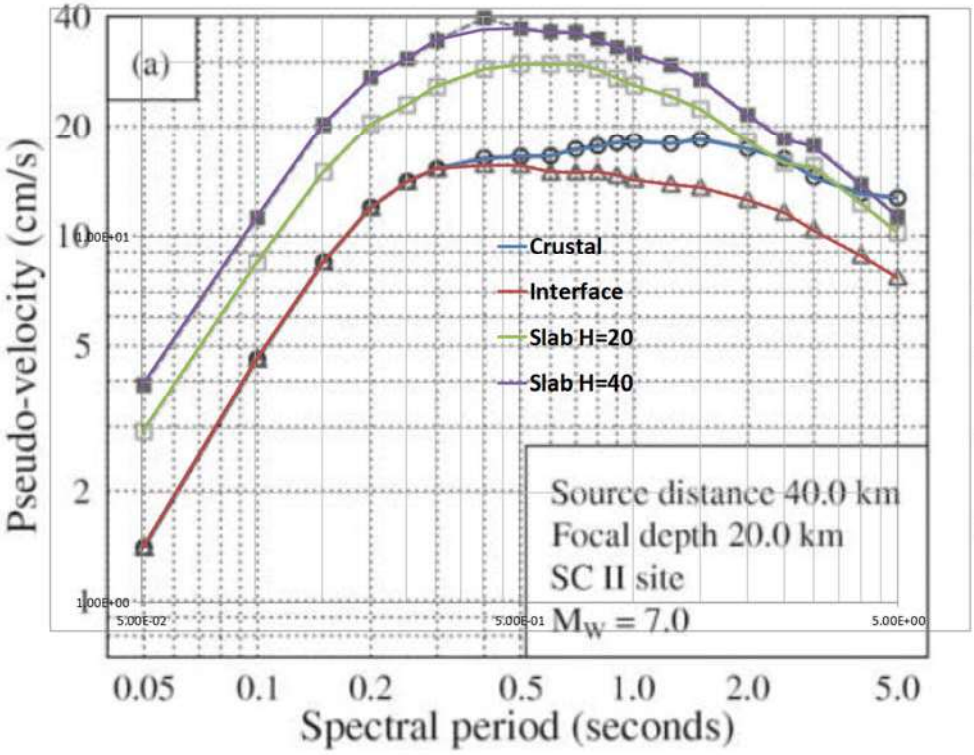

Figure 4-76 Comparison of median values between original and built-in Zhao et al. (2006) data. Full spectral range and pseudo-velocity. Source distance=40 km

Finally, Figure 4-77 shows the comparison for a similar case as the previous one but now using a source distance of 60 km. The base plot corresponds to Figure 7b of the original publication.

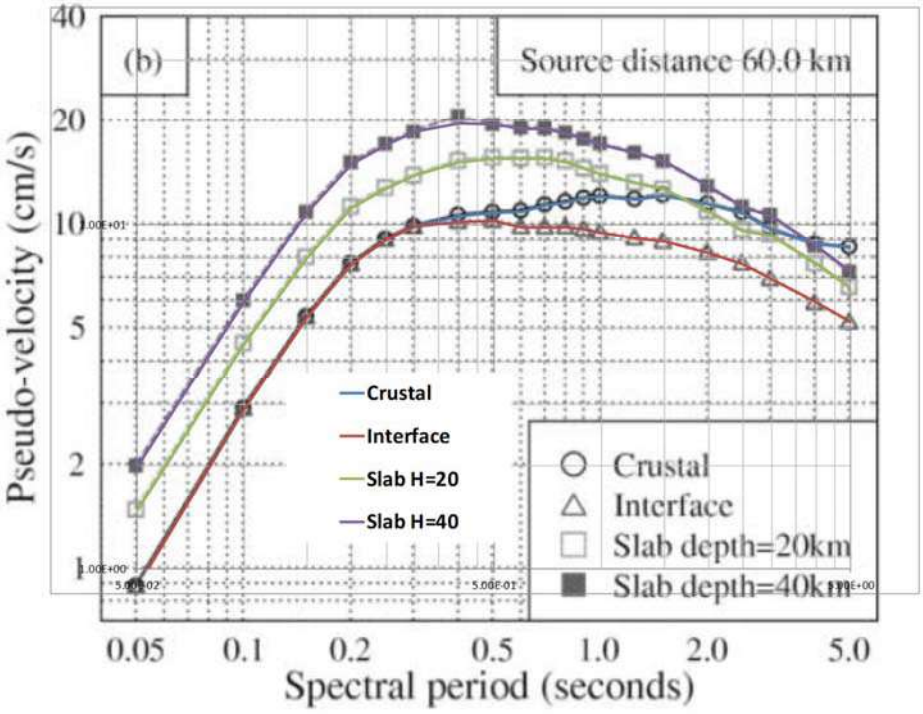

Figure 4-77 Comparison of median values between original and built-in Zhao et al. (2006) data. Full spectral range and pseudo-velocity. Source distance=60 km

For the Zhao et al. (2006) case, in all the comparisons total congruency is found between the author's values and those obtained by means of the built-in GMPM included in R-CRISIS.

Abrahamson and Silva (1997)

For this GMPM, the graphical comparison was made in terms of PGA for different mechanisms as shown in Figure 4-78 (for M=7 and rock) and for the full spectral range considering different magnitudes and soil conditions as shown in Figure 4-79. This last figure corresponds to Figure 9 of the original reference.

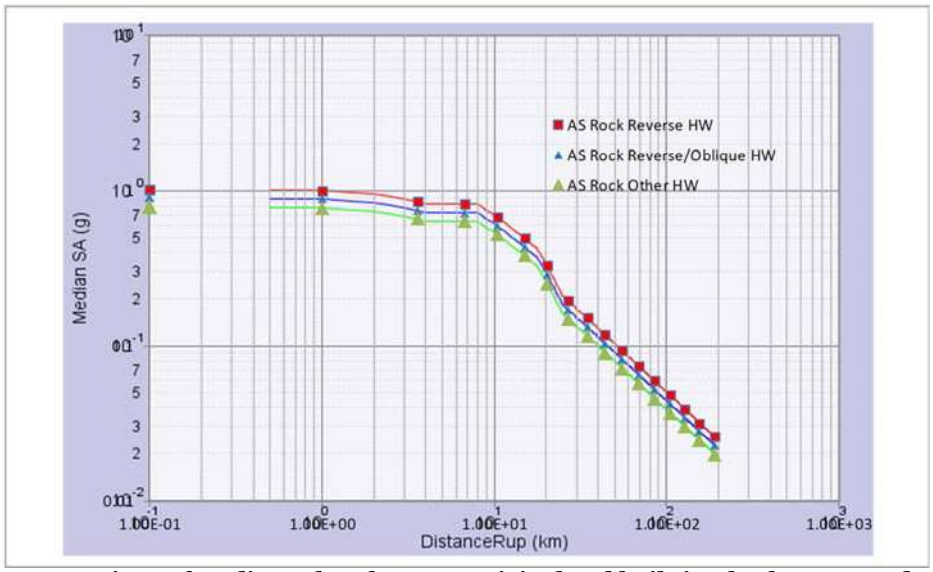

Figure 4-78 Comparison of median values between original and built-in Abrahamson and Silva (1997) GMPM. M=7, PGA, rock and different mechanisms

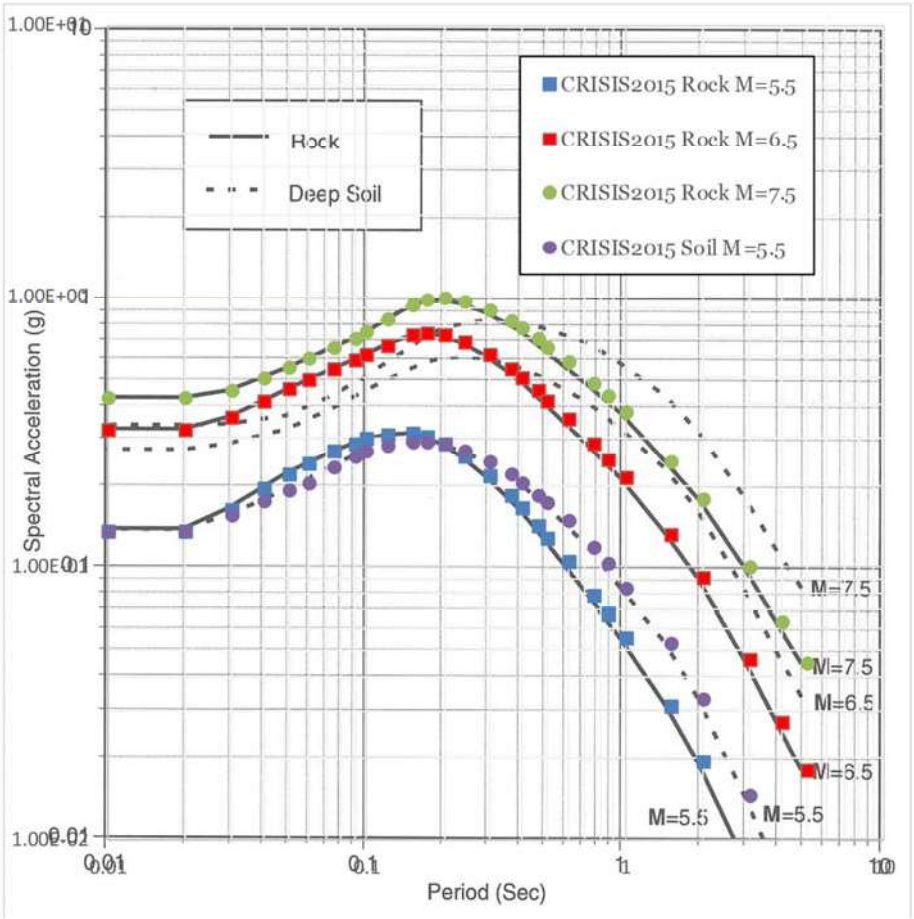

Figure 4-79 Comparison of median values between original and built-in Abrahamson and Silva (1997) GMPM. Strike-slip earthquake at a rupture distance of 10km. Average horizontal component

Chiou and Youngs (2008)

The validation of the Chiou and Youngs (2008) GMPM was made by means of the graphical comparison shown in Figure 4-80 which base data corresponds to Figure 14 of the Chiou and Youngs (2014) publication. This comparison is made for different magnitudes (3.5, 4.5, 5.5 and 8.5) in terms of the attenuation plots using V_{S30}=760 m/s, average Z_{TOR} and ΔDPP=0. The comparison was made for *Sa*=0.01s and 3.0s.

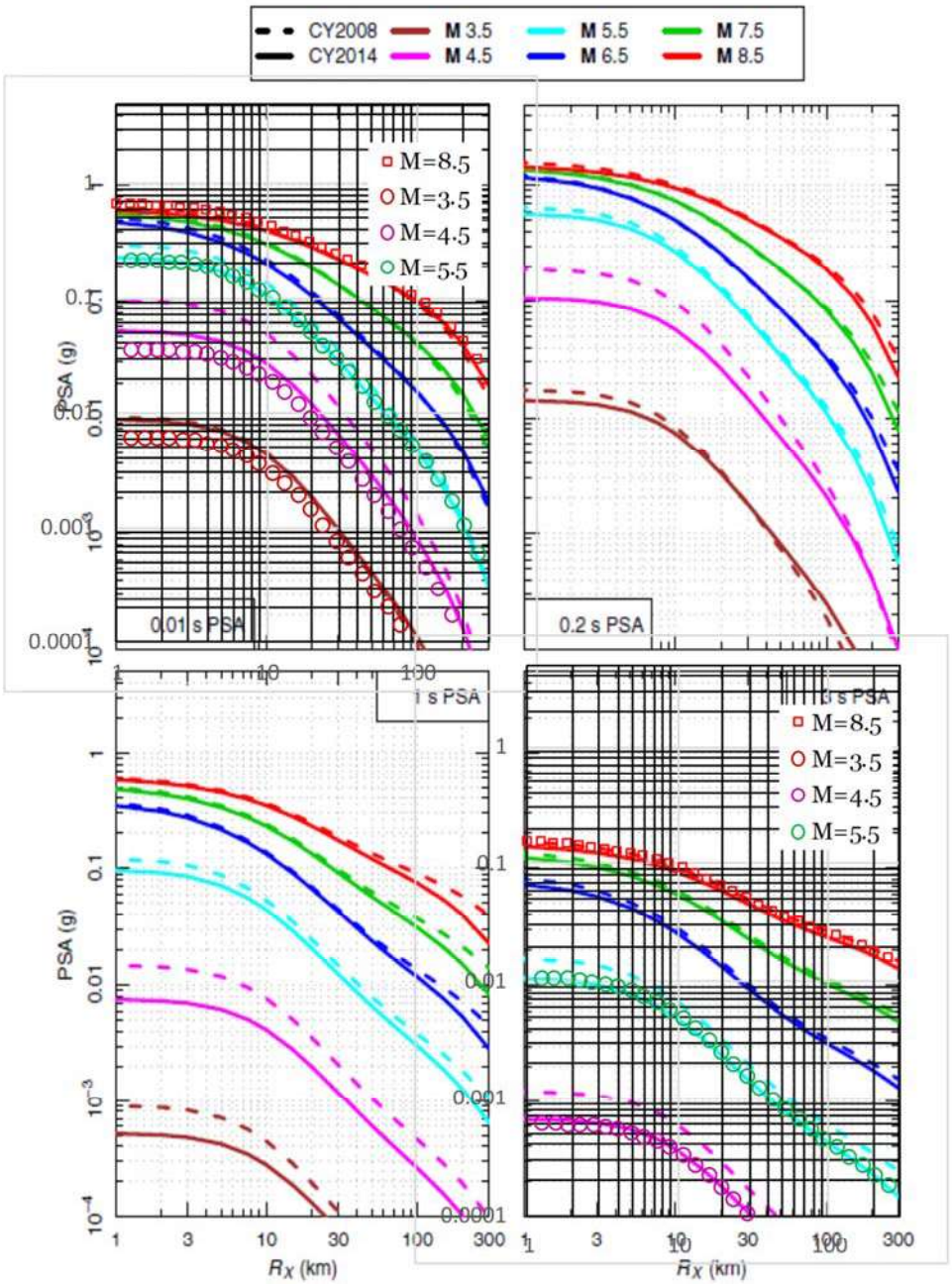

Figure 4-80 Comparison of median values between original and built-in Chiou and Youngs (2008) GMPM. 0.01s and 3.0s

Akkar and Bommer (2010)

The graphical comparison for the Akkar and Bommer (2010) GMPM was made, as shown in Figure 4-81, using as base data Figure 9 of the original publication in Seismological Research Letters. This comparison is made in terms of pseudo-spectral accelerations for rock sites at 10km. The mechanism corresponds to strike slip and three different magnitudes (5.0, 6.3 and 7.6) are used.

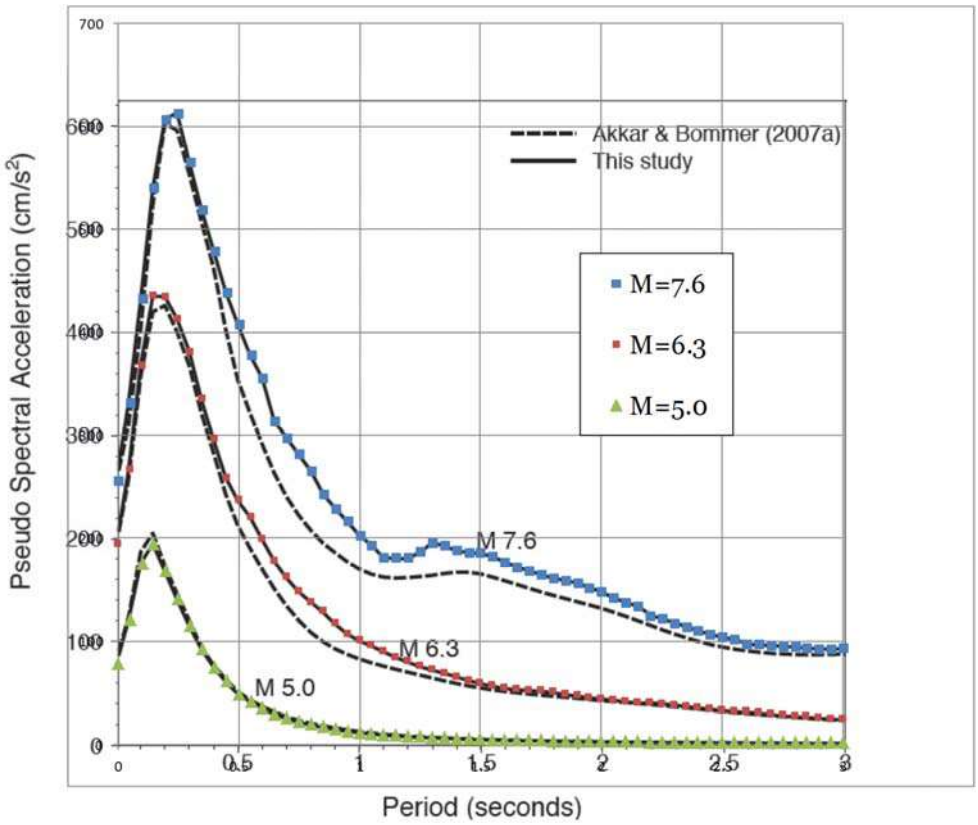

Figure 4-81 Comparison of pseudo spectral accelerations between original and built-in Akkar and Bommer (2010) GMPM

Cauzzi et al. (2017)

The validation of the built-in GMPM has been done for the Cauzzi et al. (2017) case by making graphical comparisons against the original figures provided in the article by the authors as shown in Figures 4-82 and 4-83.

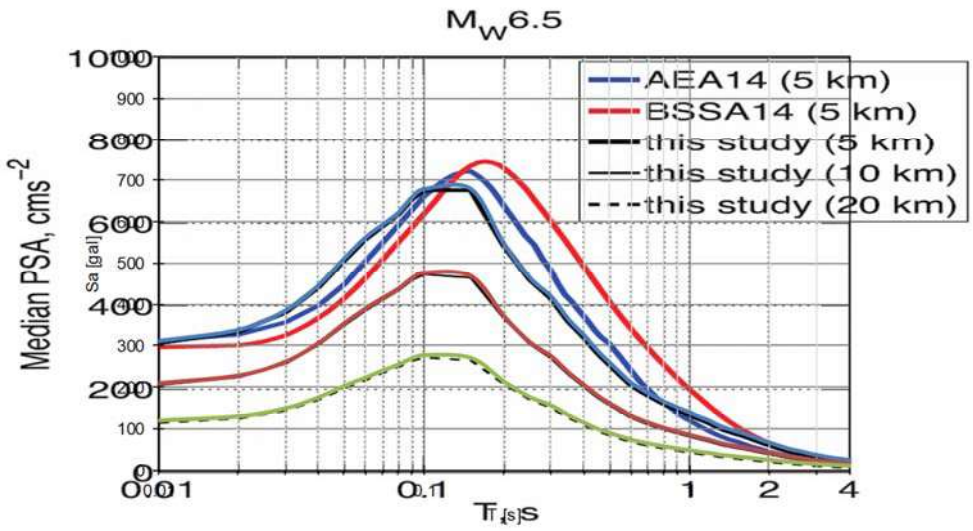

Figure 4-82 Comparison in terms of median PSA spectra at rock sites among the predictive equations of Cauzzi et al. (2017) for Mw 6.5

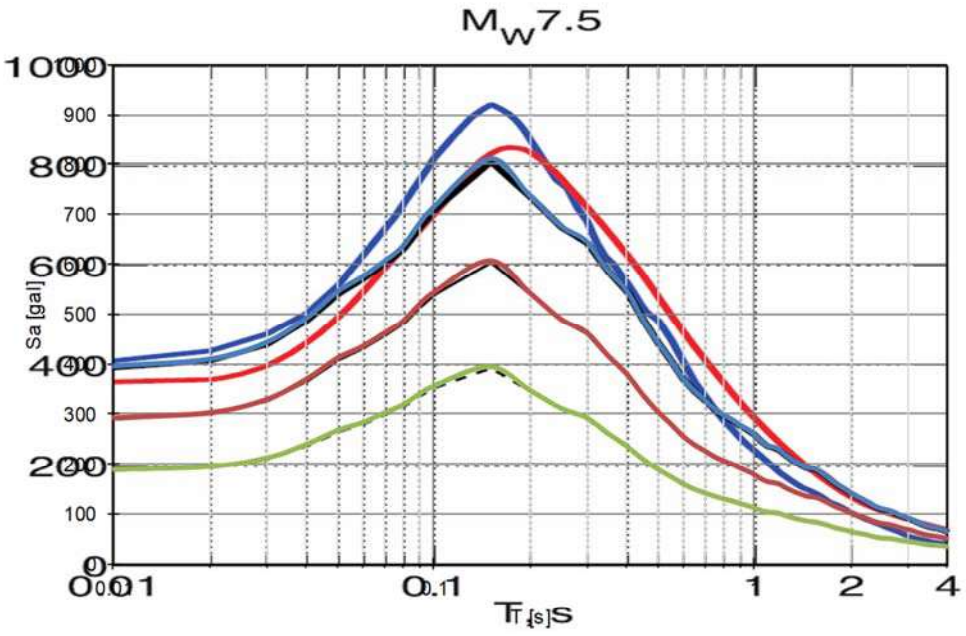

Figure 4-83 Comparison in terms of median PSA spectra at rock sites among the predictive equations of Cauzzi et al. (2017) for Mw 6.5

Montalva et al. (2017)

The validation of the built-in GMPM has been done for the Montalva et al. (2017) case by making graphical comparisons against the original figures provided in the article by the authors as shown in Figures 4-84 to 4-91.

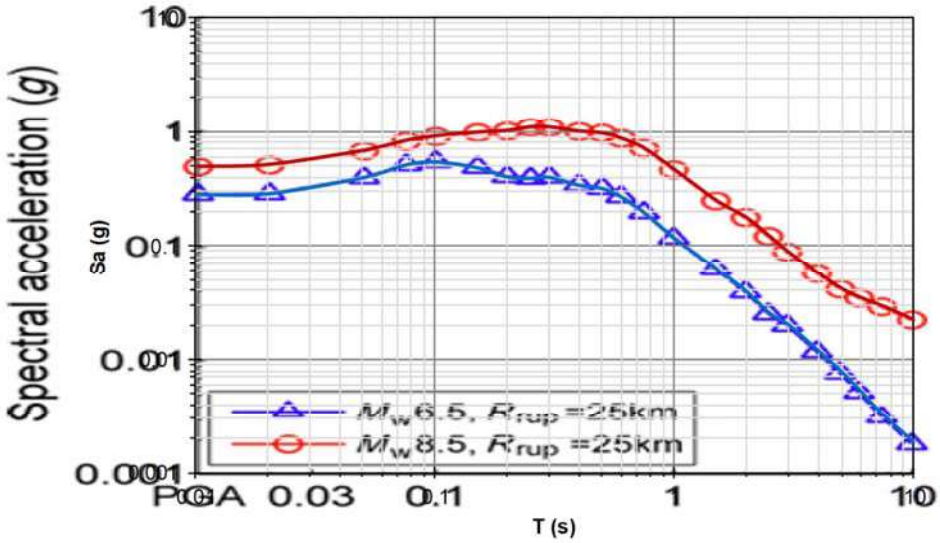

Figure 4-84 Comparison of response spectra for a fore-arc with Vs30=300 m/s for intraplate earthquake with Montalva et al. 2017 GMPM. Mw=6.5 and 8.5; R_{RUP}=25km

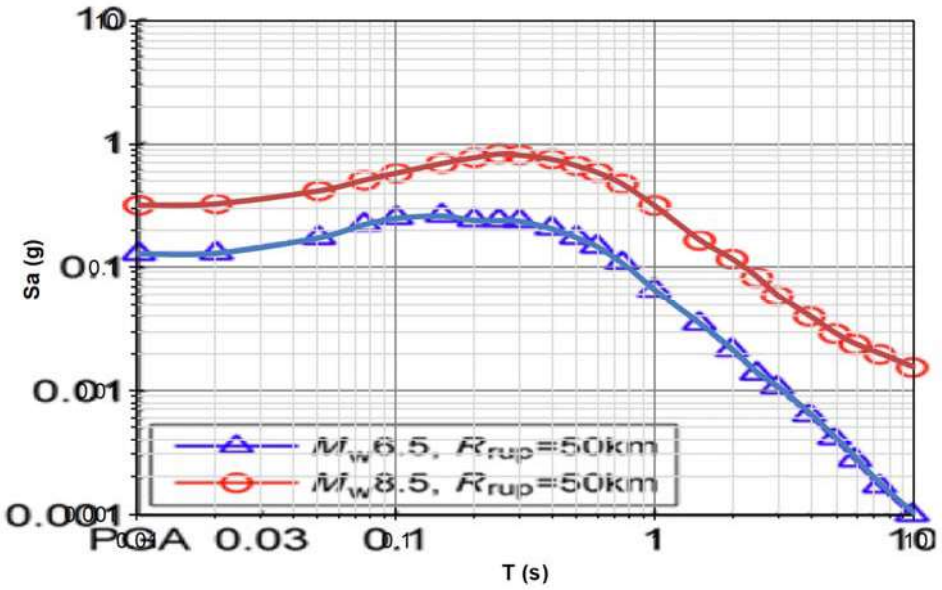

Figure 4-85 Comparison of response spectra for a fore-arc with Vs30=300 m/s for intraplate earthquake with Montalva et al. 2017 GMPM. Mw=6.5 and 8.5; R_{RUP}=50km

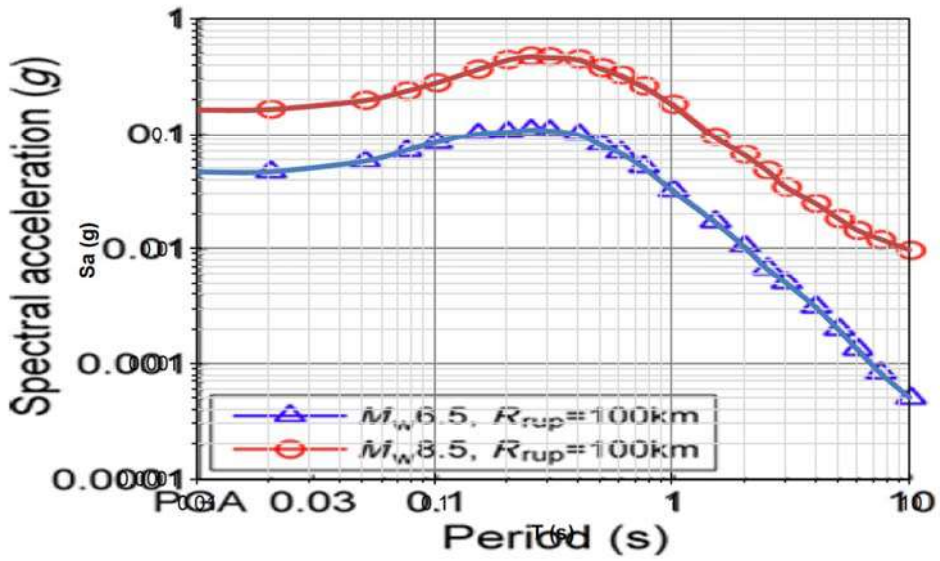

Figure 4-86 Comparison of response spectra for a fore-arc with Vs30=300 m/s for intraplate earthquake with Montalva et al. 2017 GMPM. Mw=6.5 and 8.5; RRUP=100km

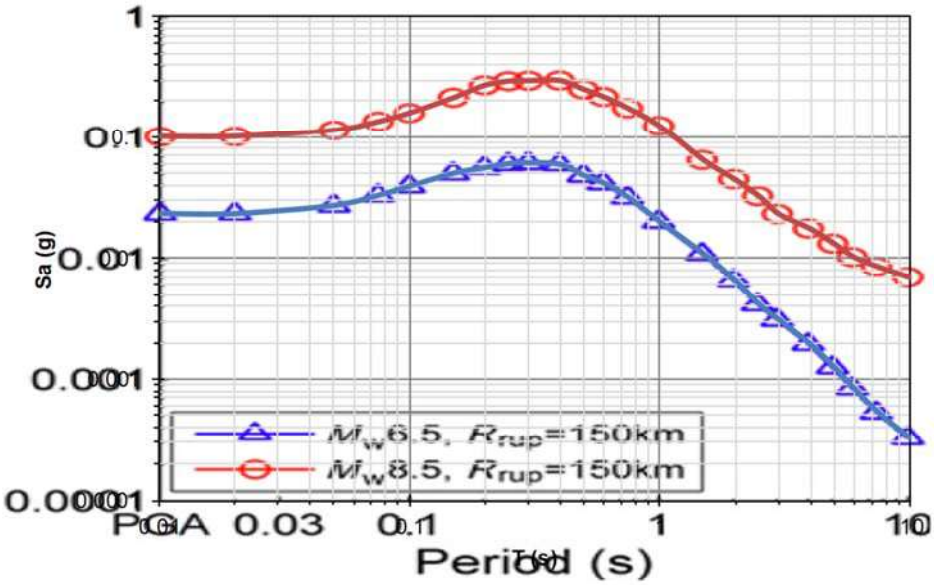

Figure 4-87 Comparison of response spectra for a fore-arc with Vs30=300 m/s for intraplate earthquake with Montalva et al. 2017 GMPM. Mw=6.5 and 8.5; RRUP=150km

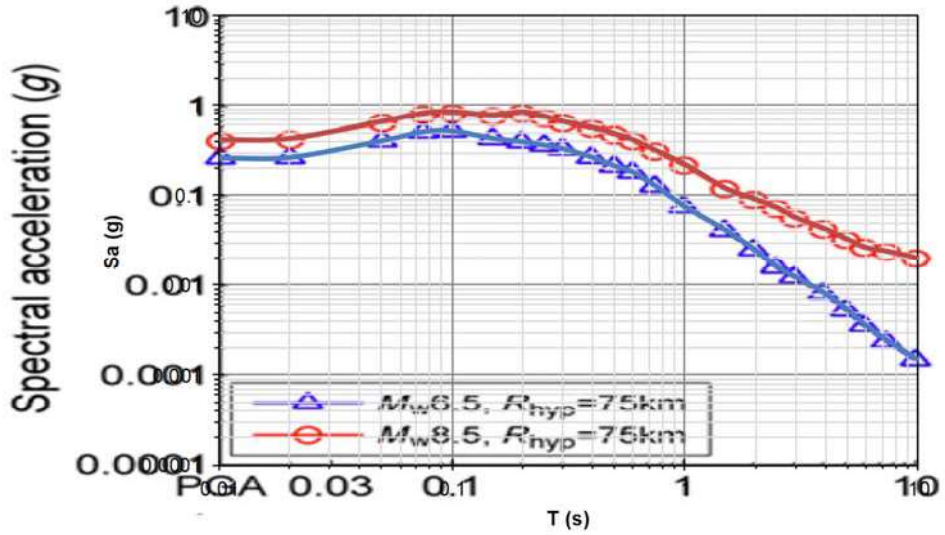

Figure 4-88 Comparison of response spectra for a fore-arc with Vs30=300 m/s for in-slab earthquake with Montalva et al. 2017 GMPM. Mw=6.5 and 8.5; R_F=75km

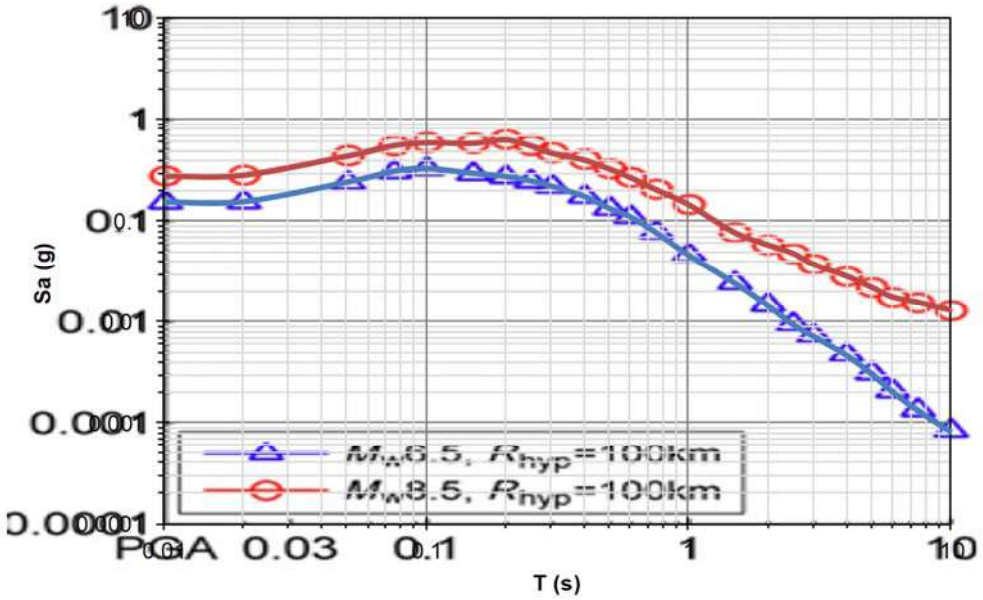

Figure 4-89 Comparison of response spectra for a fore-arc with Vs30=300 m/s for in-slab earthquake with Montalva et al. 2017 GMPM. Mw=6.5 and 8.5; R_F=100km

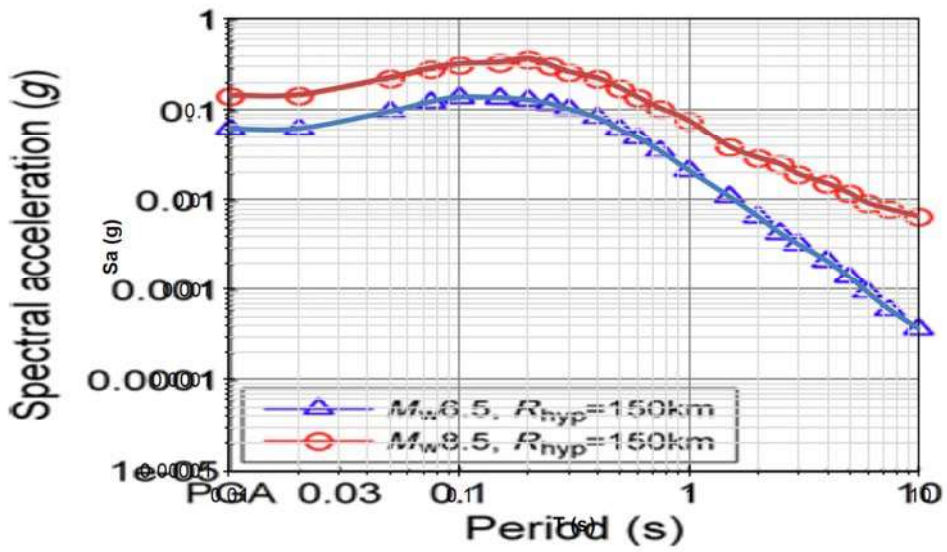

Figure 4-90 Comparison of response spectra for a fore-arc with Vs30=300 m/s for in-slab earthquake with Montalva et al. 2017 GMPM. Mw=6.5 and 8.5; R_F=150km

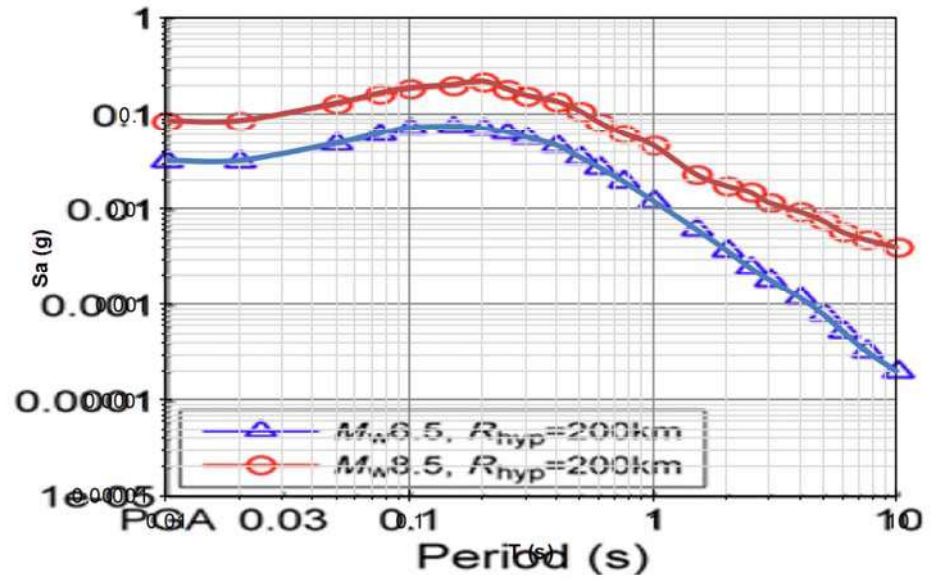

Figure 4-91 Comparison of response spectra for a fore-arc with Vs30=300 m/s for in-slab earthquake with Montalva et al. 2017 GMPM. Mw=6.5 and 8.5; R_F=200km

Bindi et al. (2017)

The validation of the built-in GMPM has been done for the Bindi et al. (2017) case by making graphical comparisons against the original figures provided in the article by the authors as shown in Figures 4-92 to 4-94.

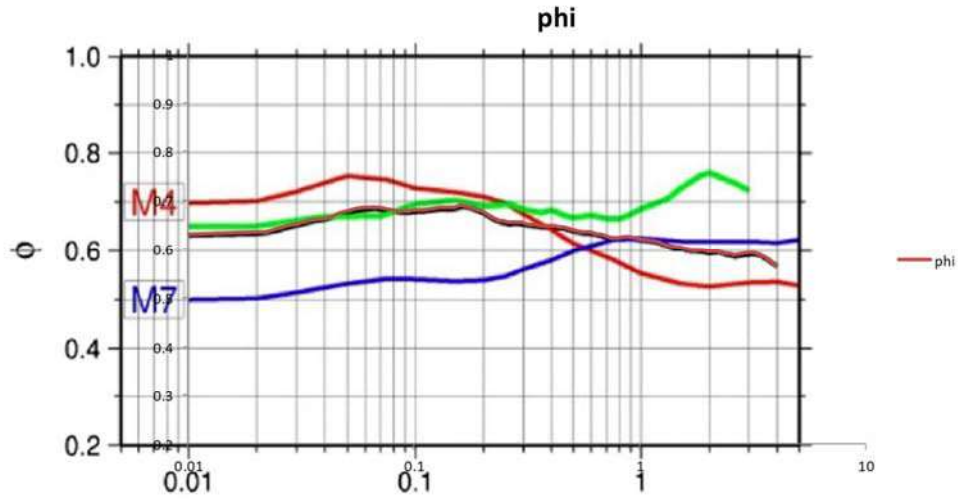

Figure 4-92 Within event standard deviation versus periods for Bindi et al. (2017) GMPM

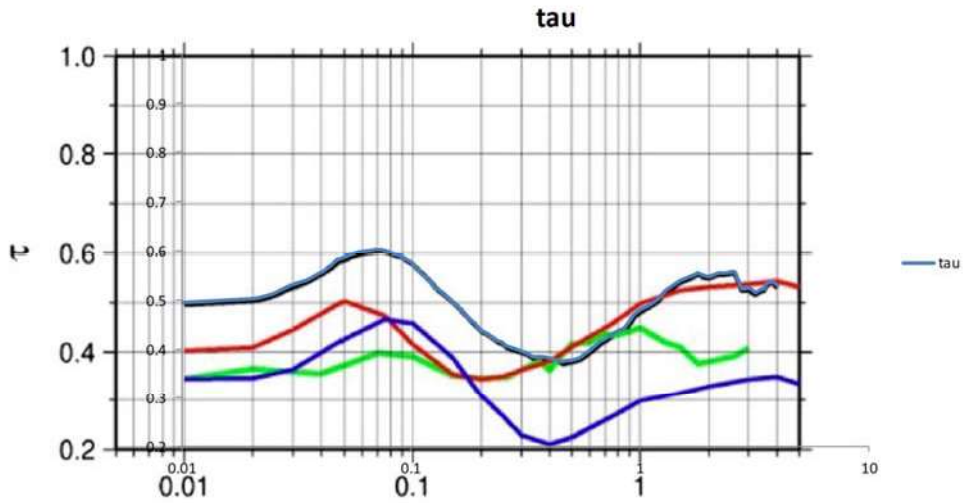

Figure 4-93 Between event standard deviation versus periods for Bindi et al. (2017) GMPM

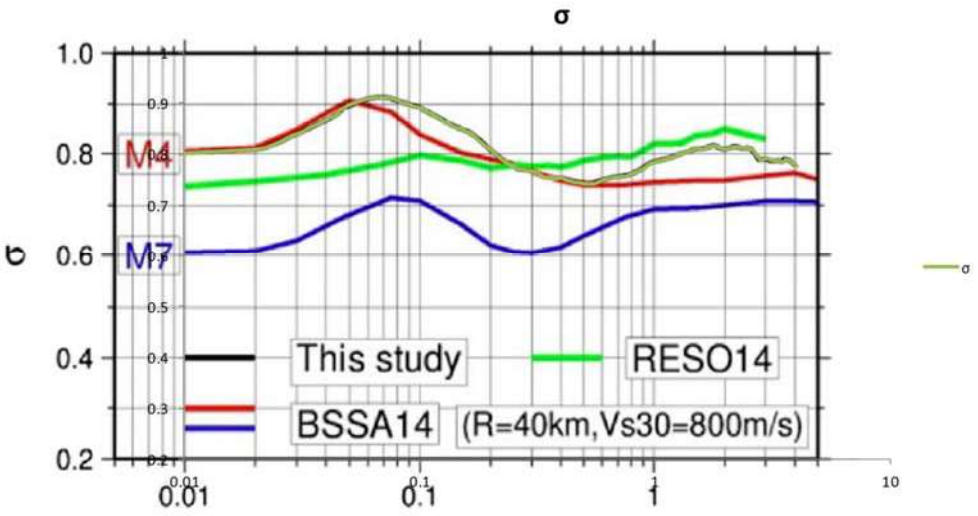

Figure 4-94 Total standard deviation versus periods for Bindi et al. (2017) GMPM

Derras et al. (2014)

The validation of the built-in GMPM has been done for the Derras et al. (2014) case by making graphical comparisons. Figures 4-95 to 4-100 show these comparison in terms of pseudo-spectral accelerations for different magnitude and Vs30 values.

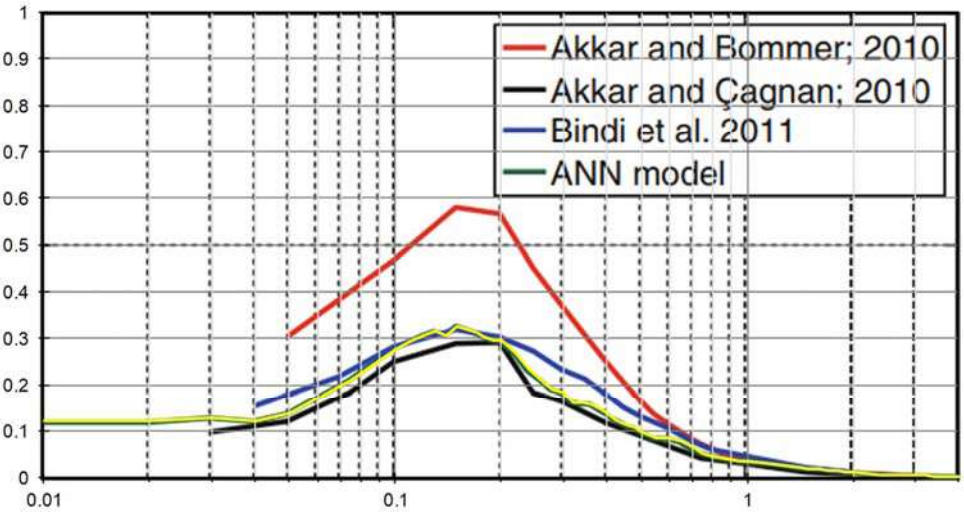

Figure 4-95 Comparison of the period-dependence of median pseudo spectral accelerations derived from Derras et al. (2014) with those proposed in other European GMPEs. Mw=5, Vs30=800m/s

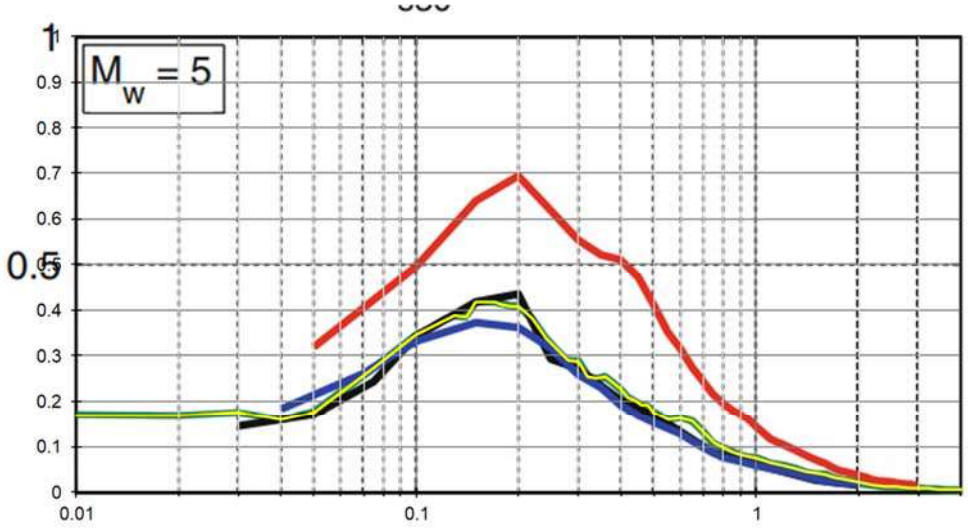

Figure 4-96 Comparison of the period-dependence of median pseudo spectral accelerations derived from Derras et al. (2014) with those proposed in other European GMPEs. Mw=5, Vs30=300m/s

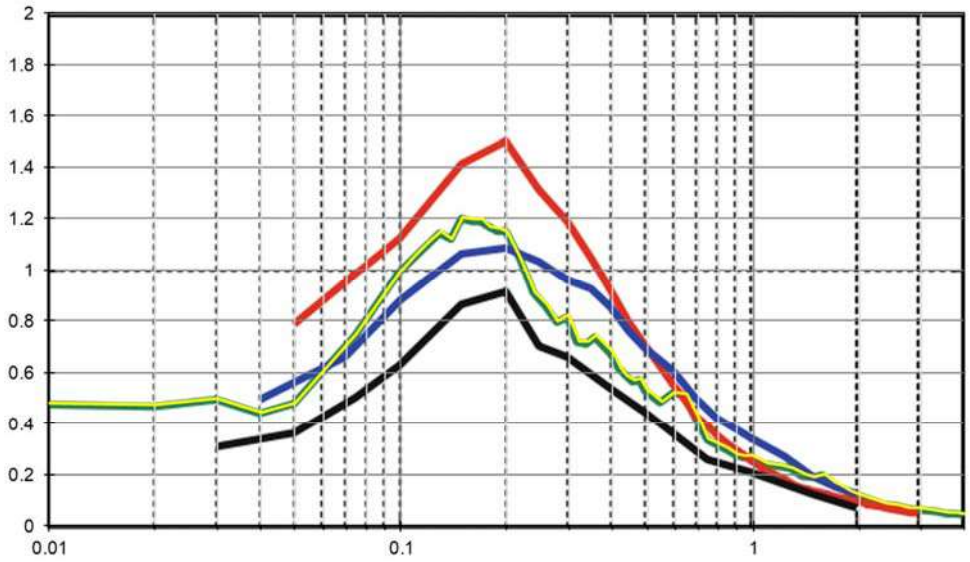

Figure 4-97 Comparison of the period-dependence of median pseudo spectral accelerations derived from Derras et al. (2014) with those proposed in other European GMPEs. Mw=6, Vs30=800m/s

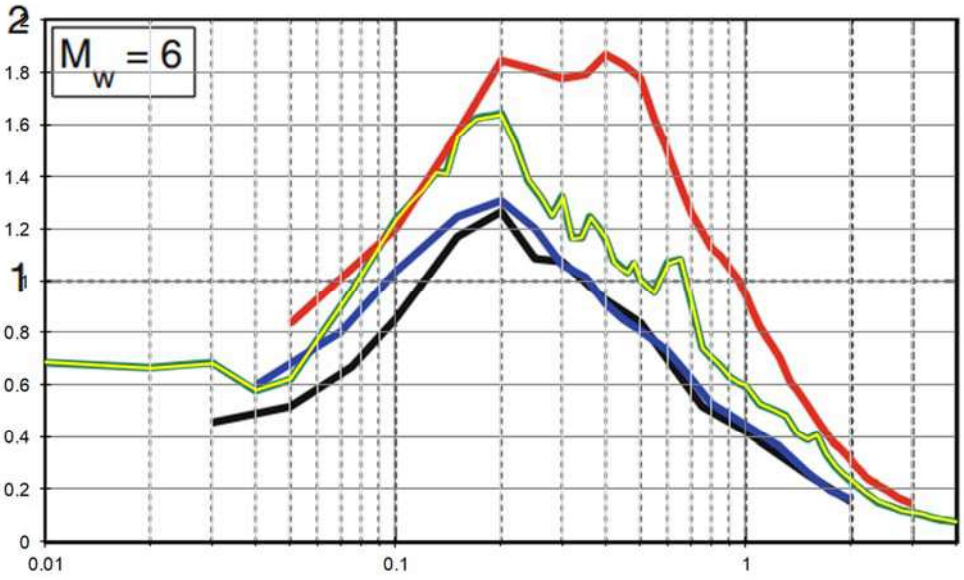

Figure 4-98 Comparison of the period-dependence of median pseudo spectral accelerations derived from Derras et al. (2014) with those proposed in other European GMPEs. Mw=6, Vs30=300m/s

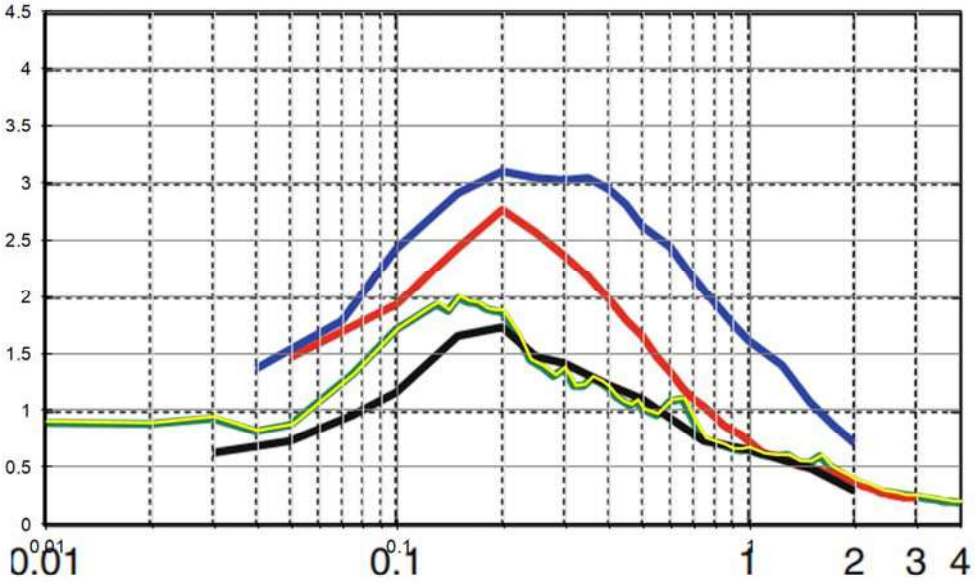

Figure 4-99 Comparison of the period-dependence of median pseudo spectral accelerations derived from Derras et al. (2014) with those proposed in other European GMPEs. Mw=7, Vs30=800m/s

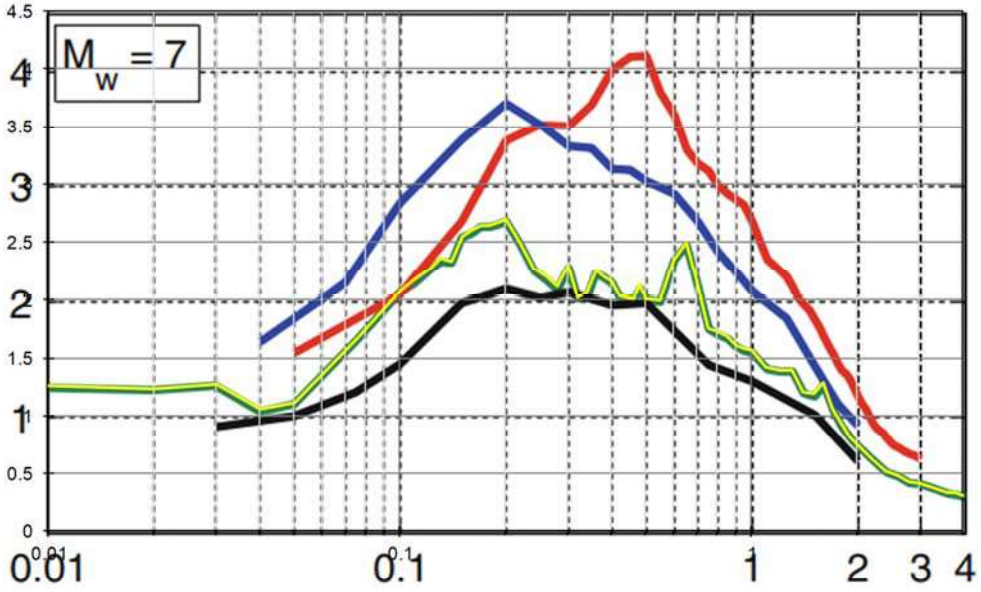

Figure 4-100 Comparison of the period-dependence of median pseudo spectral accelerations derived from Derras et al. (2014) with those proposed in other European GMPEs. Mw=5, Vs30=300m/s

Pankow and Pechmann (2004)

The validation of the built-in GMPM has been done for the Pankow and Pechmann (2004) case by making graphical comparisons, as shown in Figure 4-101, in terms of peak horizontal velocity as the data provided in the original reference.

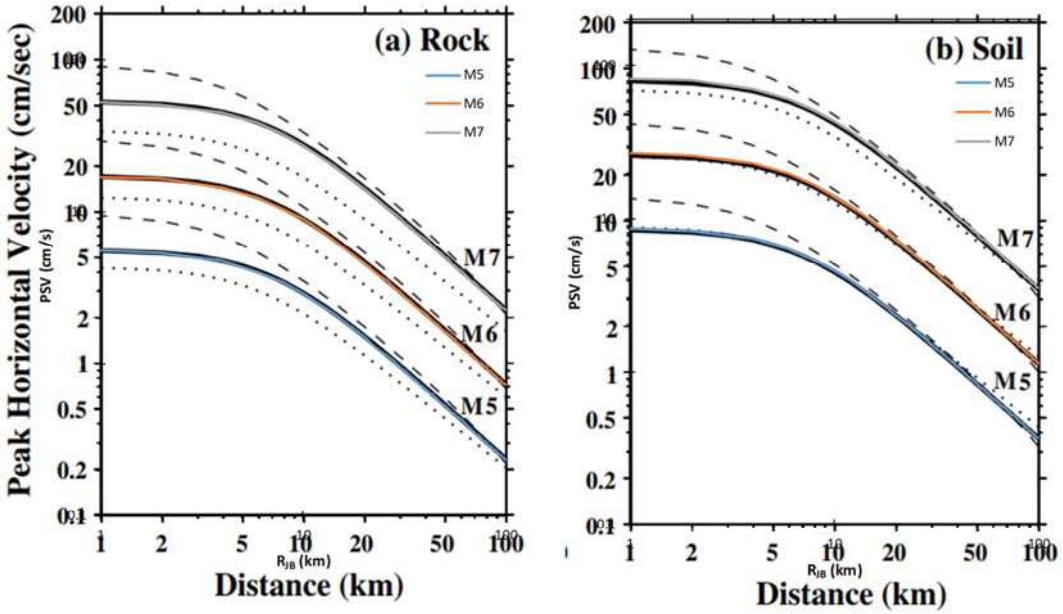

Figure 4-101 Validation of the predictions for peak horizontal velocities for Mw 5.0, 6.0 and 7.0. Left: rock; right: soil

Derras et al. (2016)

The validation of the built-in GMPM has been done for the Derras et al. (2016) case by making graphical comparisons. Figure 4-102 shows the comparison of median spectra for different magnitudes (3.5-7.5) at a stiff site and 30km distance, whereas Figure 4-103 shows the comparison for the total aleatory variability for two magnitudes (4.0 and 7.0) and two site conditions (Vs30=270 m/s and Vs30=600 m/s).

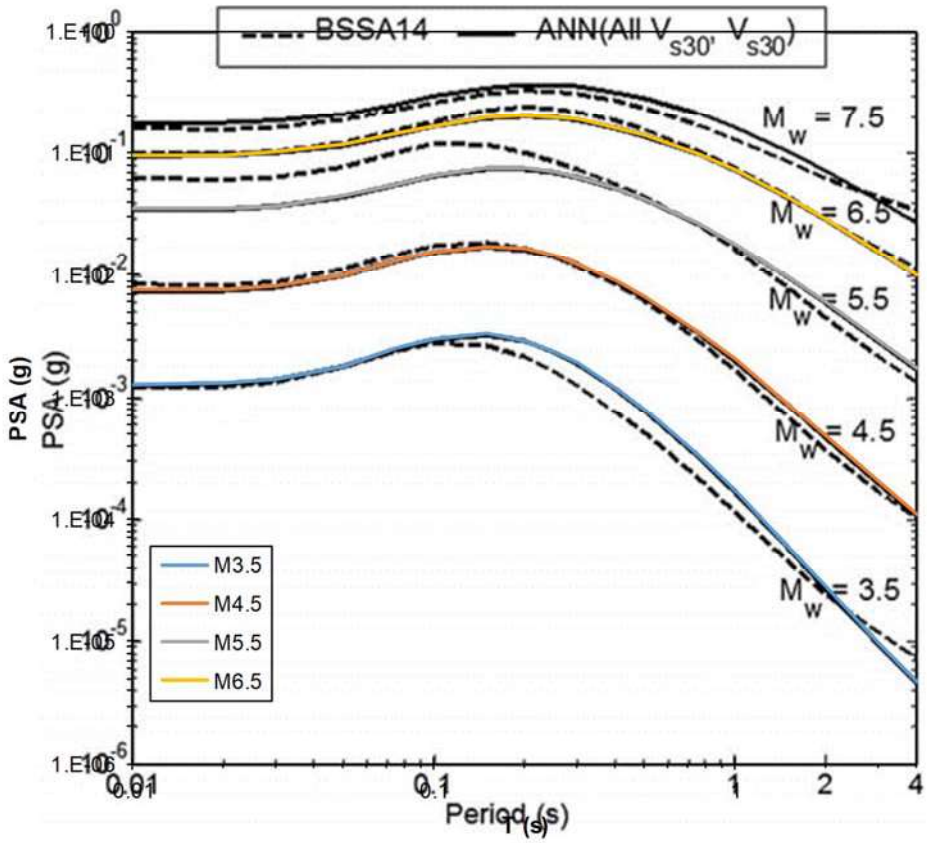

Figure 4-102 Validation of the median spectra predicted for increasing magnitudes at stiff site and 30km distance

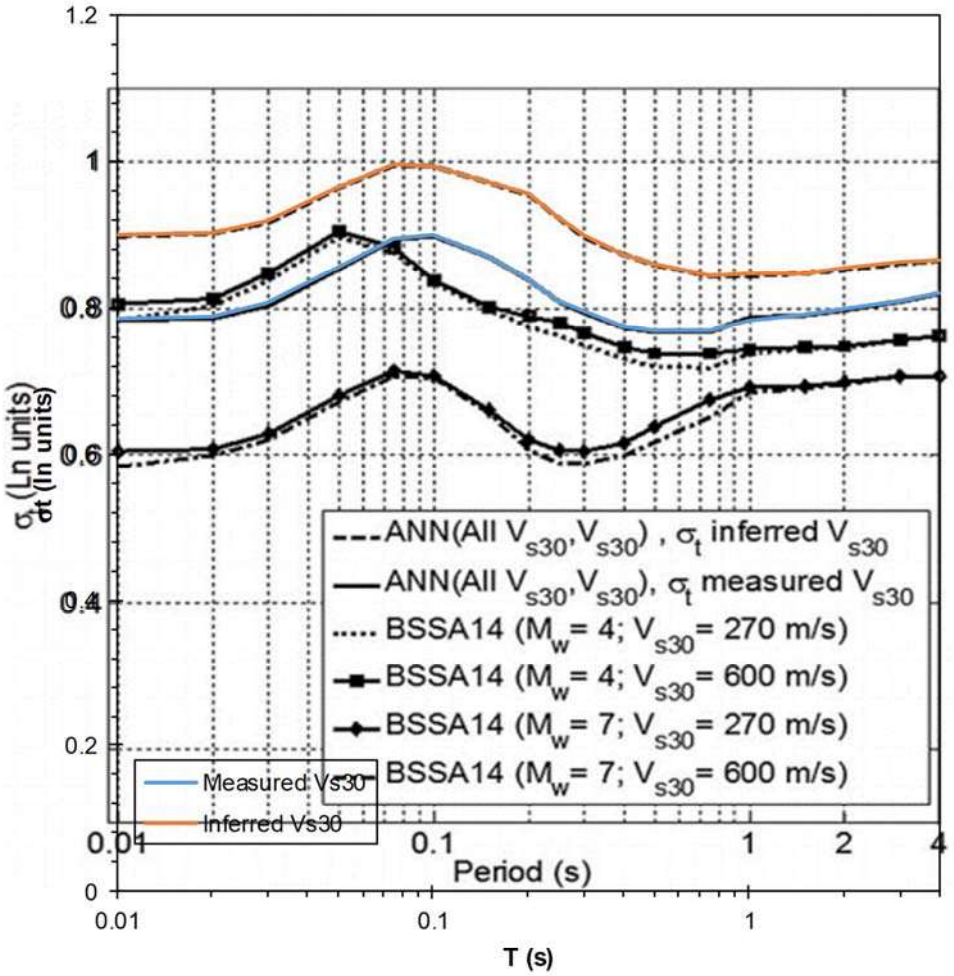

Figure 4-103 Validation of the total aleatory variability for two magnitudes (4.0 and 6.0) and soft and stiff soil conditions

Pezeshk et al. (2018)

The validation of the built-in GMPM has been done for the Pezeshk et al. (2018) in terms of graphical comparisons. Figures 4-104 to 4-106 show these comparisons which are made in terms of the response spectra predicted by the model for different distances and magnitudes using the stochastic and empirical scaling approaches together with the PGA and pseudo-acceleration response spectral values for four spectral ordinates.

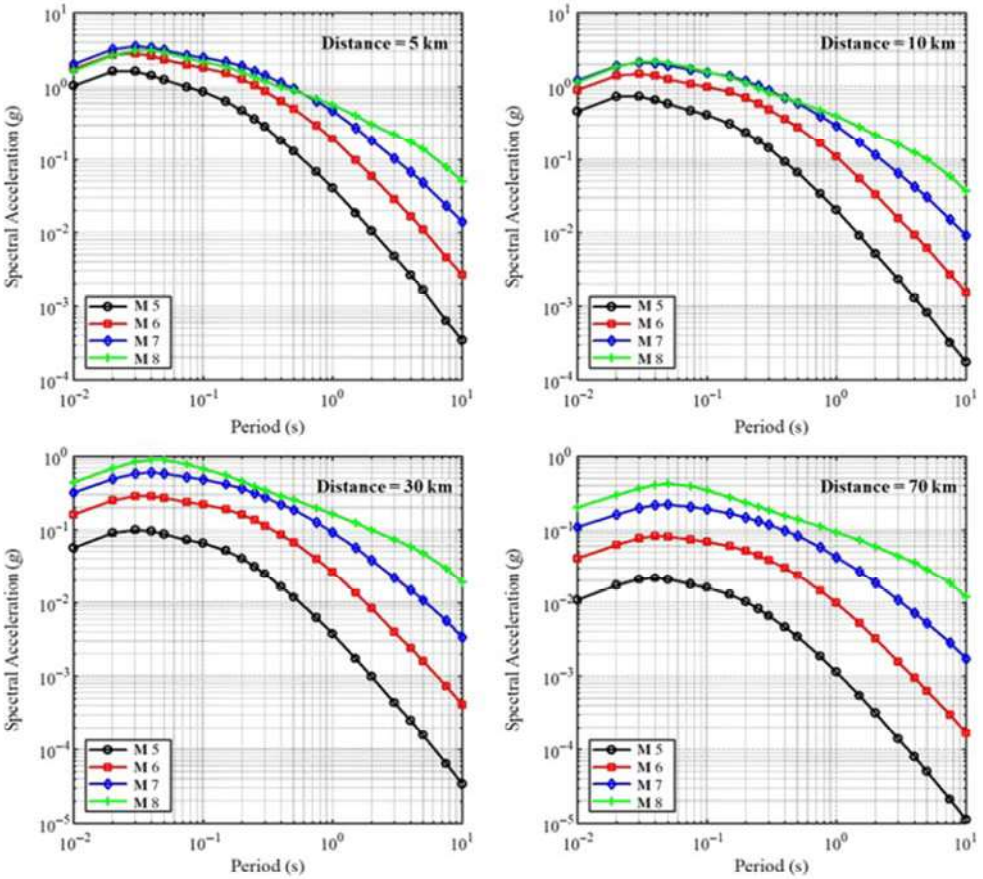

Figure 4-104 Validation of the response spectra predicted by the Pezeshk et al. (2018) GMPM based on the stochastic-scaling approach

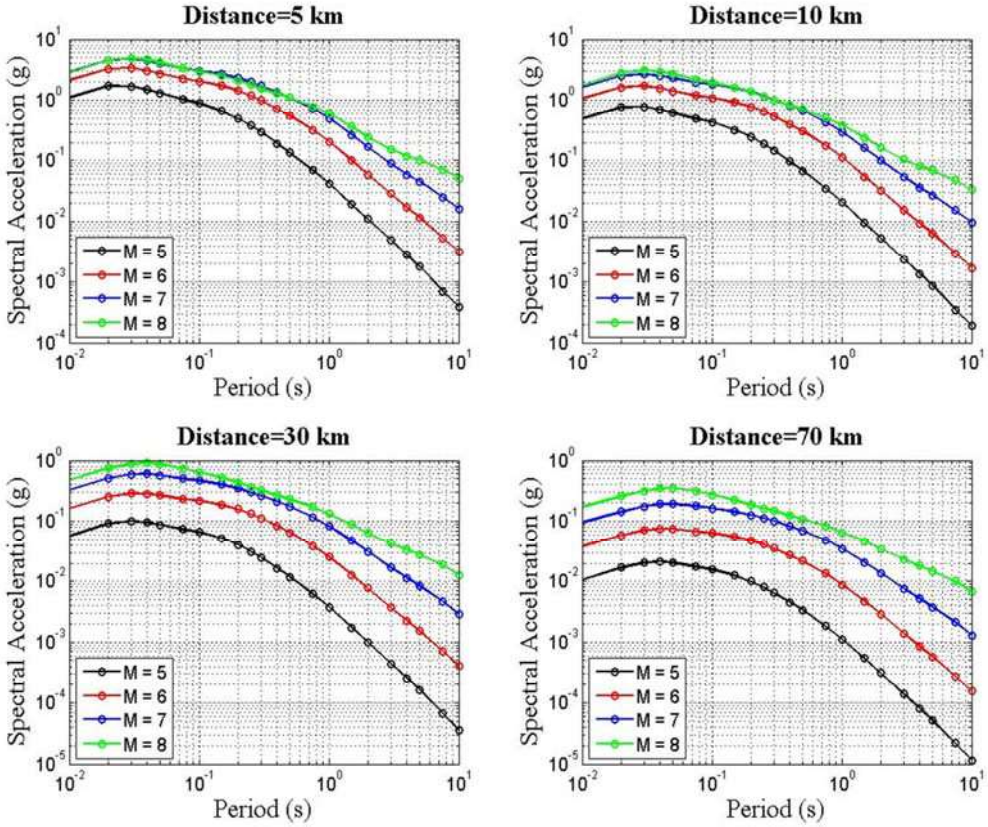

Figure 4-105 Validation of the response spectra predicted by the Pezeshk et al. (2018) GMPM based on the empirical-scaling approach

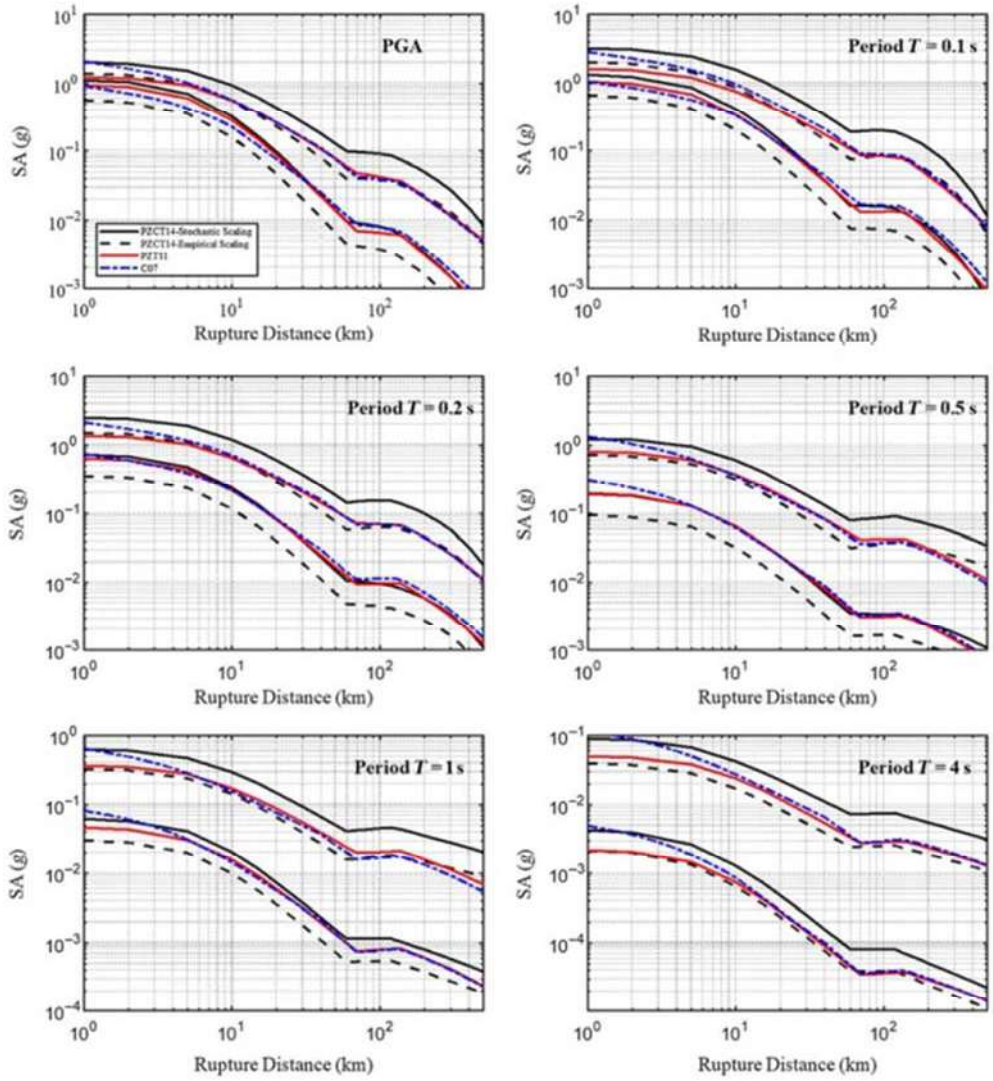

Figure 4-106 Validation of the PGA and PSA for four spectral ordinates

Yenier and Atkinson (2015)

The validation of the Yenier and Atkinson (2015) GMPM has been done for the two regions for which parameters are provided in the article: Central and Eastern North America (CENA) and California. Given that this can be considered as a "plug-and-play" GMPM, CRISIS allows incorporating in a simple manner the calibrated parameters for other regions so that its use can be expanded. Figure 4-107 shows the pseudospectral acceleration for the CENA region for different magnitudes, d=10km and Vs30=760 m/s.

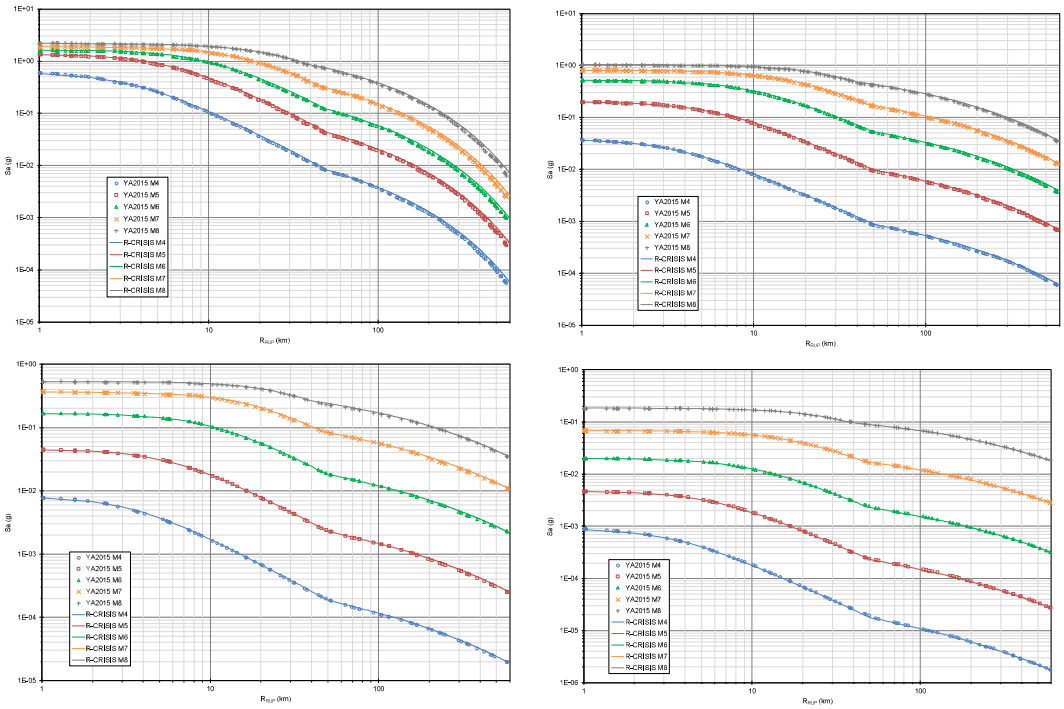

Figure 4-107 Validation of the CENA-adjusted GMPM for T=0.1s (top left), T=0.5s (top right), T=1.0s (bottom left) and T=3.0s (bottom right)

Figure 4-108 shows the validation for the response spectra for CENA and California regions using different D_{RUP} values (10 and 100km).

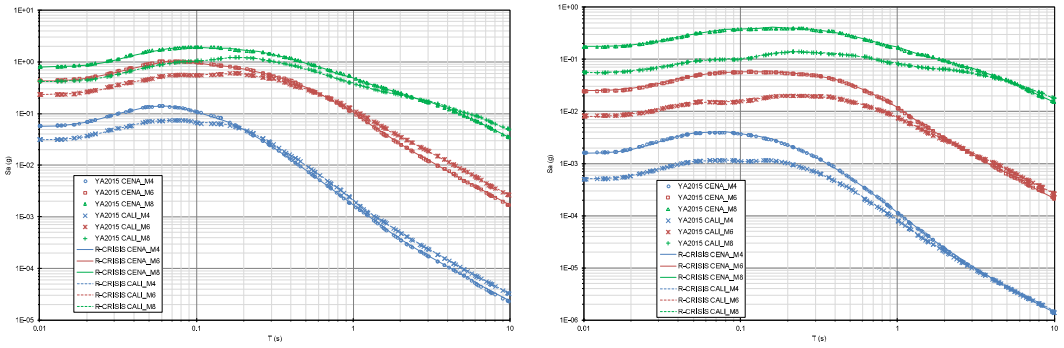

Figure 4-108 Validation of the CENA and California adjusted response spectra for D_{RUP}=10km (left) and D_{RUP}=100km (right)

Darzi et al. (2019)

The validation of the Darzi et al. (2019) GMPM has been done in a graphical manner considering the regional and global models. Figure 4-109 shows the PGA values for Mw 5.5 and 7.0, whereas Figure 4-10 shows the pseudo-accelerations for the same magnitudes and T=1.0s.

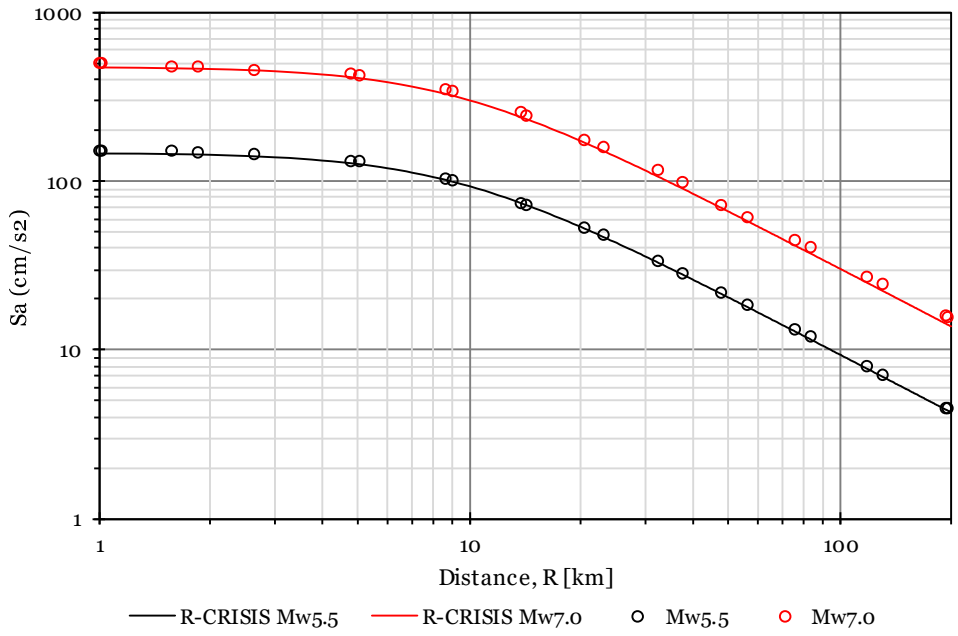

Figure 4-109 Validation of the PGA predictions of the Darzi et al. (2019) model for Mw 5.5 and 7.0

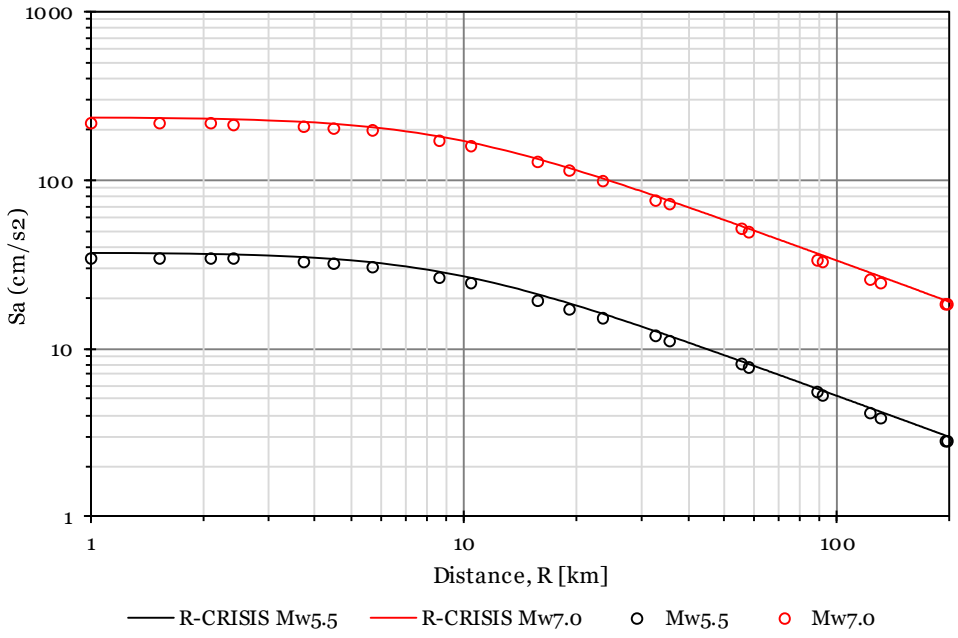

Figure 4-110 Validation of the T=1.0s predictions of the Darzi et al. (2019) model for Mw 5.5 and 7.0

Additionally, the validation of the consideration of different soil conditions was performed, as shown in Figure 4-111 where the median pseudo-acceleration for soil classes I, II and III are shown for R_{JB}=5km and M_W 5, 6 and 7.

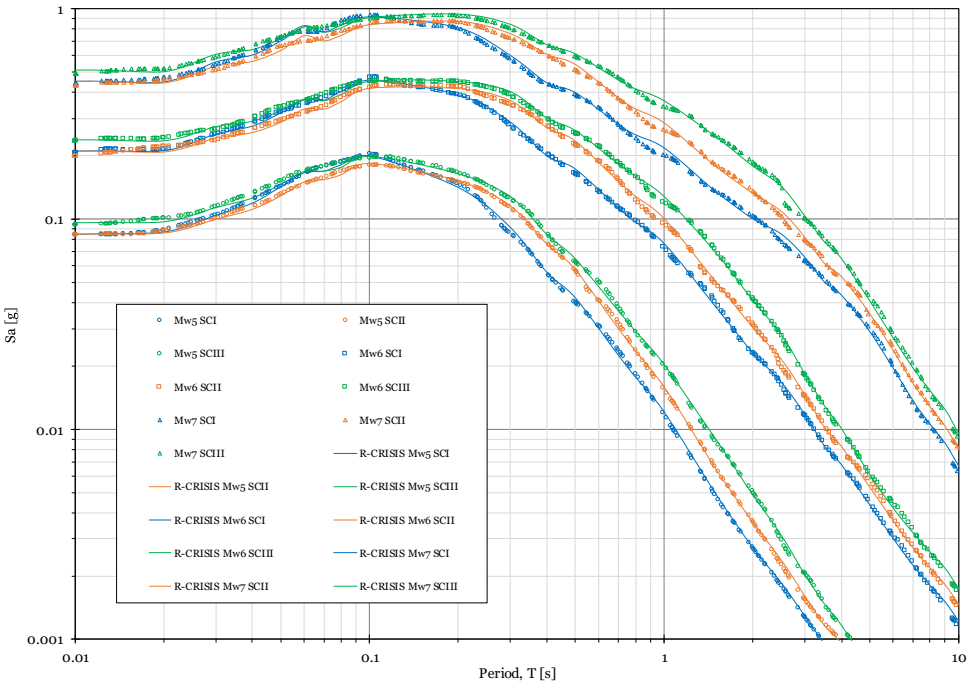

Figure 4-111 Validation of predicted median pseudo-acceleration of the Darzi et al. (2019) model for different soil classes. R_{JB}=5km

Lanzano et al. (2019)

The validation of the Lanzano et al. (2019) GMPM, denoted in the following plots as ITA18, has been performed in a graphical manner. Figure 4-112 shows the predictions of the model for T=1.0s for Mw 4.0 and 6.8, normal faulting and Vs30=600 m/s whereas Figure 4-113 shows the comparisons for the same spectral ordinate and magnitude values for strike-slip faulting mechanism and Vs30=300 m/s.

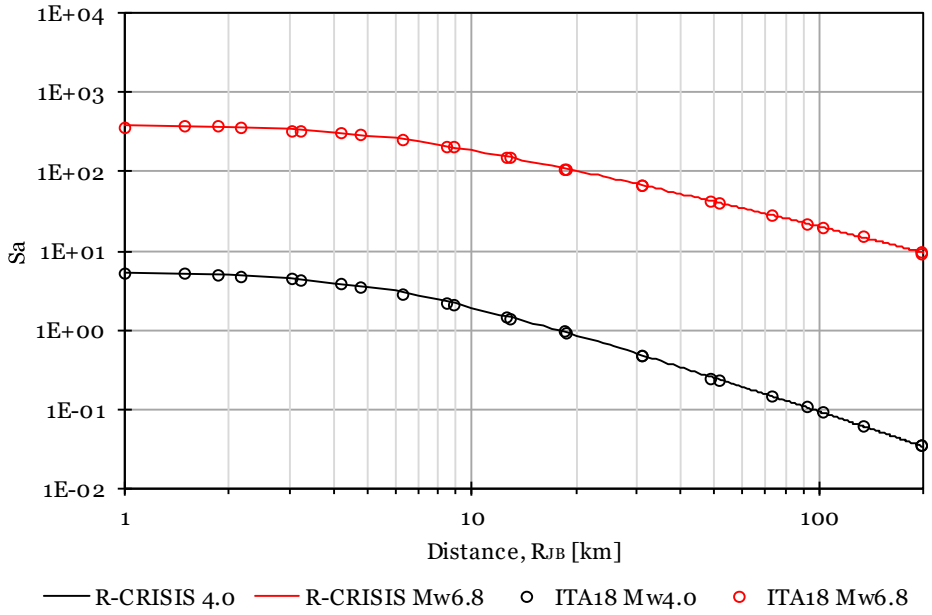

Figure 4-112 Validation of the T=1.0s predictions of the Lanzano et al. (2019) model for Mw 4.0 and 6.8, Vs30=600 m/s and normal faulting mechanism

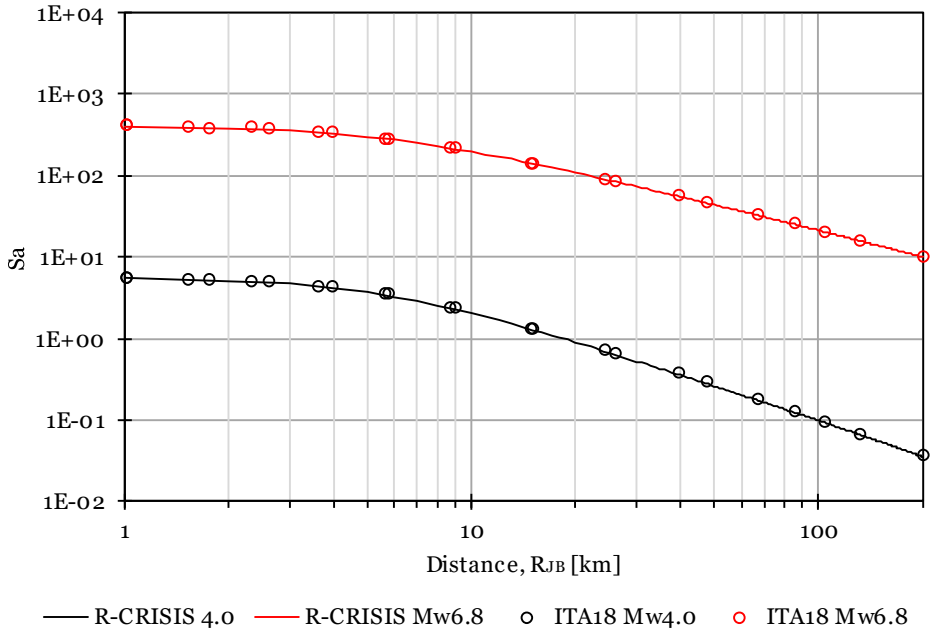

Figure 4-113 Validation of the T=1.0s predictions of the Lanzano et al. (2019) model for Mw 4.0 and 6.8, Vs30=300 m/s and strike-slip faulting mechanism

4.5.3 GMPM where R-CRISIS developers are authors

Since in some of the built-in GMPM the CRISIS developers are authors, those are assumed to have been validated and therefore, well implemented in the program. The GMPM within this category are listed next:

- Arroyo et al. (2010)
- García et al. (2005)
- Jaimes et al. (2006)

4.5.4 GMPM data provided directly by the authors

For some cases, the source code for the GMPM included as built-in models in R-CRISIS has been provided directly by their authors. That is the case of Cauzzi and Faccioli (2008) and Faccioli et al. (2010). In these cases, the GMPM are considered as validated.

4.6 Additional validation tests

4.6.1 Hybrid GMPM vs. Logic trees calculations

The comparison of both approaches has been tested in R-CRISIS using the PEER benchmark -Set 2, case 5b- (Thomas et al., 2014; Hale et al., 2018) in which a particular case among the hybrid GMPM is used. That case corresponds to a *composite model* which in summary is a weighted combination of GMPM with the same mean but different sigma (i.e. unimodal). The following table shows the comparison of the hazard intensity annual exceedance probabilities[22] between the results obtained in R-CRISIS after (**1**): using logic-trees and (**2**) using a hybrid GMPM – mixture model). From Table 4-63 it can be seen that both approaches yield in the same results.

Table 4-63 Comparison of annual exceedance probabilities with logic-trees and hybrid GMPM approaches

[22] This is done in terms of exceedance probabilities for the reasons well explained in Ordaz and Arroyo (2016)

Amax	Annual exceedance probability	
	1	2
1.00E-03	1.590E-02	1.591E-02
1.00E-02	1.590E-02	1.590E-02
5.00E-02	1.410E-02	1.413E-02
1.00E-01	8.880E-03	8.880E-03
2.00E-01	2.740E-03	2.743E-03
4.00E-01	4.380E-04	4.384E-04
6.00E-01	1.210E-04	1.214E-04
8.00E-01	4.380E-05	4.381E-05
1.00E+00	1.850E-05	1.846E-05
1.25E+00	7.240E-06	7.244E-06
1.50E+00	3.190E-06	3.193E-06
2.00E+00	7.910E-07	7.910E-07
2.50E+00	2.450E-07	2.453E-07
3.00E+00	8.900E-08	8.898E-08
4.00E+00	1.620E-08	1.615E-08
5.00E+00	3.930E-09	3.930E-09
6.00E+00	1.170E-09	1.168E-09
7.00E+00	4.020E-10	4.019E-10

Note: when performing these calculations, results compared in terms of exceedance rates may change for the reasons explained in Ordaz and Arroyo (2016).

4.6.2 Verification of the handling of the non-Poissonian occurrence probabilities

The way of computing hazard based on occurrence probabilities of events and probabilities of exceedance of intensity values and not anymore on exceedance rates is checked through a test in which Poissonian probabilities are treated in a non-Poissonian way.

The geometry of the source is very simple: a point source located at a depth of 15km. In spite of this simplicity, the test is general enough since, internally, R-CRISIS performs all the arithmetic related to exceedance probability calculations with discrete point sources. For this example, the computation site is located on the surface of the Earth, 0.2° west and south of the point source.

The seismicity is described by means of a modified G-R relation with λ_o=0.07/year, β=2 (treated as deterministic), M_o=5 and M_U=8 (treated as deterministic). Once these seismicity parameters are known, it is possible to compute, under the Poissonian assumption, the discrete probabilities of having 0, 1,....., N events in given time frames. These probabilities were externally computed and later provided to R-CRISIS as if they were probabilities obtained from a non-Poissonian model of unspecified type. Results are compared with those obtained providing R-CRISIS the same seismicity parameters in the form of a Poissonian source. Figures 4-114 to 4-116 show these comparisons, for time frames of 20, 50 and 100

years, respectively. In each case, the hazard plots are coincident, which means that the non-Poissonian occurrence probabilities are correctly handled by the R-CRISIS code.

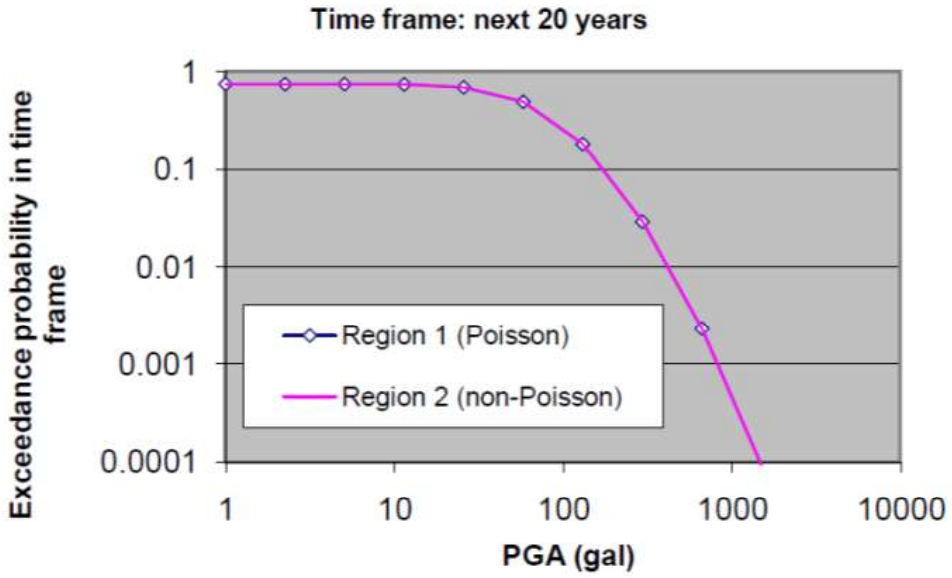

Figure 4-114 Comparison of the results obtained with Poissonian and non-Poissonian sources for 20 years timeframe

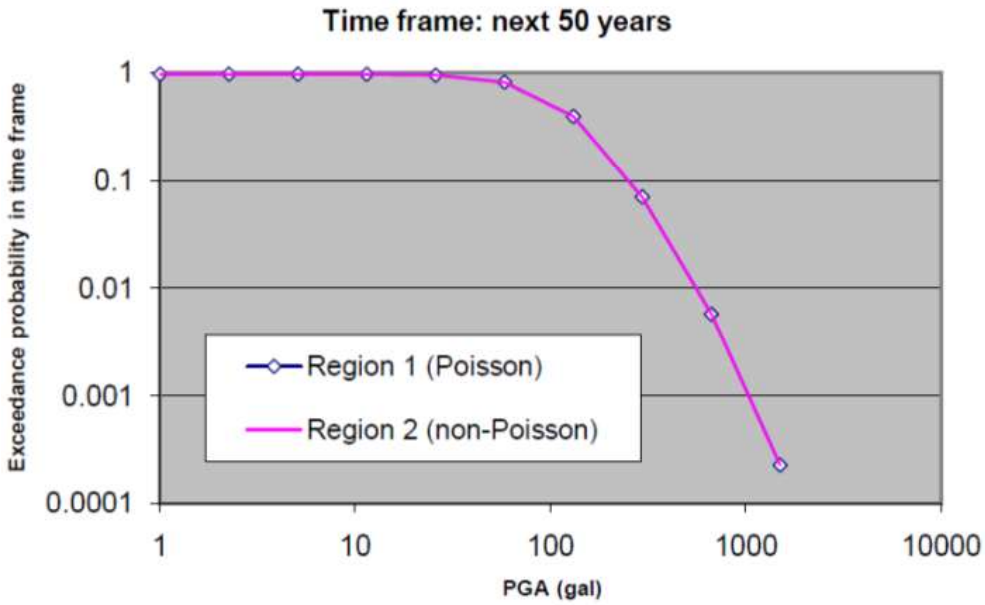

Figure 4-115 Comparison of the results obtained with Poissonian and non-Poissonian sources for 50 years timeframe

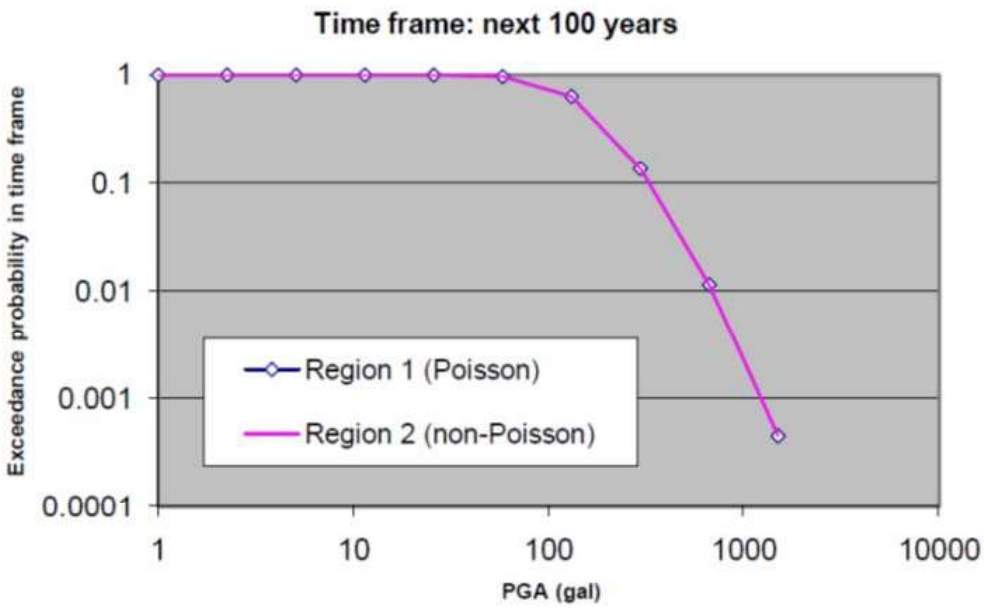

Figure 4-116 Comparison of the results obtained with Poissonian and non-Poissonian sources for 100 years timeframe